ANATOMICAL AND NEUROCHEMICAL INVESTIGATION OF THE BRAIN IN AUTISM

by

LAUREN E. LIBERO

RAJESH K. KANA, CHAIR
FRED J. BIASINI
INGRID MARIA HOPKINS
DAVID C. KNIGHT
ADRIENNE C. LAHTI

A DISSERTATION

Submitted to the graduate faculty of The University of Alabama at Birmingham,
in partial fulfillment of the requirements for the degree of
Doctor of Philosophy

BIRMINGHAM, ALABAMA

2014

ANATOMICAL AND NEUROCHEMICAL INVESTIGATION OF THE BRAIN IN AUTISM

LAUREN E. LIBERO

LIFESPAN DEVELOPMENTAL PSYCHOLOGY

ABSTRACT

Autism spectrum disorder (ASD) is a complex neurodevelopmental disorder with widespread behavioral symptoms and a strong neurobiological origin. Neuroimaging studies of ASD have uncovered evidence for widespread abnormalities in brain anatomy and functioning. Abnormalities reported by structural brain imaging, diffusion tensor imaging (DTI), and proton magnetic resonance spectroscopy (1H-MRS) studies have aided in characterizing ASD as a complex, systems-wide disorder. The overarching goal of this project was to use multiple modalities of neuroimaging to investigate the underlying neural mechanisms of ASD. The following techniques were used to collect and analyze multimodal neuroimaging data from a relatively large number of participants with autism and matched typically developing (TD) peers: (1) Surface-based morphometry (SBM) examining cortical features (e.g., volume, cortical thickness, surface area, gyrification); (2) Diffusion tensor imaging (DTI) to study the integrity of major white matter tracts; (3) Proton magnetic resonance spectroscopy (1H-MRS) to assess the concentration of neurochemicals; and (4) Pattern classification modeling using measures from multimodal brain imaging to determine the diagnostic utility of neural markers found from these imaging methods. The current study is novel in that it applies relatively new techniques for analyzing DTI and anatomical data, reports more detailed brain measures from each modality, includes large sample sizes with children and adults, and reports on a classification analysis utilizing multimodal brain measures for predictors

of diagnosis. We found significant differences in surface based features of brain structure, fractional anisotropy and radial diffusivity of major white matter tracts, as well as brain metabolite levels in children and adults with ASD, compared to TD participants. Specifically, we uncovered significant alterations in cortical volume and surface area in right posterior cingulate cortex and left temporoparietal junction, and a significant reduction in gyrification in right precentral gyrus in children and adults with ASD. In addition, we found significantly reduced fractional anisotropy (FA) and increased radial diffusivity (RD) along the left superior longitudinal fasciculus in children and adults with ASD. The 1H-MRS analysis uncovered significantly reduced levels of N-acetylaspartate in the dorsal anterior cingulate cortex in adults with ASD. Finally, an analysis utilizing brain measures as predictors for diagnosis revealed that measures of cortical thickness and white matter integrity (FA and RD) were the most effective at classifying participants with ASD, with some variables also predicting symptom severity. In summary, we observed significant alterations in brain structure, white matter connectivity, and neuronal health in participants with ASD. These measures were also useful in developing a classification model for identifying participants with ASD. Multimodal brain imaging evidence from this study provides a comprehensive characterization, which spans several levels and layers, of the neural architecture of autism.

Keywords: MRI, DTI, 1H-MRS, morphometry, fractional anisotropy, autism spectrum disorder, neurochemicals, diffusion

DEDICATION

This dissertation is dedicated to my participants, students, and friends with autism. Thank you for believing in my work and teaching me so many things. This project is for you.

ACKNOWLEDGMENTS

Thank you to my mentor Dr. Rajesh K. Kana for his support and guidance throughout my graduate career. Thank you for giving me a strong foundation in neuroimaging and autism research, and never discouraging my ambition to learn several modalities (when one technique was not enough to answer my questions).

Thank you to my graduate studies committee for their time and suggestions in the development of my studies.

I would like to that the members of the Cognition, Brain, and Autism Lab for their contribution to the data acquisition and analysis.

Thanks to the director of my graduate program Dr. Fred Biasini for your advisement and support. I would also like to thank the Lifespan Developmental Psychology students for their help and kind words during my graduate studies at UAB. Thank you to the Department of Psychology for their administrative and financial support during my Ph.D. training.

Thank you to my participants and their families for continuing to be a part of my research projects. These studies could not be done without your generosity and willingness to contribute to science.

A special thank you to my parents, Peter and Elizabeth, and my brother Peter for their encouragement and unwavering support throughout my academic career. I am so grateful to have such amazing people behind me in everything that I do.

TABLE OF CONTENTS

Page

LIST OF TABLES

Table *Page*

LIST OF FIGURES

Figures *Page*

MORPHOMETRY OF THE SOCIAL BRAIN IN AUTISM SPECTRUM DISORDER: CORTICAL THICKNESS, CORTICAL VOLUME, SURFACE AREA, AND GYRIFICATION

INVESTIGATING WHITE MATTER INTEGRITY OF MAJOR FIBER TRACTS IMPLICATED IN AUTISM SPECTRUM DISORDER USING DIFFUSION TENSOR IMAGING

CEREBRAL METABOLITE ABNORMALITIES IN THE ANTERIOR CINGULATE CORTEX IN AUTISM: AN MR SPECTROSCOPY STUDY

MULTIMODAL NEUROIMAGING BASED CLASSIFICATION OF AUTISM SPECTRUM DISORDER USING ANATOMICAL, NEUROCHEMICAL, AND WHITE MATTER CORRELATES

INTRODUCTION

Neuroscience research over the last few decades has illuminated our understanding of the neurobiological underpinnings of autism spectrum disorders (ASD). Although electrophysiological, cellular, and animal models have contributed significantly to a better conceptualization of ASD, the advent of modern in vivo human neuroimaging techniques have indeed revolutionized neuroscience research in autism. Specifically, the development and implementation of magnetic resonance imaging (MRI) techniques has facilitated an explosion of research and discovery in the field. Most importantly, the last few decades of neuroscience research has played an important role in eliminating speculative psychoanalytic accounts of autism and in dispelling the misconceptions about the disorder. With the advent of MRI, it was possible to examine the autism brain in vivo with high contrast sensitivity and spatial resolution (Chen, Jiao, & Herskovits, 2011). This has allowed researchers to examine the human brain at different levels: anatomy, organization and connectivity, and neurochemistry. Such multilayered information can be valuable in understanding the biological bases of behaviorally defined neurodevelopmental disorders like autism.

ASD has been characterized as a disorder of neurodevelopmental origin, and neuroimaging studies have provided evidence for widespread functional and structural brain abnormalities, seen early on in babies and toddlers with ASD (Williams & Minshew, 2007). Although such abnormalities at focal as well as at global levels have led to a systems-level characterization of the disorder, a firm neurobiological marker for autism has been elusive, with little information on the neurodevelopmental trajectory.

With no known neural biomarker, ASD continues to be diagnosed exclusively by clinical observation of behavior and by gathering evidence about developmental history through interviews. The treatment for ASD is thus more focused on cognitive and behavioral therapeutic approaches aimed primarily at minimizing symptoms. Identification of a neural signature may be critical in targeted treatment as well as in making treatment available early in life. Neuroimaging studies of autism, due to their focus on a single modality (e.g., functional MRI, diffusion tensor imaging, or structural MRI), have been limited by a single level of inference (e.g., brain function, white matter connectivity, or cortical anatomy) which ends up being insufficient in characterizing a biologically and behaviorally complex disorder like autism. A promising new direction in this regard is to employ multimodal imaging techniques in order to gain inference at different levels of brain organization and functioning from the same set of individuals. In this way, the inherent limitations of one modality could be addressed by another. The primary goal of the current study is to utilize multimodal neuroimaging techniques (MRI based cortical morphometry, diffusion tensor imaging, and proton magnetic resonance spectroscopy) to derive a comprehensive characterization of the neuropathology of autism. In the sections below, these different modalities of imaging are examined in the context of ASD to better understand the current state of research.

Neuroanatomy

Neuroanatomical investigations provide precise information about the structural integrity of individual regions and areas which are extremely important in understanding how the brain functions as a system. Abnormal cortical anatomy is often seen in several neuropsychiatric disorders, and has been a central feature of ASD (Amaral, Schumann, &

Nordahl, 2008, Nickl-Jockschat et al., 2012). Studies of brain volume assess anatomical differences in the brain, regional concentrations, and total brain size (Ashburner & Friston, 2000). Numerous studies have reported increased total brain volume in ASD (Hazlett et al., 2005; Hazlett et al., 2011; Stanfield et al., 2008), while several others did not find any significant differences in overall volume (Hallahan et al., 2009). Abnormally large brain may entail alterations in individual structures and can result in widespread consequences spanning function, organization, and connectivity (Herbert, 2005). Although regional volumetric differences in ASD are variable and inconsistent, the relatively more consistent findings include increased gray matter volume in frontal, temporal, parietal, and limbic areas, decreased white matter volume in frontal, temporal, and limbic areas (Chen et al., 2011; Stanfield et al., 2008), and volumetric abnormalities in amygdala, hippocampus, corpus callosum, and cerebellum (Brambilla et al., 2003; Stanfield et al., 2008). Most of the neuroanatomical studies of ASD, to date, have employed voxel-based morphometry (VBM), a technique that allows the quantification and statistical comparison of the concentration of gray matter tissue between groups. While this technique has been valuable in providing information about volumetric differences between participants with ASD and controls, VBM has many limitations, including potential inaccuracies in normalization which lead to problems when attempting to directly compare two different groups of participants (Bookstein, 2001; Davatzikos, 2004). Considering reports of anatomic shifting and alterations in the shape of sulci in the brains of children with ASD (Auzias et al., 2014; Levitt et al., 2003; Nordahl et al., 2007), normalization through VBM pipelines may result in inconsistency and/or error. Abnormal cortical patterns of sulci and gyri could dramatically alter the automated normalization included in VBM software, thus invalidating any comparison

with control groups (Bookstein, 2001; Davatzikos, 2004). Surface-based morphometry (SBM) techniques using non-linear alignment to cortical folding patterns (the sulci and gyri) provide more accurate normalization of subjects and are perhaps more useful and appropriate when attempting to examine participants with different diagnostic status (Ghosh et al., 2011).

Surface-based morphometric methods allow subdivision of cortical volume into its two main constituents, cortical thickness and surface area, which in turn, can be further subdivided into the area of the exposed cortical surface (gyrus) and the area of the non-exposed hidden surface (sulci) (Raznahan et al., 2011). Cortical thickness findings point to increased thickness in the parietal lobule, and differences (both increased and decreased findings) in frontal and temporal regions (Ecker et al. 2013; Hadjikhani, Joseph, Snyder, & Tager-Flusberg, 2006; Hardan, Muddasani, Vemulapalli, Keshavan, & Minshew, 2006; Hardan, Libove, Keshavan, Melhem, & Minshew, 2009; Hyde, Samson, Evans, & Mottron, 2010; Jiao et al., 2010; Mak-Fan et al., 2012; Scheel et al., 2011; Wallace, Dankner, Kenworth, Geidd, & Martin, 2010; see Chen et al., 2011 for a review). Gyrification, the degree of cortical folding, is another index that can be measured by the ratio of total to outer cortical contour (Hardan, Jou, Keshavan, Varma, & Minshew, 2004; Zilles, Armstrong, Schleicher, & Kretschmann, 1988). Measuring regional volume, cortical thickness, and gyrification provide information about different aspects of cortical anatomy that are subtle and important, in ASD. Findings of gyrification measures in ASD have been slightly more consistent than volume and cortical thickness investigations, finding increased GI in ASD, particularly in parietal lobule (Kates, Ikuta, & Burnette, 2009), inferior frontal gyrus (Jou, Minshew, Keshavan, & Hardan, 2010), and temporal

and occipital cortex (Wallace et al., 2013), and alterations in sulcal depth in insula and intraparietal sulcus (Shokouhi, Williams, Waiter, & Condon, 2012) and inferior frontal gyrus (Nordahl et al., 2007). Overall, despite widespread brain structural abnormalities in ASD, the results have been largely inconsistent. Alterations in volume and surface based measures have appeared in different and spatially discrete regions, and the location and direction of these differences have also varied from study to study. This may be due in part to the heterogeneity of the ASD population, to the fairly limited sample sizes in most studies, as well as to the potential inconsistencies in methodology. As significant neuroanatomical differences are still apparent in ASD, further research is needed to derive a global characterization of the deficiencies.

White matter Integrity

Volumetric studies have suggested an early overgrowth of white matter among young children with autism, followed by reduced white matter in adolescence and adulthood relative to typical control individuals (Courchesne et al., 2001; Courchesne, Carper, & Akshoomoff, 2003; Ecker et al., 2012; Herbert et al., 2004; Waiter et al., 2005). Such volumetric abnormalities may have resulted from aberrations in axonal density or organization, or from myelin abnormalities, either of which could result in aberrant connectivity. Diffusion Tensor Imaging (DTI) provides the opportunity to go beyond measurement of the volume of white matter to examine its structural integrity on a voxel-by-voxel basis. Fractional anisotropy (FA), a measure derived from diffusion tensor data, is sensitive to developmental changes and pathological differences in axonal density, size, myelination, and the coherence of organization of fibers within a voxel, and thus provides an index of the structural integrity of the white matter (Basser, 1995;

Beaulieu, 2002; Pierpaoli & Basser, 1996). In addition to FA, DTI also produces measures of mean diffusivity (MD), axial diffusivity (AD) and radial diffusivity (RD). DTI studies in ASD have found reduced FA and increased MD in a number of white matter tracts including corpus callosum, cingulum, and tracts in the temporal lobes (Alexander et al., 2007; Bloemen et al., 2010; Barnea-Goraly et al., 2004; Keller, Kana & Just, 2007; Lee et al., 2009; see Travers et al., 2012 for a review). However, while these tracts have been implicated somewhat consistently in DTI studies on ASD, results related to other major white matter tracts remain inconsistent, with some studies reporting reductions in FA across the brain and others reporting no differences. Abnormalities in overall white matter volume, in addition to studies pointing to disrupted cortical connectivity (see Kana, Libero & Moore, 2011 for a review), suggest alterations in white matter integrity and connectivity in ASD. More detailed DTI studies are needed in order to establish a reliable picture of white matter abnormalities in autism, and to relate such microstructural alterations with disruptions in functional connectivity.

Neurochemical Concentration

Neurochemicals serve as markers for various functions at the cellular level (e.g., intracellular mechanisms, cell metabolism, neuronal and synaptic health), and alterations in neurochemical levels can serve as markers for disease or neuronal damage. Proton Magnetic resonance spectroscopy (1H-MRS) measures relative tissue metabolite concentrations in the brain. Thus, as a method, 1H-MRS has proved to be a powerful tool for the assessment of various pathologic conditions, including epilepsy, multiple sclerosis, stroke, cancer, and metabolic diseases (Ross & Bluml, 2001). 1H-MRS studies have uncovered abnormal levels of brain metabolites in ASD children and adults across

the brain (see Ipser et al., 2012 for a review). MRS is a function of MRI that provides the only non-invasive technique for measuring metabolite concentration in the living brain (Stanley, 2002), and is often utilized as a method for identifying disease-related abnormalities (Fayed, Olmos, Morales, & Modrego, 2006). This method allows for measurement of a number of metabolites, including N-Acetylaspartate (NAA), Choline (Cho), Glutamate/Glutamine (Glx), and Creatine (Cr). NAA is a neuronal marker, representing neuronal and axonal health and density, and reductions in NAA concentrations can be a marker for disease (Fayed et al., 2006; Maddock & Buonocore, 2012; Meyerhoff et al., 1993). Cho levels represent cellular membrane proliferation and degradation (Fayed et al., 2006; Maddock & Buonocore, 2012). Glutamate is related to oxidative energy production and excitatory neurotransmitter functions, while glutamine is involved with glutamate recycling and regulation of brain ammonia metabolism (Maddock & Buonocore, 2012; Waagepetersen, Sonnewald, & Schousboe, 2007). The combined Glx thus represents overall glutamate/glutamine levels and their functioning in the brain (Maddock & Buonocore, 2012; Rothman, Behar, Hyder, & Shulman, 2003; Yuksel & Ongur, 2010). Finally, Cr plays a role in central nervous system energy homeostasis, and represents the most stable cerebral metabolite (Fayed et al., 2006; Maddock & Buonocore, 2012). Because Cr is stable, it is often used as an internal reference value, and other metabolites are reported in terms of their ratio to Cr (e.g., NAA/Cr for the measurement of NAA).

1H-MRS applied to study autism has uncovered a number of abnormalities in neurochemical levels, with significant decrease or increase in concentration reported by several studies. See Table 1 for a detailed list of the 1H-MRS studies in ASD literature

and the corresponding direction of the differences found in neurochemicals between ASD and TD groups.

Neurochemical	Brain Region	Direction	Author(s)
NAA	Hippocampus-amygdala	↓	Gabis et al., 2008; Mori et al., 2001; Otsuka, Harada, Mori, Hisaoka, & Nishitani, 1999
	Thalamus	↓	Hardan et al., 2008; Perich-Alsina, Aduna de Paz, Valls, & Munoz-Yunta, 2002
	Cerebellum	↓	Chugani, Sundaram, Behan, Lee, & Moore, 1999; DeVito et al., 2007; Mori et al., 2001
	Prefrontal Cortex	↑	Murphy et al., 2002
		↓	DeVito et al., 2007; Kleinhans et al., 2007
	Anterior Cingulate Cortex	↓	Fujii et al., 2010
		↑	Oner et al., 2007
	Temporal Cortex	↓	DeVito et al., 2007; Endo et al., 2007; Friedman et al., 2003
	Occipital Cortex	↓	DeVito et al., 2007
	Basal Ganglia	↓	Friedman et al., 2003
Glx	Cerebellum	↓	DeVito et al., 2007
	Prefrontal Cortex	↓	DeVito et al., 2007
	Anterior Cingulate Cortex	↓	Bernardi et al., 2011
	Temporal Cortex	↓	DeVito et al., 2007; Endo et al., 2007; Friedman et al., 2003
	Occipital Cortex	↓	DeVito et al., 2007
Cho	Thalamus	↓	Hardan et al., 2008
	Prefrontal Cortex	↑	Murphy et al., 2002
	Anterior Cingulate Cortex	↑	Vasconcelos et al., 2007
		↓	Levitt et al., 2003
	Caudate	↑	Levitt et al., 2003
Cr	Thalamus	↓	Hardan et al., 2008
	Occipital Cortex	↓	Levitt et al., 2003
	Basal Ganglia	↓	Friedman et al., 2003
	Caudate	↑	Levitt et al., 2003
No Difference	Amygdala	N.S.	Kleinhans et al., 2009
	Cerebellum	N.S.	Gabis et al., 2008; Otsuka et al., 1999
	Parietal Cortex	N.S.	Page et al., 2006
	Centrum semiovale	N.S.	Fayed & Modrego, 2005

Table 1. Alterations in neurochemical levels between autism (ASD) and typically developing (TD) control groups from proton magnetic resonance spectroscopy (1H-MRS) studies.

Overall, studies have indicated abnormalities in metabolite concentrations in the brain in ASD, especially in the hippocampus-amygdala formation, frontal cortex, cingulate, and temporo-occipital brain regions (Endo et al., 2007; Friedman et al., 2003;

Fujii et al., 2010; Gabis et al., 2008; Mori et al., 2001; Otsuka et al., 1999). However, the results vary greatly in terms of the specific neurochemicals responsible for differences in ASD, and in many cases the results are contradictory (finding increases and decreases of the same metabolites in the same brain regions). The overwhelming majority of 1H-MRS studies also includes children only; so alterations in levels of neurochemicals in adults and any potential neurodevelopmental effects are still relatively unknown. In addition, as the 1H-MRS data are collected at one specified region at a time, studies typically include results from only a few brain regions. As a result, MRS findings are specific, and limited to a few regions. As the entire brain has not been studied utilizing this technique, and findings are still limited and inconsistent, future studies are desperately needed using 1H-MRS.

Pattern Classification of Individuals with ASD based on Neuroimaging Data

An important question emerging from the large number of neuroimaging studies of autism is about the utility of such findings at a translational and applied level. One of the aims of neuroscience research has been to identify a valid and reliable biological marker for autism. With the advent of sophisticated machine learning techniques in understanding complex datasets, studies have begun to test the diagnostic utility of neuroimaging measures using pattern classification. For example, several recent studies have used functional brain activation and connectivity data to classify participants into ASD and TD groups successfully (Anderson et al., 2011; Coutanche, Thompson-Schill, & Schultz, 2011; Deshpande, Libero, Sreenivasan, Deshpande, & Kana, 2013; Kaiser & Pelphrey, 2012; Murdaugh et al., 2012; Spencer et al., 2011). A few studies have also conducted pattern classification using volumetric and surface based structural measures (Akshoomoff et al., 2004; Ecker et al., 2010a; Ecker et al., 2010b; Jiao et al., 2010; Uddin

et al., 2011) and DTI data (Ingalhalikar, Parker, Bloy, Roberts, & Verma, 2011; Lange et al., 2010) as predictors. A combination of cortical volume and thickness, along with single-nucleotide polymorphisms (Jiao et al., 2011) have also been used to predict group membership. Yet another study used brain structure to classify females with ASD apart from TD females (Calderoni et al., 2012). Out of these studies, only one so far has attempted to apply classification to a validation cohort (i.e., they applied their classifier to predict ASD diagnostic status of individuals from a different pool of participants, and not from the original pool used to develop the classifier) (Kaiser & Pelphrey, 2010), and only one has sought to compare the diagnostic utility of their classification of ASD subjects to another diagnostic population for validation (in this case, determining whether their classifier could predict ASD participants separate from TD and ADHD peers) (Ecker 2010a).

Thus, these studies suggest that the field of neuroimaging in autism is indeed considering the translational potential of basic research findings. Nevertheless, it is too early to use any such indices for a firm diagnosis of autism. The heterogeneity seen in autism (differences in the presentation of symptoms from one individual to the next, wide variation in IQ, as well as differences between males and females) is a major factor that hinders the reliability of classification findings. Another issue is that most previous classification studies have relied on functional brain imaging, through the use of experimental tasks which require one to follow directions and pay attention to visual or auditory stimuli to do a cognitive or social task. For many individuals with ASD, particularly low-functioning individuals and young children (who are also more difficult to diagnose), these methods may not be appropriate or viable. Thus, the classification results of these studies may not accurately represent the entire autism spectrum. In

addition, the neuroimaging literature shows ASD is a complex disorder, with alterations in varied and spatially separate regions of the brain. Thus, previous studies have failed to identify a focal cause for the disorder. Rather, systems or networks are affected, and these differences have been found across many neuroimaging modalities. ASD has been identified as a neural systems disorder with complex neurobiology and any biomarker will need to be multivariate, possibly including several aspects of biology and behavior (Ecker, Spooren, & Murphy, 2013). Since neural abnormalities in ASD have been measured in a number of neuroimaging modalities (e.g., brain structure, white matter integrity, neurochemical levels) in our study, information from these modalities could be included as predictors for diagnostic purposes. When all of the systems affected are included, the prospect of finding a more comprehensive and accurate classifier may be greater. In addition, while classification models are good at separating ASD participants from TD peers, including several neural systems predictors could also potentially lead to classification of participants by symptomatology or result in classification of subgroups. Becoming more sensitive to symptomatology potentially allows us to identify clusters of neural abnormalities that are linked to clusters of ASD behaviors. Identifying and grouping individuals based on their specific neural abnormalities will make the focus of treatment more apparent. In this manner, classification of individuals and identification of their constellation of neural markers could lead to better application of interventions and improvement in cognition.

Specific Aims

Previous studies have utilized mainly a single neuroimaging modality at a time, providing only neural snapshots, not yielding a cohesive characterization of ASD. The

overarching goal of the proposed project is to use multimodal imaging techniques to examine the brain in ASD and explore potential biomarkers. We will utilize SBM, DTI, and 1H-MRS to study abnormalities (at anatomical, connectional, and neurochemical levels) in the brains of children and adults with ASD. This project has the following specific aims:

Aim 1: To examine the neuroanatomical differences (cortical volume, cortical thickness, surface area, and gyrification) in children and adults with ASD, compared to TD peers, and establish the relationship between brain measures and age.

Manuscript 1— This study used structural MRI data to measure surface based features of cortical morphology in children and adults with ASD. The purpose of this study was to identify abnormalities in surface-based features of cortex in ASD, thus groups were compared on surface features. Based on previous findings of widespread abnormalities in cortical thickness, regional volume, and gyrification (see Chen, Jiao, & Jerskovits, 2011 for a review), we expect to find significant increases in cortical thickness and significant increases in overall surface area and gyrification (particularly in tempo-parietal cortices) in children and adults with ASD, compared to their TD peers. As ASD is also a neurodevelopmental disorder, we aimed to examine the relationship between surface-based cortical measures and age to study the neurodevelopmental trajectory of brain structure in the disorder. We expect to find developmental alterations in cortical volume and cortical thickness in children and adults with ASD, compared to their TD peers.

Aim 2: To investigate the structural integrity of white matter tracts (through water diffusion along axons) in children and adults with ASD compared to TD peers utilizing

DTI, and to examine the relationship between these diffusion measures and behavioral data.

Manuscript 2—The purpose of this study is to uncover aberrant white matter integrity in major white matter tracts in ASD. To do so, we used DTI to investigate the structural integrity of white matter tracts in children and adults with ASD compared to TD peers. Utilizing a new DTI analysis technique, we explored tract properties (including FA, RD, MD, and AD) in the major tracts implicated in ASD. To better understand the differences in white matter integrity, diffusion measures were compared directly between groups. Earlier studies examining diffusivity in ASD uncovered aberrations in FA and MD for numerous white matter fiber bundles, including corpus callosum, cingulum, and tracts within the temporal lobes (see Travers et al., 2012 for a review). Thus, we predicted we would find reduced FA, increased MD, and alterations in RD and AD within the major fiber tracts (particularly the corpus callosum and cingulum bundle) in the brain in children and adults with ASD, compared to their TD peers. As ASD is also a neurodevelopmental disorder, we aimed to examine the neurodevelopmental trajectory of the disorder by exploring the relationship between measures of white matter integrity and age.

Aim 3: To assess the levels of brain metabolites (NAA/Cr, Glx/Cr, and Cho/Cr) using 1H-MRS in adults with ASD, compared to TD peers, and to investigate the relationship between these measures with assessment data.

Manuscript 3—Brain metabolite levels are often an indication of neuronal health and disease. To assess potential abnormalities in brain metabolites in ASD, this study measured the levels of brain metabolites (NAA/Cr, Glx/Cr, and Cho/Cr) using 1H-

MRS in adults with ASD, compared to TD peers. Also to explore neurodevelopment and symptomatology in connection with neurochemical levels in the brain, the current study investigated the relationship between the measures of brain metabolites with age and symptom severity. Previous MRS studies uncovered significant differences in concentrations of brain metabolites in individuals with ASD (DeVito et al., 2007; Fujii et al., 2010; Kleinhans et al., 2007; Levitt et al., 2003; Murphy et al., 2002; Oner et al., 2007). Based on these findings, we expect to find significant reductions in NAA/Cr, and alterations in Glx/Cr, and Cho/Cr ratios within the anterior and posterior cingulate cortices in adults with ASD.

Aim 4: To explore the classification accuracy of neural predictors of diagnostic status (ASD or TD), based on cortical thickness, DTI metrics, and neurochemical levels.

Manuscript 4—The final study included in this project explored the convergence of results from multimodal brain imaging in ASD. As ASD is currently diagnosed clinically by behavioral observation, identification of a neural signature of ASD could potentially lead to applied classification of individuals and ultimately improved diagnosis of ASD. By examining one cohort of subjects utilizing the three modalities described in the previous papers (surface based morphometry, DTI, and 1H-MRS), we examined differences in several neural systems in adults with ASD, compared to their TD peers. In addition, we investigated the potential of multimodal neuroimaging for diagnostic utility; analyzing the best neural markers for classification of individuals with ASD and the interplay between these neural measures and symptom severity.

MORPHOMETRY OF THE SOCIAL BRAIN IN AUTISM SPECTRUM DISORDER: CORTICAL THICKNESS, CORTICAL VOLUME, SURFACE AREA, AND GYRIFICATION

by

LAUREN E. LIBERO, THOMAS P. DERAMUS, HRISHIKESH D. DESHPANDE, AND RAJESH K. KANA

Submitted to *Neuropsychologia*

Format adapted for dissertation

Abstract

Neuroimaging studies of autism spectrum disorder (ASD) have uncovered widespread structural brain abnormalities. Such abnormalities in cortical anatomy may have a significant impact on brain function and connectivity which in turn may contribute to the behavioral symptoms of autism. The findings of previous structural MRI studies have largely been distributed across several different areas, with very few consistent and reliable findings. The current study examined neuroanatomical abnormalities by comparing surface-based measures of cortical morphology (cortical thickness, surface area, cortical volume, and gyrification) in 55 high-functioning children and adults with ASD to 60 age and IQ matched typically developing (TD) peers. The ASD participants had significantly reduced cortical thickness in right rostral anterior cingulate cortex, and right superior parietal lobule; and reduced gyrification in the right precentral gyrus. On the other hand, significantly greater cortical volume was found in ASD in the right posterior cingulate, and left temporoparietal junction (TPJ); increased cortical thickness for right pars orbitalis, left TPJ, and left superior frontal, and increased surface area for right posterior cingulate cortex and left TPJ. Thus, alterations in cortical morphology in ASD were seen primarily in regions associated with social cognition. Significant age-related relationships emerged for both groups for many of the regions that were significant, with several correlations differing between ASD and TD groups. Overall, these findings represent widespread alterations in surface brain measures in children and adults with ASD, particularly in the social brain. These differences in cortical

morphology may underlie the social behavioral abnormalities that are characteristic of autism.

Keywords: autism spectrum disorder, surface-based morphometry, Freesurfer, anatomy

Introduction

Abnormal cortical anatomy has been identified as a central feature of the neuropathology of autism spectrum disorders (ASD) (Amaral, Schumann, & Nordahl, 2008; Nickl-Jockschat, et al., 2012), with specific and consistent abnormalities found in brain volume (Courchesne, Campbell, & Solso, 2011; Hazlett, et al., 2005; Hazlett, et al., 2011; Stanfield, et al., 2008), indicating early overgrowth, followed by abnormal decline and degeneration during adolescence and adulthood (Courchesne, et al., 2011). Studies of head circumference indicate larger head mass in ASD (Dawson, et al., 2007; Elder, Dawson, Toth, Fein, & Munson, 2008; Hazlett, et al., 2005), and studies of brain volume have indeed reported greater total volume in ASD as well (Hazlett, et al., 2005; Piven, et al., 1995). However, a closer look at regional volumetric differences reveals variable findings, with the relatively more consistent findings being increased gray matter volume in frontal, temporal, parietal, and limbic areas, decreased white matter volume in frontal, temporal, and limbic areas (Chen, Jiao, & Herskovits, 2011; Stanfield, et al., 2008), and volumetric abnormalities in amygdala, hippocampus, corpus callosum, and cerebellum (Brambilla, et al., 2003; Stanfield, et al., 2008). Findings from previous studies examining neurodevelopment in ASD have further complicated the picture, reporting abnormal development of brain volume in infants and young children, but rather inconsistent results in older children and adults (Courchesne, et al., 2001; McAlonan, et al., 2002; Redcay & Courchesne, 2005).

Thus, studies examining brain anatomy in ASD have varied not only in their findings, but also in the nature of participants included; with age, IQ, and symptom severity differing widely from study to study, perhaps contributing to the inconsistencies

in the findings. In addition, most of the studies comparing brain structure between typical controls and individuals with ASD have employed voxel-based morphometry (VBM), a technique that allows the quantification and statistical comparison of the concentration of gray matter tissue. While this technique has been valuable in providing information about structural differences in the ASD brain, VBM has many limitations, including potential inaccuracies in normalization which lead to problems when attempting to directly compare two different groups of participants (Bookstein, 2001; Davatzikos, 2004). This is troubling in terms of brain structure findings for ASD, considering reports of anatomical shifting and alterations in the shape of sulci in the brains of children with ASD (Auzias, et al., 2014; Levitt, et al., 2003; Nordahl, et al., 2007). Abnormal cortical patterns of sulci and gyri could dramatically alter the automated normalization procedure included in VBM software, thus invalidating any comparison with control groups. Surface-based morphometry (SBM) techniques using non-linear alignment to cortical folding patterns (the sulci and gyri), on the other hand, provide more accurate normalization of subjects' brains and are perhaps more useful, especially when attempting to examine the cortical morphology of participants with differing diagnostic status (Ghosh, et al., 2010).

SBM as a technique not only marks a more accurate determinant of differences in brain volume, but also allows the comparison of the measurements that contribute to the volume of specific regions. For example, the use of surface-based morphometric methods allows subdivision of cortical volume (CV) into its two main constituents, cortical thickness (CT; the distance between the boundary of white matter/gray matter division and gray matter/pial surface) and surface area (SA; the total area of the surface

encompassing a brain region), which in turn, can be further subdivided into the area of exposed cortical surface area (gyrus) and the non-exposed hidden surface area (sulci) (Raznahan, et al., 2011). SBM also allows measurement of gyrification, the degree of cortical folding. This measure can be gained as a ratio of the total to outer cortical contour (A. Y. Hardan, Jou, Keshavan, Varma, & Minshew, 2004; Zilles, Armstrong, Schleicher, & Kretschmann, 1988). Gyrification is an important measure of brain organization, as the degree of gyrification is associated with overall brain size, and the amount of cortical folding is relevant to the development of neuronal connections in the brain (Armstrong, Schleicher, Omran, Curtis, & Zilles, 1995). Cortical thickness represents dendritic arborization and pruning in gray matter in the brain (Huttenlocher, 1990) and alterations in myelination at the merging of gray and white matter tissue (Sowell, et al., 2004). Cortical surface area is related to the maintenance and division of progenitor cells (Chenn & Walsh, 2002). Grey matter volume is a function of cortical surface area and cortical thickness, which are found to be globally and regionally independent (Panizzon, et al., 2009; Winkler, et al., 2010). Both cortical thickness and surface area are related to the migration of neurons and organization of minicolumns (Rakic, 1988). Investigation of the contributions of these more specific surface-based measures of SA, CT, and gyrification can aid in understanding abnormalities in volume, adding information beyond the basic volumetric abnormalities uncovered in ASD. Such fine-grained investigation may be especially important in complex disorders like autism, where neuroanatomical abnormalities are usually subtle. Since these measures stem from different genetic and cellular mechanisms in the brain (Armstrong, et al., 1995; Panizzon, et al., 2009; Raznahan, et al., 2011), they have the potential to elucidate the underlying

causes of alterations in brain structure and the cognitive processes impacted by these abnormalities. By measuring regional volumes, cortical thickness, gyrification, and surface area, neuroanatomical investigations using MRI may be able to uncover the underlying cortical and organizational problems in the brain in ASD.

Many neuroimaging findings in ASD pertain to abnormalities within brain areas related to social information processing. Particularly, abnormalities have been found in the function and synchronization of *social brain* regions (see (Just, Keller, Malave, Kana, & Varma, 2012; Kana, Libero, & Moore, 2011; Minshew & Williams, 2007) for reviews) in those with ASD. The regions implicated in the social brain include the amygdala, fusiform gyrus, cingulate cortex, superior temporal sulcus, and temporoparietal junction (TPJ), parts of frontal cortex and premotor cortices (Adolphs, 2001; Pelphrey & Carter, 2008a, 2008b). fMRI studies in ASD have uncovered functional differences in many of the regions in this network (Bernier, Dawson, Webb, & Murias, 2007; Castelli, Frith, Happé, & Frith, 2002; Dapretto, et al., 2005; Kaiser, et al., 2010; Kana, Keller, Cherkassky, Minshew, & Just, 2009; Kana, Keller, Minshew, & Just, 2007; Kana, Libero, Hu, Deshpande, & Colburn, 2012; Luna, et al., 2002; Manjaly, et al., 2007; Martineau, Cochin, Magne, & Barthelemy, 2008; Nishitani, Avikainen, & Hari, 2004; Oberman, et al., 2005; Pelphrey, Morris, & McCarthy, 2005; Philip, et al., 2012; Ring, et al., 1999; Schulte-Rüther, Markowitsch, Fink, & Piefke, 2007; Wang, Lee, Sigman, & Dapretto, 2007; Williams, et al., 2006), in addition to disrupted functional connectivity among these regions (see (Just, et al., 2012; Kana, et al., 2011; Schipul, Keller, & Just, 2011) for reviews). Alterations in overall volume (based on VBM) in social brain regions, particularly cingulate, fusiform, amygdala, temporal, and frontal cortices (see (Cauda, et

al., 2011; Nickl-Jockschat, et al., 2012) for reviews) have been reported in studies of ASD. However, information on surface-based measures (CT, SA, gyrification, and CV) underlying volume, function and connectivity problems in ASD are still relatively uncharted. A few, if any, studies to date have examined all of these measures together in participants with ASD. Information regarding CT, SA, and gyrification could provide a comprehensive picture of the neuroanatomical differences, and potentially help explain the mechanisms driving differences in ASD. Considering impaired social interaction and communication are key symptoms of ASD, understanding the neural basis of the social behavioral dysfunction will be critical in characterizing the neuropathology of autism as well as in targeting treatments to improve alterations in the brain. To gain a better understanding of the anatomical differences in the brain in ASD, the current study examined surface-based measures of CT, SA, gyrification, and CV in children and adults with ASD. This study is novel in a few different ways: 1) it examines multiple indices of brain structure in autism; 2) it investigates a relatively large group of participants at different age groups providing information about the developmental trajectory of surface-based cortical features of ASD; and 3) it utilizes a surface-based morphometry approach to measuring brain structure features. With a relatively large number of participants and multiple measures of brain structure, the findings of this study provide valuable information about the neuroanatomy of autism in general and the structural integrity of the social brain in particular.

Method

Participants

MRI data was collected from 60 high-functioning children, adolescents, and adults with ASD and 61 typically developing (TD) peers. Data from one TD participant and four ASD participants were excluded due to motion or scanner artifacts. One additional ASD subject was excluded due to an incidental finding in his brain. The resulting fifty five particpants with ASD (49 males/6 females; mean age: 18.2 years) and 60 TD peers (55 males/5 females; mean age: 18.5 years) participated in this study (see Table 1 for demographic information). The two groups did not differ on age or IQ. Children were classified as those aged 8-18 years and adults were classified as those aged 19-40 years. The ASD group was made up of 30 children and 25 adults, while the TD group was made up of 30 children and 30 adults. IQ was assessed using the Wechsler Abbreviated Scale of Intelligence (WASI) (Wechsler, 1999), and handedness using the Edinburgh Handedness Inventory (Oldfield, 1971). To assess ASD symptom severity, adults completed the self-report Autism-Spectrum Quotient (AQ), and parents completed the AQ for children on their behalf (Auyeung, Baron-Cohen, Wheelwright, & Allison, 2008; Baron-Cohen, Wheelwright, Skinner, Martin, & Clubley, 2001). Adult participants additionally completed the Ritvo Autism Asperger Diagnostic Scale-Revised (RAADS-R) (Ritvo, et al., 2011). Participants with ASD had received a previous diagnosis of an ASD based on Autism Diagnostic Interview (ADI-R) (Lord, Rutter, & Le Couteur, 1994) symptoms, and Autism Diagnostic Observation Schedule (ADOS) (Lord, et al., 2000). TD participants were screened through a self-report history questionnaire to rule out neurological disorders, such as ASD, ADHD, or Tourette's Disorder, that could

potentially confound the results. The study was approved by the Institutional Review Board of the University of Alabama at Birmingham, and all participants (and parents/guardians, if applicable) provided informed consent for their participation in the study. Several ASD participants reported taking medications, including stimulant medication (n=12), antidepressants (n=15), anxiety medication (n=1), and antipsychotic medication (n=7). Thirty-six ASD participants reported no medications, and no TD participants reported taking medication.

MRI Data Acquisition & Analysis

MRI images were acquired using a 3T Siemens Allegra head-only scanner (Siemens Medical Inc., Erlangen, Germany) housed at the Civitan International Research Center, University of Alabama at Birmingham (UAB). Anatomical images have been acquired using high resolution T1-weighted scans using a 160 slice 3D MPRAGE volume scan with a TR = 200ms, TE = 3.34 ms, flip angle = 12, FOV = 25.6, 256 x 256 matrix size, and 1mm slice thickness. 3D volumes were visually examined by three researchers independently to confirm data quality. Five participants with significant distortion due to head motion or scanner artifact were excluded.

Structural images were analyzed using *FreeSufer* image analysis suite, which is documented and freely available (http://surfer.nmr.mgh.harvard.edu/) (Fischl, 2012; Fischl & Dale, 2000). The technical details of these procedures can be found in previous publications (Dale, Fischl, & Sereno, 1999; Dale & Sereno, 1993; Fischl & Dale, 2000; Fischl, Liu, & Dale, 2001; Fischl, Salat, et al., 2004; Fischl, Sereno, & Dale, 1999; Fischl, Sereno, Tootell, & Dale, 1999; Han, et al., 2006; Jovicich, et al., 2006; Ségonne, et al., 2004). Images underwent skull stripping using a watershed/surface deformation

procedure to remove non-brain tissue (Ségonne, et al., 2004), transformation to Talairach space, segmentation of subcortical white and gray matter structures (Fischl, et al., 2002; Fischl, van der Kouwe, et al., 2004), intensity normalization (Sled, Zijdenbos, & Evans, 1998) in order to correct for MR intensity non-uniformity mainly arising from variations in the sensitivity of the reception coil and from gradient-driven eddy currents (Sled, et al., 1998), tessellation of the gray matter/white matter boundaries, automated topology correction (Fischl, et al., 2001; Ségonne, Pacheco, & Fischl, 2007), and surface deformation following intensity gradients to optimally place the gray/white and gray/CSF borders that most accurately define the transition to the other tissue class (Dale, et al., 1999; Dale & Sereno, 1993; Fischl & Dale, 2000). Segmented images were visually inspected for acceptable segmentation. These images were then inflated and registered to a spherical atlas which separated the cortex into 66 regions of interest (Desikan, et al., 2006; Fischl, Salat, et al., 2004; Fischl, Sereno, & Dale, 1999) (See Figure 1 for included regions of interest). Segmented data were then parceled into units based on gyral and sulcal structure, resulting in values for cortical thickness, surface area, and volume (Desikan, et al., 2006; Fischl, Salat, et al., 2004). To measure local cortical gyrification, a ratio was computed between the surface of a circular region of interest on the outer surface, centered at this point, and the surface of the corresponding ROI on the pial surface (Schaer, et al., 2008). Cortical thickness measurements as implemented in FreeSurfer have been validated against manual measurements (Kuperberg, et al., 2003; Salat, et al., 2004) and histological analysis (Rosas, et al., 2002). Previous studies have found FreeSurfer morphometric procedures to have sufficient test-retest reliability across

scanner manufacturers, field strengths, and other imaging parameters (Han, et al., 2006; Jovicich, et al., 2006; Wonderlick, et al., 2009).

Groups were compared on the resulting values using ANCOVAs conducted using SPSS 22.0 software. Significant results are reported at $p < 0.05$, uncorrected. In addition, potential gender differences were assessed by comparing the six ASD female participants with six age and IQ matched ASD males. Age was used as a covariate for all between-group analyses. For cortical thickness comparisons, average hemispheric cortical thickness was used as an additional covariate and for volume comparisons, total intracranial volume (ICV) was used as an additional covariate. For regions returning significant between-group results, exploratory Pearson's correlations were computed for the relationship between the surface measures and age and AQ scores.

Results

Cortical Volume

Differences in cortical volume were found in two regions that are considered part of the social brain. Volume of the right posterior cingulate cortex was significantly increased in ASD participants ($F[2,113]=4.39$, $p=0.03$) compared to controls, as well as left TPJ ($F[2,113]=7.00$, $p=0.009$). See Figure 1 and Table 2 for results.

Cortical Thickness

Cortical thickness was significantly increased in ASD participants, relative to TD controls, in right pars orbitalis ($F[2,113]=7.07$, $p=0.009$), left superior frontal cortex ($F[2,113]=8.50$, $p=0.004$), and left TPJ ($F[2,113]=4.04$, $p=0.004$). Regions with significant reduction in cortical thickness in ASD participants, compared to TD peers,

included right rostral anterior cingulate cortex (F[2,113]=6.17, p=0.014), and right superior parietal cortex (F[2,113]=5.38, p=0.022). See Figure 1 and Table 2 for results.

Cortical Surface Area

Similar to the cortical volume results, the surface area for right posterior cingulate cortex was found to be significantly increased in ASD participants (F[2,113]=5.53, p=0.02), as well as left TPJ (F[2,113]=5.14, p=0.025). See Figure 1 and Table 2 for results.

Gyrification Index

Gyrification indices for right precentral gyrus were significantly reduced for ASD participants, compared to their TD peers (F[2,113]=5.02, p=0.027). See Figure 2 and Table 2 for results.

Gender Differences

Gender differences in the ASD brain were explored by comparing the six ASD females to six age and IQ matched ASD males. No significant differences were found between the males and females. Perhaps with a larger number of females for comparison, there would be more power to detect possible differences.

Correlation Analyses

For regions returning significant between-group results, exploratory Pearson's correlations were computed for the relationship between the surface measures and age and ASD symptoms. ASD participants showed a significant negative correlation of age with cortical thickness of the right superior parietal area (r= -0.274, p=0.04), and with the volume of the left TPJ (r= -0.46, p<0.001). For TD participants, only the latter was significant (r= -0.48, p<0.001). Significant positive correlations also emerged between

age and gyrification for right precentral gyrus for both ASD ($r=0.46$, $p<0.001$) and TD ($r=0.57$, $p<0.001$) participants. TD participants had a significant negative correlation between age and right PCC surface area ($r= -0.31$, $p=0.01$), between age and right pars orbitalis thickness ($r=0.28$, $p=0.029$), and age and right rostral ACC cortical thickness ($r=0.51$, $p<0.001$). Finally, TD participants also had a significant correlation between age and right PCC volume ($r= -0.61$, $p<0.001$). See Figures 3 & 4 and Table 3 for all of the significant correlations between age and surface-based measures for the ASD and TD groups.

As the significant finding for gyrification included the precentral gyrus, a region critical for motor functions, we conducted a post-hoc analysis to examine the relationship between precentral gyrus gyrification index and sensory motor subscale scores from the RAADS-R for adult participants. As a result, no significant correlations were found for all adult subjects ($r= -0.23$, $p=0.19$), TD adults alone ($r= -0.43$, $p=0.10$), and ASD adults alone ($r= -0.11$, $p=0.19$) between gyrification index for precentral gyrus and sensory motor symptoms.

No significant correlations were found within the ASD group for the SBM measures and autism symptom severity, measured by the AQ scores. However, a significant correlation emerged between AQ scores and age for ASD subjects ($r=-0.427$, $p=0.008$), with older participants having significantly lower symptom severity. This could be a result of improvements in behavior over time (due to treatment, maturity, etc.). However, it may also be due to the nature of reporting in the questionnaire, as parents reported the symptoms of the children in this study while adults with ASD reported on themselves. Since all participants with ASD are considered high-functioning and have

FSIQ in the average and above-average range, a significant correlation between AQ and age is unexpected. It should be noted that there is no significant difference in mean AQ scores in comparing the children with ASD to the adults with ASD ($F=1.50$, $p=0.211$). However, bias in either of the parents' view of their child's self-awareness could have skewed the scores of the AQ measure, rendering relationships between AQ and brain measures potentially unreliable.

Discussion

Overall, this study found widespread differences in the social brain in ASD, with significant alterations in cortical morphology (volume, cortical thickness, surface area, and gyrification) in children and adults with ASD, compared to their TD peers. These findings are important considering the social and behavioral symptoms that are hallmark of the autism phenotype. Below, we discuss the implications of these findings.

Alterations in Cortical Volume

Two social brain areas that showed alterations (increase) in cortical volume in ASD children and adults are the right PCC and left TPJ. Based on a meta-analyses of volumetric findings in studies of ASD, these results are in line with the consensus emerging from previous studies combined which found increased volume of the cingulate cortex (specifically PCC), as well as alterations in volume of the middle and superior temporal gyri (Cauda, et al., 2011; Duerden, Mak-Fan, Taylor, & Roberts, 2012). While previous studies have also indicated abnormal volume measurements in many other regions, our results were limited to statistically significant differences in volume in PCC and TPJ. Potential differences in methodology (e.g., VBM versus SBM) and inclusion of participants (differences in age, IQ, ASD symptom severity) may explain why other

regions were reported previously, but not found to be significant in the current study. Nonetheless, our findings are relevant considering altered functioning of PCC (Luna, et al., 2002; Pierce & Redcay, 2008) and TPJ (Kaiser, et al., 2010; Kana, et al., 2009; Kana, et al., 2012; Lombardo, Chakrabarti, Bullmore, & Baron-Cohen, 2011; Pelphrey, et al., 2005) reported widely in autism. PCC is considered as a hub in the default mode network (Fransson & Marrelec, 2008), and has shown altered functional and anatomical connectivity with frontal cortex in autism (Lynch, et al., 2013). Recent studies involving multivariate pattern classification analyses have revealed that children and adolescents with ASD could be discriminated from typically developing individuals with 92% accuracy based on gray matter in the PCC (Uddin, et al., 2011). In addition, PCC cytoarchitecture, through post mortem studies, has been considered as an important characteristic of the brains of individuals with autism (Oblak, Rosene, Kemper, Bauman, & Blatt, 2011). The temporoparietal junction, on the other hand, especially the right TPJ has been found to show a degree of functional specialization for coding mental state information (Saxe & Kanwisher, 2003; Saxe & Powell, 2006). This region has been found to show functional differences in autism in tasks of theory-of-mind (Kana, Libero, Hu, Deshpande, & Colburn, 2014; Murdaugh, Nadendla, & Kana, 2014). Thus, volumetric differences in these regions may have an impact on multiple levels of cortical organization and social functioning in autism, while reflecting inherent differences in cell structure, organization, and cortical development.

Alterations in Cortical Surface Area

Regarding cortical surface area, the current study found increased SA for right PCC, and left TPJ. Few studies have examined cortical surface area in individuals with

ASD, with rather inconsistent results. For example, one study found reduced SA for orbitofrontal cortex, PCC, inferior temporal, and SMA/premotor regions, and increased SA in TPJ, and superior parietal cortices for individuals with ASD (Ecker, et al., 2013). Another study found increased SA for frontal, temporal, and parieto-occipital regions (Hazlett, et al., 2011) in very young children with ASD compared to their peers. And yet another study reported no significant differences in SA between ASD and TD groups (Raznahan, et al., 2010). Our finding of increased SA in TPJ is consistent with a previous study by Ecker and colleagues, which found increased SA for TPJ in the ASD group (Ecker, et al., 2013). It should be noted that our findings overlap with volumetric differences we found in these same regions, providing another index of alteration in these areas. Surface area is strongly positively correlated with head size and brain size (Dickerson, et al., 2009), and is also related to the number of minicolumns in cortex (Rakic, 1988). Numerous studies have found enlargement in head size and brain size in ASD (Courchesne, Carper, & Akshoomoff, 2003; Hazlett, et al., 2005; Lainhart, et al., 1997; Redcay & Courchesne, 2005), with one study finding a significant relationship between brain overgrowth and surface area in young children with ASD (Hazlett, et al., 2011). In addition, previous studies have found an increased number of minicolumns in ASD (Casanova, Buxhoeveden, Switala, & Roy, 2002; Casanova, et al., 2006). Alterations in SA in ASD may be explained by abnormal minicolumn counts, or overall differences in brain size. However, few studies have examined the biological underpinnings of SA and its link to brain function. Future studies should examine this avenue in ASD.

Alterations in Cortical Thickness

Our findings of increased cortical thickness in pars orbitalis/IFG and superior frontal cortex are in line with previous studies of ASD (Ecker, et al., 2013; Hyde, Samson, Evans, & Mottron, 2010; Mak-Fan, Taylor, Roberts, & Lerch, 2012), as well as our finding of increased cortical thickness for the TPJ (Chung, et al., 2005; Ecker, et al., 2013), while past studies have also reported reduced cortical thickness in ACC (Hadjikhani, Joseph, Snyder, & Tager-Flusberg, 2006), and superior parietal lobule (Hadjikhani, et al., 2006). Overall cortical thickness is impacted by proliferation of myelin, a reduction in the size or number of neurons, and changes in synaptic processes (Sowell, et al., 2003; Sowell, et al., 2004). Cortical thickness also reflects the size and density of cells (Narr, et al., 2005; Parent & Carpenter, 1995), including the number of cells present in minicolumns (Rakic, 1988). Thus, alterations in CT in children and adults with ASD may reflect abnormality in underlying cell counts and organization. Indeed, abnormalities in the number and density of minicolumns have been reported in ASD postmortem samples (Casanova, Buxhoeveden, Switala, et al., 2002; Casanova, et al., 2006). In addition, studies examining correlations in cortical thickness between brain regions have suggested that such correlations may be related to the function of the participating networks and underlying white matter connectivity (He, Chen, & Evans, 2007; Lerch, et al., 2006; Worsley, Chen, Lerch, & Evans, 2005). Alterations in CT in one brain region could then potentially impact connectivity with other brain regions and the ultimate functioning of those networks. Considering disrupted connectivity has been suggested as an explanation for ASD (Just, et al., 2012; Kana, et al., 2011; Maximo, Cadena, & Kana, 2014; Schipul, et al., 2011), and significant reductions in white matter

integrity have been found in the disorder (see (Travers, et al., 2012) for a review), alterations in CT in ASD should be examined further for their possible role in affecting brain function and connectivity in ASD.

Alterations in Gyrification

Finally, reduced gyrification has been found previously in inferior parietal, precentral, IFG, and parieto-occipital cortices (Schaer, et al., 2013), with increased gyrification in occipital and precuneus (Wallace, et al., 2013), parietal lobule (Kates, Ikuta, & Burnette, 2009), and frontal cortices (A. Hardan, Muddasani, Vemulapalli, Keshavan, & Minshew, 2006; Jou, Minshew, Keshavan, & Hardan, 2010). Our finding of reduced gyrification index in precentral gyrus in ASD is in line with a previous study (Schaer, et al., 2013), and underscores potential alterations in the structure and organization of gyri and sulci in the brain in ASD (Levitt, et al., 2003). Cortical folding is a developmental process related to myelination, synaptogenesis, pruning, and tension of axons (Casey, Tottenham, Liston, & Durston, 2005; Su, White, Schmidt, Kao, & Sapiro, 2013; Van Essen, 1997; White, Su, Schmidt, Kao, & Sapiro, 2010), which begins in the fetal brain and continues into childhood (Mangin, Jouvent, & Cachia, 2010; White, et al., 2010; Zilles, et al., 1988). The development of gyrus and sulcus in the brain promotes cortical organization and more efficient connectivity and overall brain functioning (White, et al., 2010). Previous studies have found abnormality in gyrification (A. Y. Hardan, et al., 2004; Jou, et al., 2010; Kates, et al., 2009; Schaer, et al., 2013; Wallace, et al., 2013) and sulcal maps (Auzias, et al., 2014; Levitt, et al., 2003; Nordahl, et al., 2007) in participants with ASD. Coupled with our findings, there is ample evidence to suggest significant alterations in cortical folding exist in the ASD brain. Considering the cellular

processes underlying the development of sulci and gyri (e.g., myelination, axonal connectivity, etc.), altered gyrification in ASD points to abnormal brain development at a cellular level as a potential explanation for altered organization of landmark cortical features.

Conclusions on Surface-Based Abnormalities in ASD

That our findings of surface-based alterations in ASD are not focal, but spread across a number of regions in the brain, may also speak to the functional and behavioral abnormalities that have been seen in autism, particularly given that the regions we found to be affected in the current study are all regions relevant for social cognition. Functional brain imaging studies in ASD have noted abnormalities in the function of many regions within the social brain network, including TPJ (Castelli, et al., 2002; Kaiser, et al., 2010; Kana, et al., 2009; Kana, et al., 2012; Pelphrey, et al., 2005), IFG (Bernier, et al., 2007; Dapretto, et al., 2005; Martineau, et al., 2008; Nishitani, et al., 2004; Oberman, et al., 2005; Philip, et al., 2012; Williams, et al., 2006), superior frontal (Philip, et al., 2012), and cingulate/MPFC (Castelli, et al., 2002; Kana, et al., 2009; Kana, et al., 2007; Luna, et al., 2002; Manjaly, et al., 2007; Pelphrey, et al., 2005; Ring, et al., 1999; Schulte-Rüther, et al., 2007; Wang, et al., 2007). In addition, disrupted connectivity among these regions has been implicated in the functional alterations seen in ASD (see (Just, et al., 2012; Kana, et al., 2011; Schipul, et al., 2011) for reviews). As social cognition involves integrated functioning of these brain areas to achieve complex social understanding (Adolphs, 2001), alterations in the shape, volume, organization, and surface features of these regions may affect the functional integrity of these regions by themselves and their functioning as a network.

While one may expect the differences in surface measures to be related to one another (i.e., a difference in cortical volume is accompanied by overlapping differences in CT/SA/gyrification), for the most part we did not find this to be the case. A previous study of surface-based morphometry in ASD found that differences in SA and CT were mostly non-overlapping, and that SA and CT contribute to cortical volume uniquely (Ecker, et al., 2013). This study found that SA contributed to the differences in volume in ASD more than CT. In our study, SA was found to be relevant to the volumetric differences in both PCC and TPJ. However, CT also contributed to the TPJ difference. We also found our gyrification results were not related to uniform differences in CT, SA, or volume. We found reduced gyrification in the right precentral gyrus in ASD, with no overlapping differences in volume, SA, or cortical thickness for that region. This implies that differences in volume and organization of surface-based features of brain structures in ASD are not uniform, and may not arise from a single neural mechanism. For example, alterations in either the formation or the size of a gyrus may be arising from a source that is unrelated to the overall volume or thickness of that gyrus. Indeed, it is likely that cortical folding (and formation of gyri) is related to the tension of axons within white matter, and that cortical folding impacts the migration of neurons (Hilgetag & Barbas, 2005, 2006; Van Essen, 1997). As widespread abnormalities in the integrity of white matter have been found in ASD (Travers, et al., 2012), it is of no surprise that abnormal gyrification may arise. One study even found a link between reduced gyral window size and corpus callosum size in ASD (Casanova, et al., 2009). In addition, differences in CT and SA may arise from their relationship with cellular organization and migration. For example, we see columnar organization of cortex (Mountcastle, 1997), with a relationship

between CT and SA and the number of cells within cellular minicolumns as well as the overall number of minicolumns (Rakic, 1988). In ASD, more numerous minicolumns, that are also smaller and less compact compared to TD individuals, within middle temporal, superior and middle frontal, and temporoparietal cortices have been found (Casanova, Buxhoeveden, & Brown, 2002; Casanova, Buxhoeveden, Switala, et al., 2002; Casanova, et al., 2006), holding implications for the alterations seen in SA and CT.

CT and SA have also been found to be determined by different genetic factors (Panizzon, et al., 2009), and also develop along varied trajectories (Armstrong, et al., 1995; Raznahan, et al., 2011). Further, neuronal migration and survival are impacted by varying environmental and genetic factors (Evrard, Marret, & Gressens, 1997; Métin, Vallee, Rakic, & Bhide, 2008; Rakic, 2007; Rakic, Hashimoto-Torii, & Sarkisian, 2007). Surface-based features of the cortex (volume, SA, CT, gyrification) have different genetic, environmental, and cellular determinants, which may have huge implications for a disorder like ASD. Differences in volume and organization of the cortical surface-based features in ASD are unlikely to emerge from alterations of a single neural mechanism. Instead, various factors acting in combination may result in widespread cellular and neuroanatomical abnormalities that have been seen in the disorder. Finally, that many different mechanisms are at play in the brain that are being impacted by varying genetic and environmental factors, may be a true reflection of the complexity and heterogeneity of ASD. Such widespread differences may produce varied effects on cell migration, minicolumn density and number, and axonal integrity, ultimately producing deviant surface features which in turn result in different presentations of behavioral symptoms.

The current study did not find any significant correlations between the surface measures and symptom severity for the ASD group. However, correlations between surface measures and age uncovered differences in the development of various regions over time. Developmentally, peaks in cortical volume are seen around late adolescence, followed by reduction and stabilization in adulthood (Raznahan, et al., 2011). Indeed, the age-related relationships of right PCC and left TPJ volume were negative for TD participants, suggesting a decline in the cortical volume of those regions from children to adult participants in our study. We also found a significant negative correlation between right PCC surface area and age in TD participants, but also a number of positive correlations with age for the TD group related to cortical thickness and gyrification. The ASD participants also had a significant negative relationship between age and volume and cortical thickness measures, as well as a significant positive correlation between age and gyrification. A previous meta-analysis of regional brain volumes in ASD (Nickl-Jockschat, et al., 2012), as well as a previous study investigating CT, SA, and volume in ASD (Raznahan, et al., 2010), both uncovered altered developmental patterns, indicating desynchronization of brain volume growth and degeneration between affected brain structures and the rest of the brain. These cortical changes with age in ASD indicate that there is a complex neurodevelopmental trajectory of the disorder, with altered maturation patterns in ASD persisting through childhood and into adulthood.

Summary

The current study is novel as it is, to date, the only one to our knowledge, to examine the differences in the neuroanatomy of ASD by including analysis of all four surface-based measures (cortical volume, surface area, cortical thickness, and

gyrification). Our study also includes a relatively large sample size, compared to existing studies. A previous study estimated 50 subjects per group are required to detect a 0.25mm cortical thickness difference between groups (Pardoe, Abbott, & Jackson, 2012). Of about a dozen previously published papers utilizing surface-based morphometry in ASD, only two have reported findings that include 50 or more participants in each group (Ecker, et al., 2013; Raznahan, et al., 2010). The findings of our study are vital in revealing the importance of the alterations in the social brain anatomy in ASD.

One limitation of the current study is the application of an automated cortical segmentation technique and the resulting ability to accurately detect alterations in cortical features of ASD. A few histological studies of ASD have reported abnormal cellular patterning, specifically finding a less distinct boundary between gray and white matter in samples from ASD brains (Avino & Hutsler, 2010; Hutsler, Love, & Zhang, 2007). Alterations in laminar boundaries could impact measurements of surface-based features (such as CT, volume, and gyrification), causing comparisons with control groups to become less accurate. However, cortical thickness measures from Freesurfer software have been validated previously in typical and patient populations using histology and manual measures for comparison (Fischl, 2012; Kuperberg, et al., 2003; Rosas, et al., 2002). It is not clear whether the resolution of MRI would be able to register an alteration that is visible at the cellular level, or whether Freesurfer would be inaccurate when tracing boundaries between gray and white matter as a result of the abnormal cellular patterning in ASD cortex. Future studies should examine the potential impact of a less distinct gray/white matter boundary on MRI measures of cortical thickness and volume in ASD, and whether the cellular irregularity is related to alterations in surface features of

ASD. In addition, results reported in the current study were not corrected for multiple comparisons. However, between-group comparisons were made using mean values for each subject for predefined ROIs, reducing the total number of comparisons. In addition, total ICV and average cortical thickness were used as covariates when comparing volume and cortical thickness between groups, which is a slightly more conservative approach than using no correction at all.

In conclusion, we found differences in cortical thickness, volume, surface area, and gyrification across the social brain in children and adults with ASD. In addition, we found several developmental differences with age and surface-based measures for the affected brain regions. Together, these findings represent widespread alterations in brain structure in ASD, potentially underscoring the social abnormalities that are hallmark to the disorder.

Acknowledgments

This study was supported by funding from the UAB Department of Psychology.

References

Adolphs, R. (2001). The neurobiology of social cognition. *Current opinion in neurobiology, 11*, 231-239.

Amaral, D. G., Schumann, C. M., & Nordahl, C. W. (2008). Neuroanatomy of autism. *Trends in neurosciences, 31*, 137-145.

Armstrong, E., Schleicher, A., Omran, H., Curtis, M., & Zilles, K. (1995). The ontogeny of human gyrification. *Cerebral Cortex, 5*, 56-63.

Auyeung, B., Baron-Cohen, S., Wheelwright, S., & Allison, C. (2008). The autism spectrum quotient: Children's version (AQ-Child). *Journal of autism and developmental disorders, 38*, 1230-1240.

Auzias, G., Viellard, M., Takerkart, S., Villeneuve, N., Poinso, F., Da Fonséca, D., Girard, N., & Deruelle, C. (2014). Atypical sulcal anatomy in young children with autism spectrum disorder. *NeuroImage: Clinical*.

Avino, T. A., & Hutsler, J. J. (2010). Abnormal cell patterning at the cortical gray–white matter boundary in autism spectrum disorders. *Brain research, 1360*, 138-146.

Baron-Cohen, S., Wheelwright, S., Skinner, R., Martin, J., & Clubley, E. (2001). The autism-spectrum quotient (AQ): Evidence from asperger syndrome/high-functioning autism, malesand females, scientists and mathematicians. *Journal of autism and developmental disorders, 31*, 5-17.

Bernier, R., Dawson, G., Webb, S., & Murias, M. (2007). EEG mu rhythm and imitation impairments in individuals with autism spectrum disorder. *Brain and cognition, 64*, 228-237.

Bookstein, F. L. (2001). "Voxel-based morphometry" should not be used with imperfectly registered images. *Neuroimage, 14*, 1454-1462.

Brambilla, P., Hardan, A., di Nemi, S. U., Perez, J., Soares, J. C., & Barale, F. (2003). Brain anatomy and development in autism: review of structural MRI studies. *Brain research bulletin, 61*, 557-569.

Casanova, M. F., Buxhoeveden, D. P., & Brown, C. (2002). Clinical and macroscopic correlates of minicolumnar pathology in autism. *Journal of Child Neurology, 17*, 692-695.

Casanova, M. F., Buxhoeveden, D. P., Switala, A. E., & Roy, E. (2002). Minicolumnar pathology in autism. *Neurology, 58*, 428-432.

Casanova, M. F., El-Baz, A., Mott, M., Mannheim, G., Hassan, H., Fahmi, R., Giedd, J., Rumsey, J. M., Switala, A. E., & Farag, A. (2009). Reduced gyral window and corpus callosum size in autism: possible macroscopic correlates of a minicolumnopathy. *Journal of autism and developmental disorders, 39*, 751-764.

Casanova, M. F., van Kooten, I. A., Switala, A. E., van Engeland, H., Heinsen, H., Steinbusch, H. W., Hof, P. R., Trippe, J., Stone, J., & Schmitz, C. (2006). Minicolumnar abnormalities in autism. *Acta neuropathologica, 112*, 287-303.

Casey, B., Tottenham, N., Liston, C., & Durston, S. (2005). Imaging the developing brain: what have we learned about cognitive development? *Trends in cognitive sciences, 9*, 104-110.

Castelli, F., Frith, C., Happé, F., & Frith, U. (2002). Autism, Asperger syndrome and brain mechanisms for the attribution of mental states to animated shapes. *Brain, 125*, 1839-1849.

Cauda, F., Geda, E., Sacco, K., D'Agata, F., Duca, S., Geminiani, G., & Keller, R. (2011). Grey matter abnormality in autism spectrum disorder: an activation likelihood estimation meta-analysis study. *Journal of Neurology, Neurosurgery & Psychiatry, 82*, 1304-1313.

Chen, R., Jiao, Y., & Herskovits, E. H. (2011). Structural MRI in autism spectrum disorder. *Pediatric research, 69*, 63R-68R.

Chenn, A., & Walsh, C. A. (2002). Regulation of cerebral cortical size by control of cell cycle exit in neural precursors. *Science, 297*, 365-369.

Chung, M. K., Robbins, S. M., Dalton, K. M., Davidson, R. J., Alexander, A. L., & Evans, A. C. (2005). Cortical thickness analysis in autism with heat kernel smoothing. *NeuroImage, 25*, 1256-1265.

Courchesne, E., Campbell, K., & Solso, S. (2011). Brain growth across the life span in autism: age-specific changes in anatomical pathology. *Brain research, 1380*, 138-145.

Courchesne, E., Carper, R., & Akshoomoff, N. (2003). Evidence of brain overgrowth in the first year of life in autism. *Jama, 290*, 337-344.

Courchesne, E., Karns, C., Davis, H., Ziccardi, R., Carper, R., Tigue, Z., Chisum, H., Moses, P., Pierce, K., & Lord, C. (2001). Unusual brain growth patterns in early life in patients with autistic disorder an MRI study. *Neurology, 57*, 245-254.

Dale, A. M., Fischl, B., & Sereno, M. I. (1999). Cortical surface-based analysis: I. Segmentation and surface reconstruction. *Neuroimage, 9*, 179-194.

Dale, A. M., & Sereno, M. I. (1993). Improved localizadon of cortical activity by combining eeg and meg with mri cortical surface reconstruction: A linear approach. *Journal of cognitive neuroscience, 5*, 162-176.

Dapretto, M., Davies, M. S., Pfeifer, J. H., Scott, A. A., Sigman, M., Bookheimer, S. Y., & Iacoboni, M. (2005). Understanding emotions in others: mirror neuron dysfunction in children with autism spectrum disorders. *Nature neuroscience, 9*, 28-30.

Davatzikos, C. (2004). Why voxel-based morphometric analysis should be used with great caution when characterizing group differences. *Neuroimage, 23*, 17-20.

Dawson, G., Munson, J., Webb, S. J., Nalty, T., Abbott, R., & Toth, K. (2007). Rate of head growth decelerates and symptoms worsen in the second year of life in autism. *Biological psychiatry, 61*, 458-464.

Desikan, R. S., Ségonne, F., Fischl, B., Quinn, B. T., Dickerson, B. C., Blacker, D., Buckner, R. L., Dale, A. M., Maguire, R. P., & Hyman, B. T. (2006). An automated labeling system for subdividing the human cerebral cortex on MRI scans into gyral based regions of interest. *Neuroimage, 31*, 968-980.

Dickerson, B. C., Feczko, E., Augustinack, J. C., Pacheco, J., Morris, J. C., Fischl, B., & Buckner, R. L. (2009). Differential effects of aging and Alzheimer's disease on medial temporal lobe cortical thickness and surface area. *Neurobiology of aging, 30*, 432-440.

Duerden, E. G., Mak-Fan, K. M., Taylor, M. J., & Roberts, S. W. (2012). Regional differences in grey and white matter in children and adults with autism spectrum disorders: an activation likelihood estimate (ALE) meta-analysis. *Autism Research, 5*, 49-66.

Ecker, C., Ginestet, C., Feng, Y., Johnston, P., Lombardo, M. V., Lai, M.-C., Suckling, J., Palaniyappan, L., Daly, E., & Murphy, C. M. (2013). Brain surface anatomy in adults with autism: the relationship between surface area, cortical thickness, and autistic symptoms. *JAMA psychiatry, 70*, 59-70.

Elder, L. M., Dawson, G., Toth, K., Fein, D., & Munson, J. (2008). Head circumference as an early predictor of autism symptoms in younger siblings of children with autism spectrum disorder. *Journal of autism and developmental disorders, 38*, 1104-1111.

Evrard, P., Marret, S., & Gressens, P. (1997). Environmental and genetic determinants of neural migration and postmigratory survival*. *Acta Paediatrica, 86*, 20-26.

Fischl, B. (2012). FreeSurfer. *Neuroimage, 62*, 774-781.

Fischl, B., & Dale, A. M. (2000). Measuring the thickness of the human cerebral cortex from magnetic resonance images. *Proceedings of the National Academy of Sciences, 97*, 11050-11055.

Fischl, B., Liu, A., & Dale, A. M. (2001). Automated manifold surgery: constructing geometrically accurate and topologically correct models of the human cerebral cortex. *Medical Imaging, IEEE Transactions on, 20*, 70-80.

Fischl, B., Salat, D. H., Busa, E., Albert, M., Dieterich, M., Haselgrove, C., van der Kouwe, A., Killiany, R., Kennedy, D., & Klaveness, S. (2002). Whole brain segmentation: automated labeling of neuroanatomical structures in the human brain. *Neuron, 33*, 341-355.

Fischl, B., Salat, D. H., van der Kouwe, A. J., Makris, N., Ségonne, F., Quinn, B. T., & Dale, A. M. (2004). Sequence-independent segmentation of magnetic resonance images. *Neuroimage, 23*, S69-S84.

Fischl, B., Sereno, M. I., & Dale, A. M. (1999). Cortical surface-based analysis: II: Inflation, flattening, and a surface-based coordinate system. *Neuroimage, 9*, 195-207.

Fischl, B., Sereno, M. I., Tootell, R. B., & Dale, A. M. (1999). High-resolution intersubject averaging and a coordinate system for the cortical surface. *Human brain mapping, 8*, 272-284.

Fischl, B., van der Kouwe, A., Destrieux, C., Halgren, E., Ségonne, F., Salat, D. H., Busa, E., Seidman, L. J., Goldstein, J., & Kennedy, D. (2004). Automatically parcellating the human cerebral cortex. *Cerebral cortex, 14*, 11-22.

Fransson, P., & Marrelec, G. (2008). The precuneus/posterior cingulate cortex plays a pivotal role in the default mode network: Evidence from a partial correlation network analysis. *NeuroImage, 42*, 1178-1184.

Ghosh, S. S., Kakunoori, S., Augustinack, J., Nieto-Castanon, A., Kovelman, I., Gaab, N., Christodoulou, J. A., Triantafyllou, C., Gabrieli, J. D., & Fischl, B. (2010). Evaluating the validity of volume-based and surface-based brain image registration for developmental cognitive neuroscience studies in children 4 to 11years of age. *Neuroimage, 53*, 85-93.

Hadjikhani, N., Joseph, R. M., Snyder, J., & Tager-Flusberg, H. (2006). Anatomical differences in the mirror neuron system and social cognition network in autism. *Cerebral Cortex, 16*, 1276-1282.

Han, X., Jovicich, J., Salat, D., van der Kouwe, A., Quinn, B., Czanner, S., Busa, E., Pacheco, J., Albert, M., & Killiany, R. (2006). Reliability of MRI-derived

measurements of human cerebral cortical thickness: the effects of field strength, scanner upgrade and manufacturer. *Neuroimage, 32*, 180-194.
Hardan, A., Muddasani, S., Vemulapalli, M., Keshavan, M., & Minshew, N. (2006). An MRI study of increased cortical thickness in autism. *American Journal of Psychiatry, 163*, 1290-1292.
Hardan, A. Y., Jou, R. J., Keshavan, M. S., Varma, R., & Minshew, N. J. (2004). Increased frontal cortical folding in autism: a preliminary MRI study. *Psychiatry Research: Neuroimaging, 131*, 263-268.
Hazlett, H. C., Poe, M., Gerig, G., Smith, R. G., Provenzale, J., Ross, A., Gilmore, J., & Piven, J. (2005). Magnetic resonance imaging and head circumference study of brain size in autism: birth through age 2 years. *Archives of general psychiatry, 62*, 1366-1376.
Hazlett, H. C., Poe, M. D., Gerig, G., Styner, M., Chappell, C., Smith, R. G., Vachet, C., & Piven, J. (2011). Early brain overgrowth in autism associated with an increase in cortical surface area before age 2 years. *Archives of general psychiatry, 68*, 467-476.
He, Y., Chen, Z. J., & Evans, A. C. (2007). Small-World Anatomical Networks in the Human Brain Revealed by Cortical Thickness from MRI. *Cerebral Cortex, 17*, 2407-2419.
Hilgetag, C. C., & Barbas, H. (2005). Developmental mechanics of the primate cerebral cortex. *Anatomy and embryology, 210*, 411-417.
Hilgetag, C. C., & Barbas, H. (2006). Role of mechanical factors in the morphology of the primate cerebral cortex. *PLoS computational biology, 2*, e22.
Hutsler, J. J., Love, T., & Zhang, H. (2007). Histological and magnetic resonance imaging assessment of cortical layering and thickness in autism spectrum disorders. *Biological psychiatry, 61*, 449-457.
Huttenlocher, P. R. (1990). Morphometric study of human cerebral cortex development. *Neuropsychologia, 28*, 517-527.
Hyde, K. L., Samson, F., Evans, A. C., & Mottron, L. (2010). Neuroanatomical differences in brain areas implicated in perceptual and other core features of autism revealed by cortical thickness analysis and voxel-based morphometry. *Human brain mapping, 31*, 556-566.
Jou, R. J., Minshew, N. J., Keshavan, M. S., & Hardan, A. Y. (2010). Cortical gyrification in autistic and Asperger disorders: a preliminary magnetic resonance imaging study. *Journal of child neurology, 25*, 1462-1467.
Jovicich, J., Czanner, S., Greve, D., Haley, E., van der Kouwe, A., Gollub, R., Kennedy, D., Schmitt, F., Brown, G., & MacFall, J. (2006). Reliability in multi-site structural MRI studies: effects of gradient non-linearity correction on phantom and human data. *Neuroimage, 30*, 436-443.
Just, M. A., Keller, T. A., Malave, V. L., Kana, R. K., & Varma, S. (2012). Autism as a neural systems disorder: a theory of frontal-posterior underconnectivity. *Neuroscience & Biobehavioral Reviews, 36*, 1292-1313.
Kaiser, M. D., Hudac, C. M., Shultz, S., Lee, S. M., Cheung, C., Berken, A. M., Deen, B., Pitskel, N. B., Sugrue, D. R., & Voos, A. C. (2010). Neural signatures of autism. *Proceedings of the National Academy of Sciences, 107*, 21223-21228.

Kana, R. K., Keller, T. A., Cherkassky, V. L., Minshew, N. J., & Just, M. A. (2009). Atypical frontal-posterior synchronization of Theory of Mind regions in autism during mental state attribution. *Social Neuroscience, 4*, 135-152.

Kana, R. K., Keller, T. A., Minshew, N. J., & Just, M. A. (2007). Inhibitory control in high-functioning autism: decreased activation and underconnectivity in inhibition networks. *Biological psychiatry, 62*, 198-206.

Kana, R. K., Libero, L. E., Hu, C. P., Deshpande, H. D., & Colburn, J. S. (2012). Functional Brain Networks and White Matter Underlying Theory-of-Mind in Autism. *Social Cognitive and Affective Neuroscience*.

Kana, R. K., Libero, L. E., Hu, C. P., Deshpande, H. D., & Colburn, J. S. (2014). Functional brain networks and white matter underlying theory-of-mind in autism. *Social cognitive and affective neuroscience, 9*, 98-105.

Kana, R. K., Libero, L. E., & Moore, M. S. (2011). Disrupted cortical connectivity theory as an explanatory model for autism spectrum disorders. *Physics of life reviews, 8*, 410-437.

Kates, W. R., Ikuta, I., & Burnette, C. P. (2009). Gyrification patterns in monozygotic twin pairs varying in discordance for autism. *Autism Research, 2*, 267-278.

Kuperberg, G. R., Broome, M. R., McGuire, P. K., David, A. S., Eddy, M., Ozawa, F., Goff, D., West, W. C., Williams, S. C., & van der Kouwe, A. J. (2003). Regionally localized thinning of the cerebral cortex in schizophrenia. *Archives of general psychiatry, 60*, 878-888.

Lainhart, J. E., Piven, J., Wzorek, M., Landa, R., Santangelo, S. L., Coon, H., & Folstein, S. E. (1997). Macrocephaly in children and adults with autism. *Journal of the American Academy of Child & Adolescent Psychiatry, 36*, 282-290.

Lerch, J. P., Worsley, K., Shaw, W. P., Greenstein, D. K., Lenroot, R. K., Giedd, J., & Evans, A. C. (2006). Mapping anatomical correlations across cerebral cortex (MACACC) using cortical thickness from MRI. *Neuroimage, 31*, 993-1003.

Levitt, J. G., Blanton, R. E., Smalley, S., Thompson, P., Guthrie, D., McCracken, J. T., Sadoun, T., Heinichen, L., & Toga, A. W. (2003). Cortical sulcal maps in autism. *Cerebral Cortex, 13*, 728-735.

Lombardo, M. V., Chakrabarti, B., Bullmore, E. T., & Baron-Cohen, S. (2011). Specialization of right temporo-parietal junction for mentalizing and its relation to social impairments in autism. *Neuroimage, 56*, 1832-1838.

Lord, C., Risi, S., Lambrecht, L., Cook Jr, E. H., Leventhal, B. L., DiLavore, P. C., Pickles, A., & Rutter, M. (2000). The Autism Diagnostic Observation Schedule—Generic: A standard measure of social and communication deficits associated with the spectrum of autism. *Journal of autism and developmental disorders, 30*, 205-223.

Lord, C., Rutter, M., & Le Couteur, A. (1994). Autism Diagnostic Interview-Revised: a revised version of a diagnostic interview for caregivers of individuals with possible pervasive developmental disorders. *Journal of autism and developmental disorders, 24*, 659-685.

Luna, B., Minshew, N., Garver, K., Lazar, N., Thulborn, K., Eddy, W., & Sweeney, J. (2002). Neocortical system abnormalities in autism An fMRI study of spatial working memory. *Neurology, 59*, 834-840.

Lynch, C. J., Uddin, L. Q., Supekar, K., Khouzam, A., Phillips, J., & Menon, V. (2013). Default mode network in childhood autism: posteromedial cortex heterogeneity and relationship with social deficits. *Biological psychiatry, 74*, 212-219.

Mak-Fan, K. M., Taylor, M. J., Roberts, W., & Lerch, J. P. (2012). Measures of cortical grey matter structure and development in children with autism spectrum disorder. *Journal of autism and developmental disorders, 42*, 419-427.

Mangin, J.-F., Jouvent, E., & Cachia, A. (2010). In-vivo measurement of cortical morphology: means and meanings. *Current opinion in neurology, 23*, 359-367.

Manjaly, Z. M., Bruning, N., Neufang, S., Stephan, K. E., Brieber, S., Marshall, J. C., Kamp-Becker, I., Remschmidt, H., Herpertz-Dahlmann, B., & Konrad, K. (2007). Neurophysiological correlates of relatively enhanced local visual search in autistic adolescents. *Neuroimage, 35*, 283-291.

Martineau, J., Cochin, S., Magne, R., & Barthelemy, C. (2008). Impaired cortical activation in autistic children: is the mirror neuron system involved? *International journal of psychophysiology, 68*, 35-40.

Maximo, J. O., Cadena, E. J., & Kana, R. K. (2014). The Implications of Brain Connectivity in the Neuropsychology of Autism. *Neuropsychology review, 24*, 16-31.

McAlonan, G. M., Daly, E., Kumari, V., Critchley, H. D., van Amelsvoort, T., Suckling, J., Simmons, A., Sigmundsson, T., Greenwood, K., & Russell, A. (2002). Brain anatomy and sensorimotor gating in Asperger's syndrome. *Brain, 125*, 1594-1606.

Métin, C., Vallee, R. B., Rakic, P., & Bhide, P. G. (2008). Modes and mishaps of neuronal migration in the mammalian brain. *The Journal of Neuroscience, 28*, 11746-11752.

Minshew, N. J., & Williams, D. L. (2007). The new neurobiology of autism: cortex, connectivity, and neuronal organization. *Archives of neurology, 64*, 945.

Mountcastle, V. B. (1997). The columnar organization of the neocortex. *Brain, 120*, 701-722.

Murdaugh, D. L., Nadendla, K. D., & Kana, R. K. (2014). Differential role of temporoparietal junction and medial prefrontal cortex in causal inference in autism: An independent component analysis. *Neuroscience letters, 568*, 50-55.

Narr, K. L., Bilder, R. M., Toga, A. W., Woods, R. P., Rex, D. E., Szeszko, P. R., Robinson, D., Sevy, S., Gunduz-Bruce, H., & Wang, Y.-P. (2005). Mapping cortical thickness and gray matter concentration in first episode schizophrenia. *Cerebral Cortex, 15*, 708-719.

Nickl-Jockschat, T., Habel, U., Maria Michel, T., Manning, J., Laird, A. R., Fox, P. T., Schneider, F., & Eickhoff, S. B. (2012). Brain structure anomalies in autism spectrum disorder—a meta-analysis of VBM studies using anatomic likelihood estimation. *Human brain mapping, 33*, 1470-1489.

Nishitani, N., Avikainen, S., & Hari, R. (2004). Abnormal imitation-related cortical activation sequences in Asperger's syndrome. *Annals of neurology, 55*, 558-562.

Nordahl, C. W., Dierker, D., Mostafavi, I., Schumann, C. M., Rivera, S. M., Amaral, D. G., & Van Essen, D. C. (2007). Cortical folding abnormalities in autism revealed by surface-based morphometry. *The Journal of Neuroscience, 27*, 11725-11735.

Oberman, L. M., Hubbard, E. M., McCleery, J. P., Altschuler, E. L., Ramachandran, V. S., & Pineda, J. A. (2005). EEG evidence for mirror neuron dysfunction in autism spectrum disorders. *Cognitive Brain Research, 24*, 190-198.

Oblak, A. L., Rosene, D. L., Kemper, T. L., Bauman, M. L., & Blatt, G. J. (2011). Altered posterior cingulate cortical cyctoarchitecture, but normal density of neurons and interneurons in the posterior cingulate cortex and fusiform gyrus in autism. *Autism Research, 4*, 200-211.

Oldfield, R. C. (1971). The assessment and analysis of handedness: the Edinburgh inventory. *Neuropsychologia, 9*, 97-113.

Panizzon, M. S., Fennema-Notestine, C., Eyler, L. T., Jernigan, T. L., Prom-Wormley, E., Neale, M., Jacobson, K., Lyons, M. J., Grant, M. D., & Franz, C. E. (2009). Distinct genetic influences on cortical surface area and cortical thickness. *Cerebral Cortex, 19*, 2728-2735.

Pardoe, H. R., Abbott, D. F., & Jackson, G. D. (2012). Sample size estimates for well-powered cross-sectional cortical thickness studies. *Human brain mapping*.

Parent, A., & Carpenter, M. B. (1995). *Human neuroanatomy*: Williams & Wilkins Baltimore, MD:.

Pelphrey, K. A., & Carter, E. J. (2008a). Brain mechanisms for social perception. *Annals of the New York Academy of Sciences, 1145*, 283-299.

Pelphrey, K. A., & Carter, E. J. (2008b). Charting the typical and atypical development of the social brain. *Development and psychopathology, 20*, 1081-1102.

Pelphrey, K. A., Morris, J. P., & McCarthy, G. (2005). Neural basis of eye gaze processing deficits in autism. *Brain, 128*, 1038-1048.

Philip, R., Dauvermann, M. R., Whalley, H. C., Baynham, K., Lawrie, S. M., & Stanfield, A. C. (2012). A systematic review and meta-analysis of the fMRI investigation of autism spectrum disorders. *Neuroscience & Biobehavioral Reviews, 36*, 901-942.

Pierce, K., & Redcay, E. (2008). Fusiform function in children with an autism spectrum disorder is a matter of "who". *Biological psychiatry, 64*, 552-560.

Piven, J., Arndt, S., Bailey, J., Havercamp, S., Andreasen, N. C., & Palmer, P. (1995). An MRI study of brain size in autism. *American Journal of Psychiatry, 152*, 1145-1149.

Rakic, P. (1988). Specification of cerebral cortical areas. *Science, 241*, 170-176.

Rakic, P. (2007). The radial edifice of cortical architecture: from neuronal silhouettes to genetic engineering. *Brain research reviews, 55*, 204-219.

Rakic, P., Hashimoto-Torii, K., & Sarkisian, M. R. (2007). Genetic determinants of neuronal migration in the cerebral cortex. In *Cortical Development: Genes and Genetic Abnormalities: Novartis Foundation Symposium 288* (pp. 45-58): John Wiley & Sons, Ltd.

Raznahan, A., Shaw, P., Lalonde, F., Stockman, M., Wallace, G. L., Greenstein, D., Clasen, L., Gogtay, N., & Giedd, J. N. (2011). How does your cortex grow? *The Journal of Neuroscience, 31*, 7174-7177.

Raznahan, A., Toro, R., Daly, E., Robertson, D., Murphy, C., Deeley, Q., Bolton, P. F., Paus, T., & Murphy, D. G. (2010). Cortical anatomy in autism spectrum disorder: an in vivo MRI study on the effect of age. *Cerebral Cortex, 20*, 1332-1340.

Redcay, E., & Courchesne, E. (2005). When is the brain enlarged in autism? A meta-analysis of all brain size reports. *Biol Psychiatry, 58*, 1-9.

Ring, H. A., Baron-Cohen, S., Wheelwright, S., Williams, S. C., Brammer, M., Andrew, C., & Bullmore, E. T. (1999). Cerebral correlates of preserved cognitive skills in autism A functional MRI study of Embedded Figures Task performance. *Brain, 122*, 1305-1315.

Ritvo, R. A., Ritvo, E. R., Guthrie, D., Ritvo, M. J., Hufnagel, D. H., McMahon, W., Tonge, B., Mataix-Cols, D., Jassi, A., & Attwood, T. (2011). The Ritvo Autism asperger diagnostic scale-revised (RAADS-R): a scale to assist the diagnosis of Autism spectrum disorder in adults: an international validation study. *Journal of autism and developmental disorders, 41*, 1076-1089.

Rosas, H., Liu, A., Hersch, S., Glessner, M., Ferrante, R., Salat, D., van Der Kouwe, A., Jenkins, B., Dale, A., & Fischl, B. (2002). Regional and progressive thinning of the cortical ribbon in Huntington's disease. *Neurology, 58*, 695-701.

Salat, D. H., Buckner, R. L., Snyder, A. Z., Greve, D. N., Desikan, R. S., Busa, E., Morris, J. C., Dale, A. M., & Fischl, B. (2004). Thinning of the cerebral cortex in aging. *Cerebral cortex, 14*, 721-730.

Saxe, R., & Kanwisher, N. (2003). People thinking about thinking people: the role of the temporo-parietal junction in "theory of mind". *Neuroimage, 19*, 1835-1842.

Saxe, R., & Powell, L. J. (2006). It's the Thought That Counts Specific Brain Regions for One Component of Theory of Mind. *Psychological science, 17*, 692-699.

Schaer, M., Cuadra, M. B., Tamarit, L., Lazeyras, F., Eliez, S., & Thiran, J. (2008). A surface-based approach to quantify local cortical gyrification. *Medical Imaging, IEEE Transactions on, 27*, 161-170.

Schaer, M., Ottet, M.-C., Scariati, E., Dukes, D., Franchini, M., Eliez, S., & Glaser, B. (2013). Decreased frontal gyrification correlates with altered connectivity in children with autism. *Frontiers in human neuroscience, 7*.

Schipul, S. E., Keller, T. A., & Just, M. A. (2011). Inter-regional brain communication and its disturbance in autism. *Front Syst Neurosci, 5*, 7.

Schulte-Rüther, M., Markowitsch, H. J., Fink, G. R., & Piefke, M. (2007). Mirror neuron and theory of mind mechanisms involved in face-to-face interactions: a functional magnetic resonance imaging approach to empathy. *Journal of Cognitive Neuroscience, 19*, 1354-1372.

Ségonne, F., Dale, A., Busa, E., Glessner, M., Salat, D., Hahn, H., & Fischl, B. (2004). A hybrid approach to the skull stripping problem in MRI. *Neuroimage, 22*, 1060-1075.

Ségonne, F., Pacheco, J., & Fischl, B. (2007). Geometrically accurate topology-correction of cortical surfaces using nonseparating loops. *Medical Imaging, IEEE Transactions on, 26*, 518-529.

Sled, J. G., Zijdenbos, A. P., & Evans, A. C. (1998). A nonparametric method for automatic correction of intensity nonuniformity in MRI data. *Medical Imaging, IEEE Transactions on, 17*, 87-97.

Sowell, E. R., Peterson, B. S., Thompson, P. M., Welcome, S. E., Henkenius, A. L., & Toga, A. W. (2003). Mapping cortical change across the human life span. *Nature neuroscience, 6*, 309-315.

Sowell, E. R., Thompson, P. M., Leonard, C. M., Welcome, S. E., Kan, E., & Toga, A. W. (2004). Longitudinal mapping of cortical thickness and brain growth in normal children. *The Journal of Neuroscience, 24*, 8223-8231.

Stanfield, A. C., McIntosh, A. M., Spencer, M. D., Philip, R., Gaur, S., & Lawrie, S. M. (2008). Towards a neuroanatomy of autism: a systematic review and meta-analysis of structural magnetic resonance imaging studies. *European Psychiatry, 23*, 289-299.

Su, S., White, T., Schmidt, M., Kao, C. Y., & Sapiro, G. (2013). Geometric computation of human gyrification indexes from magnetic resonance images. *Human brain mapping, 34*, 1230-1244.

Travers, B. G., Adluru, N., Ennis, C., Tromp do, P. M., Destiche, D., Doran, S., Bigler, E. D., Lange, N., Lainhart, J. E., & Alexander, A. L. (2012). Diffusion tensor imaging in autism spectrum disorder: a review. *Autism Res, 5*, 289-313.

Uddin, L. Q., Menon, V., Young, C. B., Ryali, S., Chen, T., Khouzam, A., Minshew, N. J., & Hardan, A. Y. (2011). Multivariate searchlight classification of structural magnetic resonance imaging in children and adolescents with autism. *Biological psychiatry, 70*, 833-841.

Van Essen, D. C. (1997). A tension-based theory of morphogenesis and compact wiring in the central nervous system. *NATURE-LONDON-*, 313-318.

Wallace, G. L., Robustelli, B., Dankner, N., Kenworthy, L., Giedd, J. N., & Martin, A. (2013). Increased gyrification, but comparable surface area in adolescents with autism spectrum disorders. *Brain, 136*, 1956-1967.

Wang, A. T., Lee, S. S., Sigman, M., & Dapretto, M. (2007). Reading affect in the face and voice: neural correlates of interpreting communicative intent in children and adolescents with autism spectrum disorders. *Archives of general psychiatry, 64*, 698-708.

Wechsler, D. (1999). *Wechsler abbreviated scale of intelligence*: Psychological Corporation.

White, T., Su, S., Schmidt, M., Kao, C.-Y., & Sapiro, G. (2010). The development of gyrification in childhood and adolescence. *Brain and cognition, 72*, 36-45.

Williams, J. H., Waiter, G. D., Gilchrist, A., Perrett, D. I., Murray, A. D., & Whiten, A. (2006). Neural mechanisms of imitation and 'mirror neuron'functioning in autistic spectrum disorder. *Neuropsychologia, 44*, 610-621.

Winkler, A. M., Kochunov, P., Blangero, J., Almasy, L., Zilles, K., Fox, P. T., Duggirala, R., & Glahn, D. C. (2010). Cortical thickness or grey matter volume? The importance of selecting the phenotype for imaging genetics studies. *Neuroimage, 53*, 1135-1146.

Wonderlick, J., Ziegler, D. A., Hosseini-Varnamkhasti, P., Locascio, J., Bakkour, A., Van Der Kouwe, A., Triantafyllou, C., Corkin, S., & Dickerson, B. C. (2009). Reliability of MRI-derived cortical and subcortical morphometric measures: effects of pulse sequence, voxel geometry, and parallel imaging. *Neuroimage, 44*, 1324-1333.

Worsley, K. J., Chen, J.-I., Lerch, J., & Evans, A. C. (2005). Comparing functional connectivity via thresholding correlations and singular value decomposition. *Philosophical Transactions of the Royal Society B: Biological Sciences, 360*, 913-920.

Zilles, K., Armstrong, E., Schleicher, A., & Kretschmann, H.-J. (1988). The human pattern of gyrification in the cerebral cortex. *Anatomy and embryology, 179,* 173-179.

Table 1. Participant demographic information.

	Autism				Control				Group difference	
	N	Mean	Range	s.d.	N	Mean	Range	s.d.	*t*-value	*P*-value
Age	55	18.5	8-40	0.89	60	18.23	8-36	0.91	0.33	0.74
Children	30	--	8-18	--	30	--	8-18	--	--	--
Adults	25	--	19-40	--	30	--	19-36	--	--	--
Verbal IQ	55	108.3	80-139	1.96	60	111.7	85-134	1.70	1.33	0.18
Performance IQ	55	111.6	84-138	2.05	60	109.3	84-137	1.66	0.98	0.32
Full-scale IQ	55	110.0	80-140	2.11	60	112.2	83-139	1.62	0.85	0.39
AQ	55	37.8	9-135	4.13	60	15.8	2-65	1.98	5.01	<0.00001
RAADS-R SM	17	28.7	4-47	2.49	16	11.8	0-25	2.50	4.75	<0.00001

Table 2. Significant differences between autism (ASD) and typically developing (TD) groups on surface-based brain measures.

Domain	Region	F value	p-value	Direction	ASD Mean (s.d.)	TD Mean (s.d.)
Volume	R Posterior Cingulate	4.39	0.03	ASD>TD	4051 (636)	3807 (510)
	L TPJ	7	0.009	ASD>TD	11940 (1791)	12231 (1955)
Cortical Thickness	R Pars Orbitalis	7.07	0.009	ASD>TD	3.02 (0.27)	2.93 (0.25)
	L Superior Frontal	8.5	0.004	ASD>TD	3.05 (0.18)	3.00 (0.17)
	R Rostral Anterior Cingulate	6.17	0.014	TD>ASD	2.80 (0.24)	2.92 (0.24)
	R Superior Parietal	5.38	0.022	TD>ASD	2.19 (0.17)	2.25 (0.15)
	L TPJ	4.04	0.004	ASD>TD	2.66 (0.19)	2.71 (0.19)
Surface Area	R Posterior Cingulate	5.53	0.02	ASD>TD	1391 (205)	1301 (167)
	L TPJ	5.14	0.025	ASD>TD	4189 (648)	4338 (524)
Gyrification	R Precentral	5.02	0.027	TD>ASD	1.60 (0.04)	1.61 (0.04)

Table 3. Significant correlations between age and brain measures by group.

Domain	Group	Region	Pearson's r	p-value
Volume	ASD	L TPJ	-0.46	<0.001
	TD	L TPJ	-0.48	<0.001
	TD	R Posterior Cingulate	-0.61	<0.001
Cortical Thickness	ASD	R Superior Parietal	-0.27	0.04
	TD	R Pars Orbitalis	0.28	0.029
	TD	R Rostral Anterior Cingulate	0.51	<0.001
Surface Area	TD	R Posterior Cingulate	-0.31	0.01
Gyrification	ASD	R Precentral	0.46	<0.001
	TD	R Precentral	0.57	<0.001

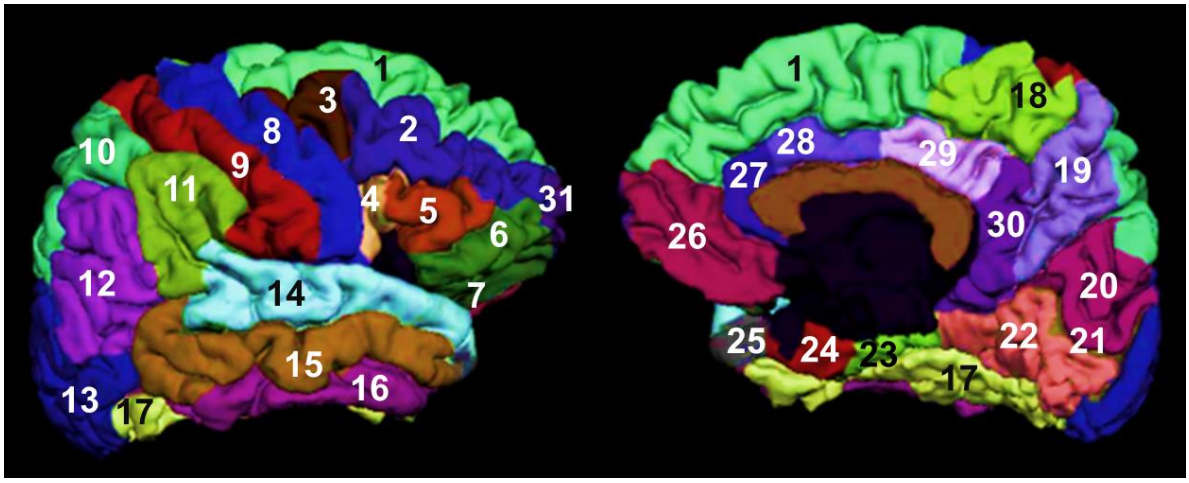

Figure 1. Regions of interest included in analyses: 1. superior frontal, 2. rostral middle frontal, 3. caudal middle frontal, 4. pars opercularis, 5. pars triangularis, 6. pars orbitalis, 7. lateral orbitofrontal, 8. precentral, 9. postcentral, 10. superior parietal, 11. temporoparietal junction, 12. inferior parietal, 13. lateral occipital, 14. superior temporal, 15. middle temporal, 16. inferior temporal, 17. fusiform, 18. paracentral, 19. precuneus, 20. cuneus, 21. peri calcarine, 22. lingual, 23. parahippocampal, 24. entorhinal, 25. temporal pole, 26. medial orbitofrontal, 27. rostral anterior cingulate, 28. caudal anterior cingulate, 29. posterior cingulate, 30. isthmus cingulate, 31. frontal pole, 32. transverse temporal (not visible), 33. superior temporal sulcus (not visible).

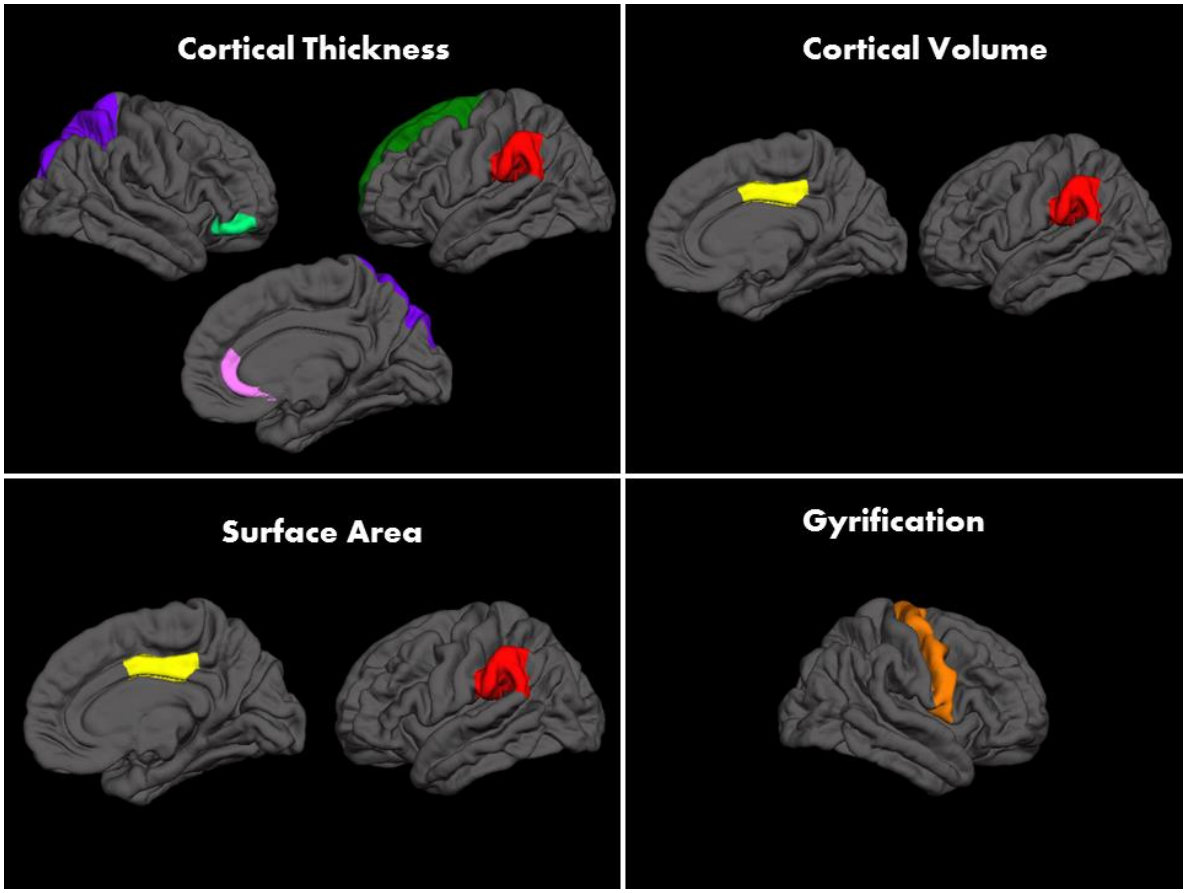

Figure 2. Results of significant differences between autism (ASD) and typically developing (TD) groups from the surface-based morphometry analysis. Cortical thickness: right pars orbitalis (teal), right rostral anterior cingulate (pink), right superior parietal (purple), left superior frontal (green), and left temporoparietal junction (TPJ) (red); Cortical volume: right posterior cingulate (yellow) and left TPJ (red); Surface Area: right posterior cingulate (yellow) and left TPJ (red); Gyrification: right precentral gyrus (orange).

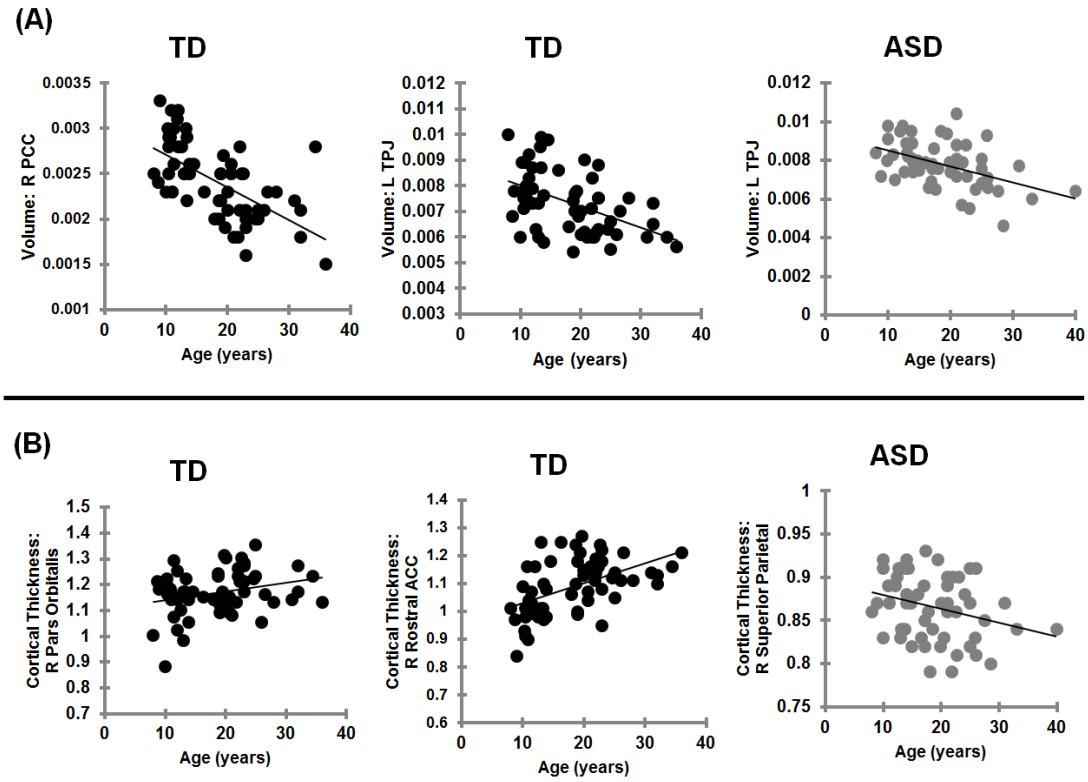

Figure 3. Results from correlation analyses between surface-based measures and age. (A) Left: Significant correlation between age and cortical volume for right posterior cingulate (R PCC) for typically developing (TD) participants; Middle: Significant correlation between age and cortical volume for left temporoparietal junction (L TPJ) for typically developing (TD) participants; Right: Significant correlation between age and cortical volume for LTPJ for participants with autism spectrum disorder (ASD). (B) Left: Significant correlation between age and cortical thickness for right pars orbitalis for the TD group; Middle: Significant correlation between age and cortical thickness for right rostral anterior cingulate (ACC); Right: Significant correlation between age and right superior parietal lobule for ASD participants.

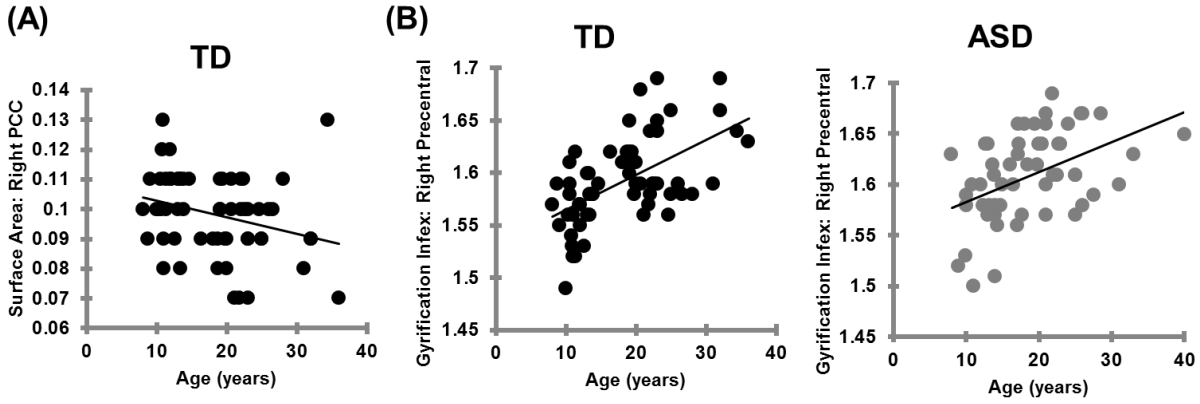

Figure 4. Results from correlation analyses between surface-based measures and age. (A) Significant correlation between age and surface area for right posterior cingulate (PCC) for typically developing (TD) participants. (B) Significant correlations between age and gyrification index for right precentral gyrus for the TD group (left) and autism (ASD) group (right).

INVESTIGATING WHITE MATTER INTEGRITY OF MAJOR FIBER TRACTS IMPLICATED IN AUTISM SPECTRUM DISORDER USING DIFFUSION TENSOR IMAGING

by

LAUREN E. LIBERO AND RAJESH K. KANA

Submitted to *Brain Structure and Function*

Format adapted for dissertation

Abstract

Autism spectrum disorder (ASD) is a neurodevelopmental disorder found to have widespread alterations in the function and synchrony of brain regions. These abnormalities may be the result of alterations in the nature and organization of white matter pathways connecting the brain. To investigate the integrity of major white matter tracts, the current study examined multiple indices of white matter diffusion in 42 children and adults with ASD, and 44 typically developing (TD) age-and-IQ-matched peers using diffusion tensor imaging (DTI). Diffusivity measures were compared between groups for the following tracts: bilateral cingulum bundle, corpus callosum, inferior longitudinal fasciculus, superior longitudinal fasciculus, and uncinate fasciculus. Results indicate a significant reduction in fractional anisotropy (FA) for the left superior longitudinal fasciculus (LSLF) in ASD children and adults, compared to their TD peers. A significant increase in radial diffusivity for ASD participants was also found in the same cluster along the LSLF. In addition, a significant positive correlation emerged for all subjects between FA for the LSLF and age, with FA increasing with age. Finally, a significant negative correlation was found between FA in the LSLF and autism symptom severity in adults with ASD, indicating greater abnormalities in white matter as the severity of autism increased. These findings point to a significant alteration in long distance white matter connectivity in children and adults with ASD, potentially underscoring the relationship between white matter microstructure and the ASD phenotype. These results also suggest that the white matter abnormalities in autism may be subtle and related to symptom severity and the developmental trajectory.

Keywords: autism spectrum disorder, diffusion tensor imaging, superior longitudinal fasciculus, fractional anisotropy

Introduction

Converging findings from the neuroimaging literature attribute the neuropathology of autism spectrum disorder (ASD) to widespread disruptions in brain connectivity (Just et al. 2012; Kana et al. 2011; Maximo et al. 2014). While most of these studies focus on functional connectivity (synchronization of brain activity across spatially distant regions), of late, alterations in white matter microstructure have also been reported in autism by diffusion tensor imaging (DTI) studies (see (Travers et al. 2012) for a review). Morphometric studies have suggested an early overgrowth of white matter among young children with autism, followed by reduced white matter volume in adolescence and adulthood relative to typically developing control individuals (Courchesne et al. 2003; Courchesne et al. 2001; Ecker et al. 2012; Herbert et al. 2004; Waiter et al. 2004). Such volumetric abnormalities seen in autism may arise from aberrations in axonal density or organization, or from myelin abnormalities, either of which could result in aberrant connectivity. Functional differences in connectivity and abnormalities in white matter volume point to potential aberrations in the integrity of white matter tracts in ASD. Thus, a comprehensive account of connectivity abnormalities in autism would warrant investigating the nature and organization of axons which may be critical in brain functioning.

Structural limits on communication between brain regions may cause computational changes to evolve to deal with a pattern of reduced connectivity. DTI provides the opportunity to go beyond measurement of functional connections and volumetric measures to examine the structural integrity of white matter tracts on a voxel-by-voxel basis. Fractional anisotropy (FA), a measure derived from diffusion tensor data,

is sensitive to developmental changes and pathological differences in axonal density, size, myelination, and the coherence of organization of fibers within a voxel, and thus provides an index of the structural integrity of the white matter (Basser 1995; Basser and Pierpaoli 1996; Beaulieu 2002). The FA measurement represents the degree of anisotropic (directional) diffusion in a 3D ellipsoid distribution (Basser and Jones 2002; Pfefferbaum et al. 2000), with the highest values in the brain measured in white matter tracts (maximum theoretical value 1) and lower values in gray matter and cerebrospinal fluid (approaching 0). In addition to FA, DTI also provides measures of the average radius of diffusion as mean diffusivity (MD), diffusivity running parallel to the white matter tract as axial diffusivity (AD), and diffusivity perpendicular to the tract as radial diffusivity (RD). These measures together provide multiple indices of diffusion along white matter tracts in the brain, enabling us to investigate potential abnormalities in the microstructure of white matter in disorders like ASD.

DTI studies in ASD have found reduced FA in a number of white matter tracts including corpus callosum, cingulum bundle, uncinate fasciculus, and tracts along the anterior-posterior direction in the brain, such as the inferior and superior longitudinal fasciculi ((Alexander et al. 2007; Barnea-Goraly et al. 2004; Bloemen et al. 2010; Keller et al. 2007; Lee et al. 2007); see (Travers et al. 2012) for a review). While alterations in FA for these tracts have been found somewhat consistently in studies on ASD, investigations reporting on multiple indices, such as MD, RD, and AD have been more sparse and inconsistent. A few studies have pointed to the relationship between structural integrity of white matter tracts and cognitive functioning in ASD. For example, reduced FA in ASD participants has been linked to increased ASD symptom severity and

behaviors (Catani et al. 2008; Noriuchi et al. 2010; Poustka et al. 2012; Thakkar et al. 2008), as well as performance IQ (Alexander et al. 2007; Lange et al. 2010; Lee et al. 2009). In developmental disorders like ASD, DTI provides a unique opportunity to investigate the structural makeup and structural limits of functional communication in the brain. In addition, applying DTI to different age groups or following a cohort longitudinally can address the neurodevelopmental trajectory of the disorder, and determine the best possible windows of time for effective treatment and intervention.

Despite the promises of diffusion tensor imaging techniques, DTI studies in general have focused on reporting differences in FA, without examining other measures that may drive changes in FA. In addition, many studies use methods that may not be ideal for investigating the brain in a population like ASD. For example, voxel-based methods like Tract-Based Spatial Statistics (TBSS), used in a large number of DTI studies on ASD, uses a projected white matter skeleton to compute white matter properties for each subject. The size and shape of fiber tracts may vary from participant to participant when examining patient populations like ASD. Thus, aligning the skeleton with actual white matter voxels in individual participants, or aligning the same tracts across participants, may not be accurate and may not be able to detect differences with the same accuracy across all tracts (Edden and Jones 2011; Wassermann et al. 2011; Yeatman et al. 2012; Yeatman et al. 2011). In other words, tract features specific to individual subjects may get misaligned in TBSS resulting in a skeleton that may not be best representing white matter tract measurements for the participant group. This is particularly troublesome for patient populations like autism, who may have abnormalities in brain size (Redcay and

Courchesne 2005) and organization, and thus could have greatly misaligned white matter skeletons resulting in inaccurate diffusion properties.

The current study examined the differences in white matter integrity in children and adults with ASD in a set of major fiber tracts implicated in the disorder: cingulum bundle, corpus callosum, inferior and superior longitudinal fasciculi, and uncinate fasciculus. To investigate diffusivity measures across the tracts, we used Automated Fiber Quantification (AFQ), a relatively novel technique which quantifies FA, MD, RD, and AD along the trajectories of major white matter tracts in the brain (Yeatman et al. 2012). This method facilitates the examination of diffusion along 100 points on a given fiber bundle instead of a single mean value for the entire tract. This is done by segmenting individual participants' white matter tracts, quantifying white matter tract properties, and evaluating differences in tract properties between groups. AFQ has been found to generate tract profiles that are consistent across subjects, but are also precise and reliable in terms of quantifying the actual white matter tracts within each subject's brain (Yeatman et al. 2012). We used this technique to investigate potential differences in white matter diffusion in participants with ASD and the relationship between the resulting diffusion measures and behavior. It is hypothesized that participants with ASD, compared to their TD peers, will exhibit a significant reduction in FA in the major tracts examined in this study. This study is novel in a few different ways: 1) it examines multiple indices of white matter integrity in autism; 2) it investigates a relatively large group of participants at different age groups providing information about the developmental trajectory of white matter in autism; and 3) unlike previous studies reporting mean FA for entire tracts, this study examines diffusion properties at 100 points

along each fiber tract. Findings from this study are significant in that they provide information related to possible alterations in diffusion measures of several major white matter tracts in the brains of those with ASD. Alterations in white matter integrity marked by DTI hold strong implications for explaining the abnormalities in function and synchrony of brain regions seen in individuals with ASD.

Method

Participants

Forty two high-functioning children, adolescents, and adults with ASD (36 males/6 females; mean age: 19.9 years) and 46 typically developing (TD) peers (37 males/7 females; mean age: 20.1 years) participated in this study (see Table 1 for demographic information). The two groups did not differ in age or IQ. Two TD adults were excluded due to excessive head motion, resulting in 44 TD participants included the data analyses. Children were classified as those aged 8-18 years and adults were classified as those aged 19-40 years. The ASD group was made up of 21 children and 21 adults, while the TD group was made up of 18 children and 26 adults. Verbal IQ (VIQ), Performance IQ (PIQ), and Full Scale IQ (FSIQ) were assessed using the Wechsler Abbreviated Scale of Intelligence (WASI) (Wechsler 1999), and handedness using the Edinburgh Handedness Inventory (Oldfield 1971). Participants who were 18 years of age and younger were classified as children. Parents of children completed the Autism-Spectrum Quotient Child (AQ) about their child, as a measure of symptom severity (Auyeung et al. 2008). Adult participants completed the Ritvo Autism-Asperger Diagnostic Scale-Revised (RAADS-R) to measure ASD symptoms (Ritvo et al. 2011). The RAADS-R has been found to be accurate in discriminating between individuals with

ASD and those without ASD (sensitivity = 97%, specificity = 100%, test–retest reliability = 0.987, accuracy = 98.5%). Participants with ASD had received a previous diagnosis of an ASD based on Autism Diagnostic Interview (ADI-R) symptoms, and Autism Diagnostic Observation Schedule-Generic (ADOS-G) (Lord et al. 2000). TD participants were screened through a self-report history questionnaire to rule out neurological disorders, such as ASD, ADHD, or Tourette's Disorder, that could potentially confound the results. The study was approved by our university's Institutional Review Board, and all participants and their guardians provided informed consent for their participation in the study. Several ASD participants reported taking medications, including stimulant medication (n=12), antidepressants (n=9), anxiety medication (n=1), and antipsychotic medication (n=4). Twenty-eight ASD participants reported no medications, and no TD participants reported taking medication.

DTI Data Acquisition

Imaging was performed on a 3T head-only scanner (Siemens Allegra, Erlangen, Germany). Anatomical images were acquired using high resolution T1-weighted scans using a 160 slice 3D magnetization-prepared rapid acquisition gradient-echo (MPRAGE) volume scan with a TR = 200ms, TE = 3.34 ms, flip angle = 12^0, FOV = 25.6 cm, 256 x 256 matrix size, and 1mm slice thickness. The diffusion weighted images were collected using a single-shot, spin-echo, EPI sequence. A diffusion weighted, single-shot, spin–echo, echo-planar imaging sequence was used (TR = 7000 ms, TE = 90 ms, bandwidth = 2790 Hz/voxel, FOV = 220 mm, and matrix size = 128 x 128 x 27, resulting in an in-plane resolution of 1.7 X 1.7 X 3 mm^3). Twenty-seven 3-mm thick slices were imaged (no slice gap) with no diffusion-weighting (b = $0s/mm^2$) and with diffusion-weighting (b

= 1000s/mm^2) gradients applied in 46 orthogonal directions. Ninety-two images of each slice by gradient direction combination were acquired and averaged to produce the final diffusion imaging dataset for each participant.

Preprocessing and DTI Tractography

Diffusion images were preprocessed using the *mrDiffusion* package (Stanford VISTA Lab). Through this pipeline, participant head motion and eddy current distortions were removed by a 14-parameter constrained non-linear co-registration based on the expected pattern of distortions for each phase-encoded direction of the data (Rohde et al. 2004). Diffusion weighted images were aligned to the unweighted (b=0) images, and then rigid-body aligned to each subject's anatomical T1 reference image. Data were resampled to 2 X 2 X 2 mm^3 voxels with a 7th order b-spline interpolation, taking into account head motion-correction, eddy-current distortion correction, and anatomical alignment transforms (Friston and Ashburner 2004). The rotation matrices from the alignment steps were combined and applied to correctly orient the resampled data to their respective vectors. Finally, the tensor model was fit using a robust least-squares algorithm, and the resulting eigenvalues were used to compute fractional anisotropy (FA), mean diffusivity (MD), radial diffusivity (RD), and axial diffusivity (AD) (Basser and Pierpaoli 1996).

The preprocessed data were analyzed using *Automated Fiber Quantification* (AFQ) (Yeatman et al. 2012). The data for each participant were subjected to whole-brain tractography (using deterministic tractography). The data were then segmented into tracts for left cingulum bundle, right cingulum bundle, callosum forceps major, callosum forceps minor, left inferior longitudinal fasciculus (LILF), right inferior longitudinal fasciculus (RILF), left superior longitudinal fasciculus (LSLF), right superior

longitudinal fasciculus (RSLF), left uncinate, right uncinate. Next, stray fibers were removed, and tract properties (FA, RD, MD, and AD) were computed for 100 points along each tract for each participant. Norms for each tract were determined using control group data. For some participants, tract properties for specific tracts could not be computed (due to artifact, head motion, or quality [e.g., size or crossing fibers] of the tissue). Tracts with greater than 10% of participants missing data (due to incomplete tractography) were removed from further analyses. These tracts included the left and right cingulum bundles (see Figure 1 for a flow chart depicting analysis procedures).

Statistical Analyses

To compare the ASD and TD groups on FA, RD, MD, and AD, t-tests were conducted point-wise along each fiber tract for 100 points. A permutation based multiple comparison correction was applied to determine statistical significance (Nichols and Holmes 2002), $p < 0.05$. We additionally compared the six ASD female participants with six age and IQ matched ASD participants to examine any potential gender differences. For fiber tracts that showed significant differences between groups, Pearson's correlations were computed between mean FA values for the significant cluster and age, and ASD symptom measures (RAADS-R and AQ). Independent samples t-tests were used to compare groups on demographic information and neuropsychological assessment data.

Results

The main finding of this study is a significant difference in white matter integrity of the left superior longitudinal fasciculus, with ASD participants showing significantly reduced FA compared to their TD peers ($p<0.05$, corrected) (See Figure 2). Differences

in FA spanned most of the LSLF, with the cluster reaching corrected statistical significance appearing in the anterior portion of the tract, and no differences in FA in the most posterior points (see Figure 3 for a graph representing mean FA for both ASD and TD groups for the statistically significant cluster on the LSLF). At the same cluster along the LSLF, a significant increase in RD for the ASD group was also found compared to the TD group ($p<0.05$, corrected). No significant differences in FA, RD, MD, or AD emerged between groups for the callosum forceps major, callosum forceps minor, left inferior longitudinal fasciculus, right inferior longitudinal fasciculus, right superior longitudinal fasciculus, left uncinate fasciculus, or right uncinate fasciculus after correcting for multiple comparisons.

To examine gender differences in white matter integrity in ASD, we compared the six ASD females with six age and IQ matched ASD males. No significant differences emerged between the male and female participants for any of the major white matter tracts.

A significant positive correlation between FA for the LSLF cluster and age emerged ($r=0.304$, $p=0.005$) for all participants (See Figure 4). When this relationship was examined within each group separately, the TD participants had a significant positive correlation between FA for the LSLF cluster and age ($r=0.348$, $p=0.021$), whereas the correlation for the ASD group was only marginally significant ($r=0.286$, $p=0.070$). The two groups did not differ significantly in their correlation coefficients ($Z=-0.308$, $p=0.757$). Thus, in all these correlations, white matter integrity, indexed by fractional anisotropy, improved as a function of age.

We also examined the relationship between diffusion measures and autism symptomatology. A significant negative correlation emerged between FA for the LSLF and RAADS-R scores in the adult participants ($r = -0.291$, $p=0.045$) (See Figure 5). However, when examined within each group, the correlation was not significant (TD $r=-0.045$, $p=0.83$; ASD $r=0.015$, $p=0.945$). In addition, the two groups did not significantly differ in their correlation coefficients ($Z=0.194$, $p=0.845$). For the children in this study, the correlation between FA for LSLF and AQ (autism symptomatology in children as measured by AQ) was negative but not significant ($r=-0.248$, $p=0.143$). Within each group, the correlation was not significant (TD $r=-0.073$, $p=0.774$; ASD $r=-0.184$, $p=0.464$), and the two groups did not significantly differ in their correlation coefficients ($Z=0.314$, $p=0.753$).

Discussion

The main finding of this study is a significant reduction in FA and a significant increase in RD in the LSLF in children and adults with autism relative to typical control participants. This reduction in FA is in line with the findings of several previous studies in ASD (Jeong et al. 2011; Jou et al. 2011a; Jou et al. 2011b; Noriuchi et al. 2010; Poustka et al. 2012; Shukla et al. 2011). Increased RD in the same tract in autism was also reported in a few previous studies (Jeong et al. 2011; Shukla et al. 2011). The SLF is a fiber tract that spans from the inferior fontal gyrus to the superior temporal gyrus and temporoparietal junction, terminating close to Broca's Area, Wernicke's Area, precentral gyrus and the supramarginal gyrus (Bernal and Altman 2010; Catani and Jones 2005; Makris et al. 2005; Wakana et al. 2004). It is a major association fiber pathway, related to regulation of motor behavior, spatial attention, and language (Makris et al. 2005). In

typically developing children, FA of the LSLF in particular has been found to be associated with attention, inhibitory control, and language skills (Urger et al. 2014), pointing to the role of this tract in many complex, higher order behaviors. In terms of ASD, SLF abnormalities could thus impact a number of behaviors, including the social and communicative impairments that are hallmark of the disorder.

The SLF is a particularly slow developing tract, not clearly visible in neonates, and its development has been associated with language use (Bengtsson et al. 2005; Hermoye et al. 2006; Huang et al. 2006; Paus et al. 1999; Thompson et al. 2000; Zhang et al. 2007). Previous studies have linked language impairments to diffusivity measures in the brain in ASD. For example, a recent study found increased RD in the left arcuate portion of the SLF in ASD to be related to poorer language index scores (Roberts et al. 2013), and another study found increased MD in the SLF to be related to increased language impairment in ASD (Nagae et al. 2012). For a disorder marked by impairment in language and communication, it comes as no surprise that the older children and adults included in this study would then have alterations in FA and RD in this fiber tract. However, considering that the SLF continues to develop slowly across infancy and childhood, and may develop in line with language skills, the impairment in LSLF in children and adults marks just how critical early intervention (especially for language) in young children with ASD is.

The LSLF in terms of our typical control norms was characterized by a peak in FA towards the anterior portion of the tract, with lower FA towards the center of the tract, and increasing FA again towards the posterior portion. While group differences were found across the majority of this tract, the cluster reaching statistical significance

appeared at the relatively anterior peak in FA for the control subjects; meanwhile, FA levels for ASD participants normalized at the posterior end of the LSLF with no statistically significant differences at that portion of the tract. These findings suggest that alterations in diffusivity may not span the entire LSLF tract; instead, some parts of this tract (in this case the anterior section) have more abnormal diffusivity than others. This alteration in the nature and orientation of the LSLF for ASD children and adults has important implications for both development, as well as connectivity abnormalities. First, a difference in the integrity of anterior and posterior aspects of this fiber bundle may be attributed to developmental abnormalities and/or differences in myelination across the tract. Thus, white matter connectivity abnormalities in ASD may not be widespread, but rather may differ across different tracts as well as along different points on a given tract. Second, cortical connectivity theories of autism have postulated aberrations in long distance connectivity in the brain in ASD, particularly with frontal brain regions holding most of the blame for abnormalities in function and connectivity (Kana et al. 2011). The anterior portion of the SLF projects to precentral gyrus (Bernal and Altman 2010; Martino et al. 2013) and is delineated at superior, middle, and inferior frontal gyri (Makris et al. 2005). With terminations in frontal cortex, reduced FA in the anterior cluster of the LSLF supports this theory of abnormal connectivity in autism, and suggests the alterations in functional connectivity may be stemming from abnormalities in white matter integrity at the anterior portion of the LSLF. Cellular abnormalities, found primarily in frontal cortex of postmortem ASD brains, also support potential abnormalities in connectivity within frontal cortex and SLF. These abnormalities include astroglial reactions and enlarged cell bodies in gray and white matter of dorsal and mesial

frontal cortex (Vargas et al. 2005), abnormal number and spacing of minicolumns in prefrontal cortex (Casanova et al. 2002a; Casanova et al. 2002b; Casanova et al. 2006), increased number of neurons in prefrontal cortex (Courchesne et al. 2011), and abnormal laminar cytoarchitecture in prefrontal neurons (Stoner et al. 2014). Cellular alterations in frontal cortex could certainly impact function and connectivity both within local (frontal) white matter and beyond (long distance white matter tracts connected to frontal cortex, i.e., SLF).

The current study also found a significant positive correlation between FA for the LSLF and age, with FA increasing with age for all participants. This is in line with previous findings of the same correlation in typically developing individuals (Ashtari et al. 2007; Lebel and Beaulieu 2011; Lebel et al. 2008). It is perhaps telling that the LSLF continues to develop into adolescence and young adulthood, implying its plasticity even in older participants. We also found a significant negative correlation between FA in the LSLF and RAADS-R scores in adults, with lower FA in this cluster related to greater ASD symptom severity. A negative, but not significant, correlation for children was found between FA in the LSLF cluster and AQ scores, with lower FA in the LSLF related to greater ASD symptom severity again. A reliable negative relationship between white matter integrity of the SLF and autism symptom severity (measured by ADI-R and ADOS-G scores) has been found by a previous study (Poustka et al. 2012). These relationships may suggest the role of healthy axons, especially in tracts like LSLF, in determining social communicative behaviors in autism.

While a significant difference in FA and RD for the LSLF emerged between TD and ASD participants, no significant differences were found in any of the diffusion

measurements for the remaining tracts studied (cingulum bundle, inferior longitudinal fasciculus, uncinate, and the forceps major and forceps minor of the corpus callosum). The tracts included in the current study have all been found to have significant FA reduction in ASD, however, studies still report inconsistencies when it comes to these white matter tracts in ASD (Travers et al. 2012). In addition, previous studies differ greatly in age, IQ, and symptom severity of their included participants. As there is variation in the development of different white matter fiber tracts, as well as links between tract integrity and ASD symptoms, subject characteristics may strongly impact findings. In addition, the tractography methodology used in previous studies varies as well. For example, while the preprocessing pipeline of the current study employs motion and eddy current distortion correction, many studies fail to report the use of any kind of correction. As diffusion imaging relies heavily on directional information, motion correction is of utmost importance if one wants reliable tractography. It should also be noted that the current study could not compare groups for the cingulum bundle, as tractography could not be computed for this tract for many subjects. The cingulum bundle is a small tract, surrounded by gray matter tissue and the corpus callosum. Its size and location make it susceptible to motion artifacts and difficult to accurately calculate statistics for. While AFQ identified unreliable quantification for participants' tracts in the current study, many other automated techniques may not do so, rendering their findings potentially insensitive to noise and thus inaccurate.

Overall, this study found strong evidence for alterations in white matter integrity in the LSLF in children and adults with ASD, and the relationship between diffusivity of this tract with age, and autism symptom severity. Using a relatively novel method of DTI

analysis, our study represents the first application of AFQ to DTI in the ASD population. This method provides the diffusion profile across an entire white matter fiber tract, and avoids potential errors from misalignment of tracts and single subject white matter voxels (present in voxel-based analysis techniques). This method is also more informative than some others, as diffusion information can be measured along the entire tract rather than relying on averaged measures across a given tract (which is unlikely to be sensitive enough to identify clinical differences in white matter integrity). With this method, we were able to gather tractography measures of the major white matter tracts in the brain and compare the tract profiles of children and adults with ASD to their TD peers. This diffusion measure may be more accurate and reliable as this approach is not impacted by significant differences in brain sizes (which may be particularly relevant in a neurodevelopmental disorder like ASD).

While a significant increase in RD was found at the same cluster on the LSLF with reduced FA in participants with ASD, this finding is difficult to interpret without further investigation. For example, studies in animals have linked increased RD to reductions in myelin (Harsan et al. 2006; Song et al. 2002; Tyszka et al. 2006). It is possible that reductions in myelin are driving the alterations in the white matter microstructure of the SLF in ASD; however, without using methods that specifically target myelination in our participants, we can only speculate. It is also possible that other abnormalities, such as number of crossing fibers, axonal density or diameter, and inflammation, could be driving a change in RD (Wheeler-Kingshott and Cercignani 2009). Indeed, one study utilizing diffusional kurtosis imaging in young adults with ASD found reduced axonal water fraction in the SLF compared to controls, indicating altered

intra-axonal volume and potentially lower axonal density (Lazar et al. 2014). Thus, evidence from the current study and from previous studies suggest that the left superior longitudinal fasciculus may be an important fiber tract that shows significant alterations in the quality of white matter microstructure in autism. Future studies should also further examine the relationship between FA in the SLF and age. It would be interesting to study this relationship in older adults, to investigate the neural development of this tract across the lifespan in ASD. In addition, in terms of early development and treatment, examining the development of the SLF in very young children with ASD could potentially lead to more targeted treatment of the disorder (especially with regard to social skills and symptom severity).

Acknowledgments

This study was funded by the UAB Center for Clinical and Translational Sciences grant (5UL1RR025777). The authors would like to thank Hrishikesh Deshpande and Wesley Burge for their assistance with computational aspects of this project. The authors would also like to thank Jason Yeatman, Dr. Brian Wandell, and the Stanford Vision and Imaging Science and Technology Laboratory for providing access to the mrDiffusion and AFQ software, and their assistance with these resources.

References

Alexander AL et al. (2007) Diffusion tensor imaging of the corpus callosum in autism Neuroimage 34:61-73

Ashtari M et al. (2007) White matter development during late adolescence in healthy males: a cross-sectional diffusion tensor imaging study Neuroimage 35:501-510

Auyeung B, Baron-Cohen S, Wheelwright S, Allison C (2008) The autism spectrum quotient: Children's version (AQ-Child) Journal of autism and developmental disorders 38:1230-1240

Barnea-Goraly N, Kwon H, Menon V, Eliez S, Lotspeich L, Reiss AL (2004) White matter structure in autism: preliminary evidence from diffusion tensor imaging Biological psychiatry 55:323-326

Basser P, Jones DK (2002) Diffusion-tensor MRI: theory, experimental design and data analysis – a technical review NMR in Biomedicine 15:456-467 doi:10.1002/nbm.783

Basser PJ (1995) Inferring microstructural features and the physiological state of tissues from diffusion-weighted images NMR in Biomedicine 8:333-344

Basser PJ, Pierpaoli C (1996) Microstructural and Physiological Features of Tissues Elucidated by Quantitative-Diffusion-Tensor MRI Journal of Magnetic Resonance, Series B 111:209-219 doi: http://dx.doi.org/10.1006/jmrb.1996.0086

Beaulieu C (2002) The basis of anisotropic water diffusion in the nervous system–a technical review NMR in Biomedicine 15:435-455

Bengtsson SL, Nagy Z, Skare S, Forsman L, Forssberg H, Ullén F (2005) Extensive piano practicing has regionally specific effects on white matter development Nature neuroscience 8:1148-1150

Bernal B, Altman N (2010) The connectivity of the superior longitudinal fasciculus: a tractography DTI study Magnetic resonance imaging 28:217-225

Bloemen OJ et al. (2010) White matter integrity in Asperger syndrome: a preliminary diffusion tensor magnetic resonance imaging study in adults Autism Research 3:203-213

Casanova MF, Buxhoeveden DP, Brown C (2002a) Clinical and macroscopic correlates of minicolumnar pathology in autism Journal of Child Neurology 17:692-695

Casanova MF, Buxhoeveden DP, Switala AE, Roy E (2002b) Minicolumnar pathology in autism Neurology 58:428-432

Casanova MF et al. (2006) Minicolumnar abnormalities in autism Acta neuropathologica 112:287-303

Catani M, Jones DK (2005) Perisylvian language networks of the human brain Annals of neurology 57:8-16

Catani M et al. (2008) Altered cerebellar feedback projections in Asperger syndrome Neuroimage 41:1184-1191

Courchesne E, Carper R, Akshoomoff N (2003) Evidence of brain overgrowth in the first year of life in autism JAMA: the journal of the American Medical Association 290:337

Courchesne E et al. (2001) Unusual brain growth patterns in early life in patients with autistic disorder Neurology 57:245-254

Courchesne E et al. (2011) Neuron number and size in prefrontal cortex of children with autism Jama 306:2001-2010

Ecker C et al. (2012) Brain anatomy and its relationship to behavior in adults with autism spectrum disorder: a multicenter magnetic resonance imaging study Archives of general psychiatry 69:195-209

Edden RA, Jones DK (2011) Spatial and orientational heterogeneity in the statistical sensitivity of skeleton-based analyses of diffusion tensor MR imaging data Journal of neuroscience methods 201:213-219

Friston KJ, Ashburner J (2004) Generative and recognition models for neuroanatomy Neuroimage 23:21-24 doi:10.1016/j.neuroimage.2004.04.021

Harsan LA et al. (2006) Brain dysmyelination and recovery assessment by noninvasive in vivo diffusion tensor magnetic resonance imaging Journal of neuroscience research 83:392-402

Herbert MR et al. (2004) Localization of white matter volume increase in autism and developmental language disorder Annals of Neurology 55:530-540

Hermoye L et al. (2006) Pediatric diffusion tensor imaging: normal database and observation of the white matter maturation in early childhood Neuroimage 29:493-504

Huang H et al. (2006) White and gray matter development in human fetal, newborn and pediatric brains Neuroimage 33:27-38

Jeong J-W, Kumar A, Sundaram SK, Chugani HT, Chugani DC (2011) Sharp curvature of frontal lobe white matter pathways in children with autism spectrum disorders: tract-based morphometry analysis American Journal of Neuroradiology 32:1600-1606

Jou R, Mateljevic N, Kaiser M, Sugrue D, Volkmar F, Pelphrey K (2011a) Structural neural phenotype of autism: preliminary evidence from a diffusion tensor imaging study using tract-based spatial statistics American Journal of Neuroradiology 32:1607-1613

Jou RJ, Jackowski AP, Papademetris X, Rajeevan N, Staib LH, Volkmar FR (2011b) Diffusion tensor imaging in autism spectrum disorders: preliminary evidence of abnormal neural connectivity Australian and New Zealand Journal of Psychiatry 45:153-162

Just MA, Keller TA, Malave VL, Kana RK, Varma S (2012) Autism as a neural systems disorder: a theory of frontal-posterior underconnectivity Neuroscience & Biobehavioral Reviews 36:1292-1313

Kana RK, Libero LE, Moore MS (2011) Disrupted cortical connectivity theory as an explanatory model for autism spectrum disorders Physics of life reviews 8:410-437

Keller TA, Kana RK, Just MA (2007) A developmental study of the structural integrity of white matter in autism Neuroreport 18:23-27

Lange N et al. (2010) Atypical diffusion tensor hemispheric asymmetry in autism Autism research 3:350-358

Lazar M, Miles LM, Babb JS, Donaldson JB (2014) Axonal deficits in young adults with High Functioning Autism and their impact on processing speed NeuroImage: Clinical 4:417-425

Lebel C, Beaulieu C (2011) Longitudinal development of human brain wiring continues from childhood into adulthood The Journal of Neuroscience 31:10937-10947

Lebel C, Walker L, Leemans A, Phillips L, Beaulieu C (2008) Microstructural maturation of the human brain from childhood to adulthood Neuroimage 40:1044-1055

Lee JE et al. (2007) Diffusion tensor imaging of white matter in the superior temporal gyrus and temporal stem in autism Neuroscience letters 424:127-132

Lee JE et al. (2009) A study of diffusion tensor imaging by tissue-specific, smoothing-compensated voxel-based analysis Neuroimage 44:870-883

Lord C et al. (2000) The Autism Diagnostic Observation Schedule—Generic: A standard measure of social and communication deficits associated with the spectrum of autism Journal of autism and developmental disorders 30:205-223

Makris N, Kennedy DN, McInerney S, Sorensen AG, Wang R, Caviness VS, Pandya DN (2005) Segmentation of subcomponents within the superior longitudinal fascicle in humans: a quantitative, in vivo, DT-MRI study Cerebral Cortex 15:854-869

Martino J, Witt Hamer P, Berger M, Lawton M, Arnold C, Lucas E, Duffau H (2013) Analysis of the subcomponents and cortical terminations of the perisylvian superior longitudinal fasciculus: a fiber dissection and DTI tractography study Brain Struct Funct 218:105-121 doi:10.1007/s00429-012-0386-5

Maximo JO, Cadena EJ, Kana RK (2014) The Implications of Brain Connectivity in the Neuropsychology of Autism Neuropsychology review:1-16

Nagae L et al. (2012) Elevated mean diffusivity in the left hemisphere superior longitudinal fasciculus in autism spectrum disorders increases with more profound language impairment American Journal of Neuroradiology 33:1720-1725

Nichols TE, Holmes AP (2002) Nonparametric permutation tests for functional neuroimaging: a primer with examples Human brain mapping 15:1-25

Noriuchi M et al. (2010) Altered white matter fractional anisotropy and social impairment in children with autism spectrum disorder Brain research 1362:141-149

Oldfield RC (1971) The assessment and analysis of handedness: the Edinburgh inventory Neuropsychologia 9:97-113

Paus T et al. (1999) Structural maturation of neural pathways in children and adolescents: in vivo study Science 283:1908-1911

Pfefferbaum A, Sullivan EV, Hedehus M, Lim KO, Adalsteinsson E, Moseley M (2000) Age-related decline in brain white matter anisotropy measured with spatially corrected echo-planar diffusion tensor imaging Magnetic resonance in medicine 44:259-268

Poustka L, Jennen-Steinmetz C, Henze R, Vomstein K, Haffner J, Sieltjes B (2012) Fronto-temporal disconnectivity and symptom severity in children with autism spectrum disorder World Journal of Biological Psychiatry 13:269-280

Redcay E, Courchesne E (2005) When is the brain enlarged in autism? A meta-analysis of all brain size reports Biol Psychiatry 58:1-9 doi:10.1016/j.biopsych.2005.03.026

Ritvo RA et al. (2011) The Ritvo Autism asperger diagnostic scale-revised (RAADS-R): a scale to assist the diagnosis of Autism spectrum disorder in adults: an international validation study Journal of autism and developmental disorders 41:1076-1089

Roberts T et al. (2013) Left Hemisphere Diffusivity of the Arcuate Fasciculus: Influences of Autism Spectrum Disorder and Language Impairment American Journal of Neuroradiology

Rohde GK, Barnett AS, Basser PJ, Marenco S, Pierpaoli C (2004) Comprehensive approach for correction of motion and distortion in diffusion-weighted MRI Magn Reson Med 51:103-114 doi:10.1002/mrm.10677

Shukla DK, Keehn B, Müller RA (2011) Tract-specific analyses of diffusion tensor imaging show widespread white matter compromise in autism spectrum disorder Journal of Child Psychology and Psychiatry 52:286-295

Song S-K, Sun S-W, Ramsbottom MJ, Chang C, Russell J, Cross AH (2002) Dysmyelination revealed through MRI as increased radial (but unchanged axial) diffusion of water Neuroimage 17:1429-1436

Stoner R et al. (2014) Patches of Disorganization in the Neocortex of Children with Autism New England Journal of Medicine 370:1209-1219

Thakkar KN, Polli FE, Joseph RM, Tuch DS, Hadjikhani N, Barton JJ, Manoach DS (2008) Response monitoring, repetitive behaviour and anterior cingulate abnormalities in autism spectrum disorders (ASD) Brain 131:2464-2478

Thompson PM, Giedd JN, Woods RP, MacDonald D, Evans AC, Toga AW (2000) Growth patterns in the developing brain detected by using continuum mechanical tensor maps Nature 404:190-193

Travers BG et al. (2012) Diffusion tensor imaging in autism spectrum disorder: a review Autism Res 5:289-313 doi:10.1002/aur.1243

Tyszka JM, Readhead C, Bearer EL, Pautler RG, Jacobs RE (2006) Statistical diffusion tensor histology reveals regional dysmyelination effects in the shiverer mouse mutant Neuroimage 29:1058-1065

Urger SE, De Bellis MD, Hooper SR, Woolley DP, Chen SD, Provenzale J (2014) The Superior Longitudinal Fasciculus in Typically Developing Children and Adolescents: Diffusion Tensor Imaging and Neuropsychological Correlates J Child Neurol doi:10.1177/0883073813520503

Vargas DL, Nascimbene C, Krishnan C, Zimmerman AW, Pardo CA (2005) Neuroglial activation and neuroinflammation in the brain of patients with autism Annals of neurology 57:67-81

Waiter GD, Williams JHG, Murray AD, Gilchrist A, Perrett DI, Whiten A (2004) A voxel-based investigation of brain structure in male adolescents with autistic spectrum disorder Neuroimage 22:619-625

Wakana S, Jiang H, Nagae-Poetscher LM, Van Zijl PC, Mori S (2004) Fiber Tract–based Atlas of Human White Matter Anatomy 1 Radiology 230:77-87

Wassermann D, Rathi Y, Bouix S, Kubicki M, Kikinis R, Shenton M, Westin C-F White matter bundle registration and population analysis based on Gaussian processes. In: Information Processing in Medical Imaging, 2011. Springer, pp 320-332

Wechsler D (1999) Wechsler abbreviated scale of intelligence. Psychological Corporation,

Wheeler-Kingshott CAM, Cercignani M (2009) About "axial" and "radial" diffusivities Magnetic Resonance in Medicine 61:1255-1260 doi:10.1002/mrm.21965

Yeatman JD, Dougherty RF, Myall NJ, Wandell BA, Feldman HM (2012) Tract profiles of white matter properties: automating fiber-tract quantification PLoS one 7:e49790

Yeatman JD, Dougherty RF, Rykhlevskaia E, Sherbondy AJ, Deutsch GK, Wandell BA, Ben-Shachar M (2011) Anatomical properties of the arcuate fasciculus predict phonological and reading skills in children Journal of cognitive neuroscience 23:3304-3317

Zhang J et al. (2007) Evidence of slow maturation of the superior longitudinal fasciculus in early childhood by diffusion tensor imaging Neuroimage 38:239-247

Table 1. Participant demographic information.

	Autism				Control				Group difference	
	N	Mean	Range	s.d.	N	Mean	Range	s.d.	*t*-value	*p*-value
Age	42	19.9	8-40	1.27	44	20.1	8-38	1.21	0.14	0.88
Children	21	--	8-18	--	18	--	8-18	--	--	--
Adults	21	--	19-40	--	26	--	19-38	--	--	--
Verbal IQ	42	110.5	80-139	2.04	44	112.4	83-141	2.05	0.63	0.52
Performance IQ	42	112.6	85-145	2.36	44	113.7	94-137	1.86	0.37	0.70
Full-scale IQ	42	112.9	92-140	1.99	44	114.7	87-140	2.00	0.61	0.53
AQ	42	33.1	20-42	5.33	44	10.3	3-25	6.25	11.9	<0.0001
RAADS-R	21	119.2	32-181	39.7	26	44.1	3-72	23.8	8.12	<0.0001

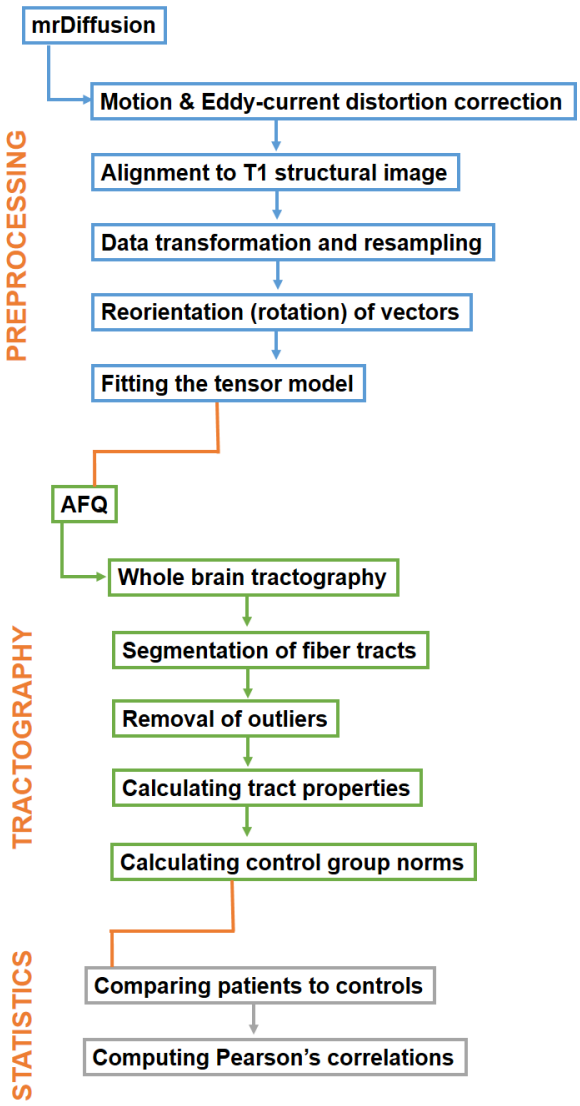

Figure 1: Flowchart depicting the main steps in the mrDiffusion preprocessing pipeline and Automated Fiber Quantification (AFQ) tractography and statistical analysis steps.

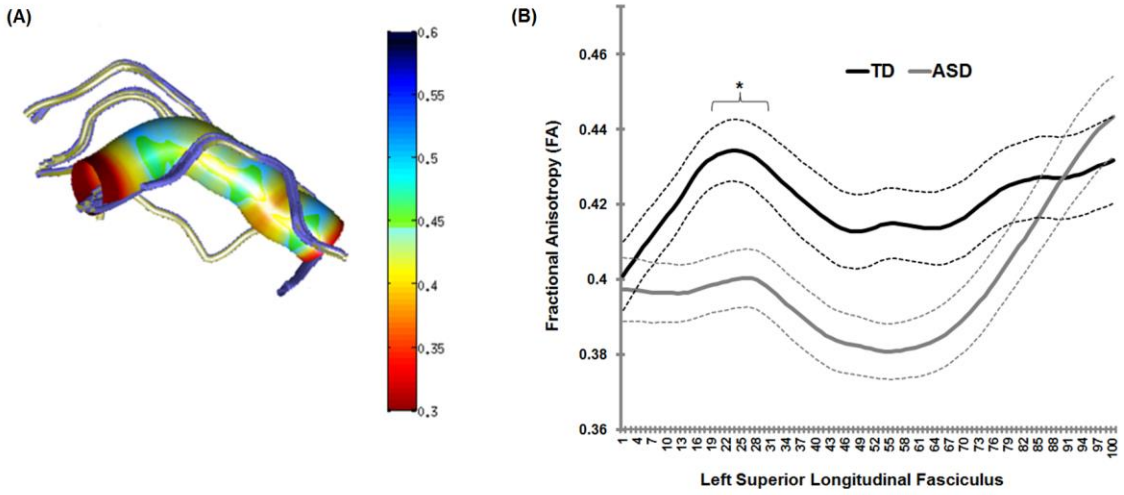

Figure 2: (A) A rendering of FA measurements for the left superior longitudinal fasciculus (LSLF) for one subject as a visualization of the tract properties; (B) Group means (solid lines) and standard deviations (dotted lines) for fractional anisotropy (FA) for the nodes along the left superior longitudinal fasciculus (LSLF) for the TD (depicted in black) and ASD (depicted in gray) groups. The cluster with a significant reduction in FA in ASD participants ($p<0.05$, corrected) is indicated with an asterisk.

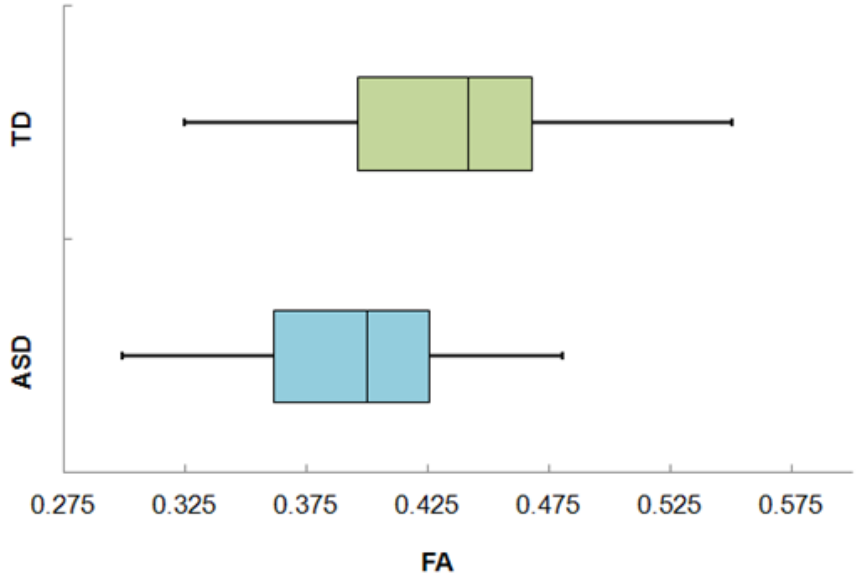

Figure 3: Mean subject fractional anisotropy (FA) values for the significant cluster on the left superior longitudinal fasciculus (LSLF) for ASD and TD groups.

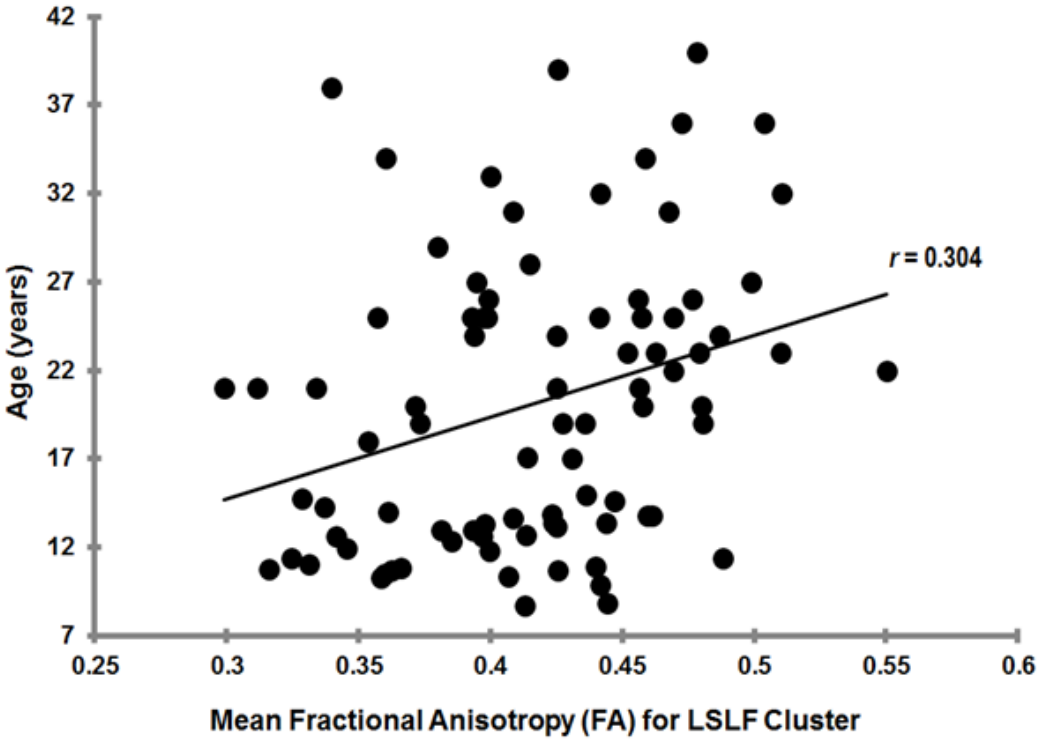

Figure 4: Graph depicting the correlation between mean fractional anisotropy (FA) values for each participant for the significant cluster on the left superior longitudinal fasciculus (LSLF) and age (r=0.304, p=0.005), indicating the development of the tract.

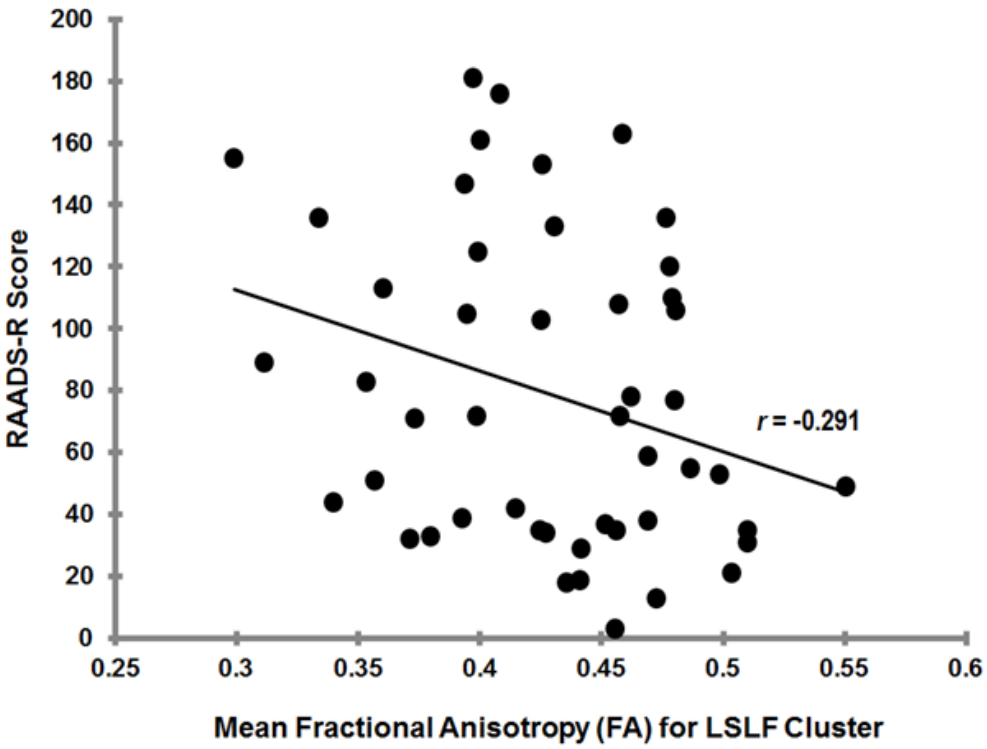

Figure 5: Graph depicting correlation between mean fractional anisotropy (FA) values for each participant for the significant cluster on the left superior longitudinal fasciculus (LSLF) and Ritvo Autism Asperger Diagnostic Scale-Revised (RAADS-R) scores of adult participants (r = -0.291, p=0.045), indicating the relationship between FA and autism symptom severity.

CEREBRAL METABOLITE ABNORMALITIES IN THE ANTERIOR CINGULATE CORTEX IN AUTISM: AN MR SPECTROSCOPY STUDY

by

LAUREN E. LIBERO, MEREDITH A. REID, DAVID M. WHITE, NOUHA SALIBI, ADRIENNE C. LAHTI, AND RAJESH K. KANA

Submitted to *Biological Psychiatry*

Format adapted for dissertation

Abstract

Background: Functional neuroimaging studies have uncovered marked abnormalities in brain functioning in individuals with autism spectrum disorder (ASD) during social cognitive tasks. The cingulate cortex in particular, especially the anterior and posterior cingulate cortices have been reported to have functional and anatomical alterations in individuals with ASD. The current study sought to examine the concentration of brain metabolites in anterior and posterior cingulate cortex in high-functioning adults with ASD.

Method: Twenty high-functioning adults with ASD and twenty age and IQ matched typically developing (TD) peers participated in this study. Proton magnetic resonance spectroscopy (1H-MRS) was used to measure the levels of N-Acetylaspartate (NAA), choline (Cho), and glutamate/glutamine (Glx), relative to creatine (Cr) level in dorsal anterior cingulate (dACC) and posterior cingulate (PCC) cortices. Groups were compared using means for the ratio of each metabolite to their respective Cr baseline.

Results: The main findings include a significant reduction in NAA/Cr in the anterior cingulate for adults with ASD, compared to their TD peers. No significant differences in Glx/Cr or Cho/Cr were found in dorsal anterior cingulate cortex. Nor were there any significant alterations in NAA/Cr, Cho/Cr, and Glx/Cr in the posterior cingulate cortex. A significant correlation between NAA/Cr and IQ in anterior cingulate in TD, but not in ASD participants, was found. In addition, a significant partial correlation between autism symptom severity and NAA/Cr for the dACC emerged for all participants.

Conclusion: Results of this study provide evidence for metabolic dysfunction in the anterior cingulate cortex in adults with ASD, suggesting poor neuronal health in that area. Poor neuronal health in dACC can have significant impact on the structural and functional integrity of this region in individuals with ASD.

Introduction

Autism spectrum disorder (ASD) is a neurodevelopmental disorder with varying levels of neuropathology spanning aberrant structure, function, and potentially poor neuronal health. Neuronal health is an integral aspect of normal brain functioning and may prove critical in understanding the pathobiology of neurodevelopmental disorders. Alterations in neurochemical levels, intracellular mechanisms, and cell metabolism can affect the integrity of neurons and ultimately the overall brain function (1). Neuronal health and alterations in neurochemical levels have been linked to neurodegenerative diseases like Alzheimer's disease, as well as traumatic brain injury and stroke (1, 2). Abnormalities associated with the integrity of neurons would impact local function within the affected area, but could also disrupt connectivity with other brain regions and the whole brain, ultimately causing the disruption of important cognitive and social functions. Such functions (e.g., social interaction, communication, decision-making) are found to be markedly impaired in individuals with ASD.

An intriguing aspect of the neuropathology of autism is that it is complex and cuts across multiple levels. Previous neuroimaging studies point to diffuse functional and anatomical abnormalities in the brains of participants with ASD (3, 4). Post mortem studies of the brain in ASD have uncovered altered cell counts and density (5, 6), abnormal cytoarchitecture (7, 8), and indications of cellular stress and inflammation (9-12). These findings demonstrate widespread neurological abnormalities in autism. However, structural and functional neuroimaging studies do not have the fine-grained resolution to gather information about neuronal health. Post mortem studies, on the other

hand, are often dependent on smaller tissue samples and are only able to link cellular abnormalities to behaviors characteristic of ASD retrospectively.

Proton Magnetic resonance spectroscopy (1H-MRS) is the only non-invasive MRI technique available for measuring tissue metabolite concentration in the living brain (13), and is often used for identifying disease-related abnormalities (14). It has proven to be an effective tool for the assessment of various pathologic conditions, including epilepsy, multiple sclerosis, stroke, cancer, and metabolic diseases (15). 1H-MRS can be applied to study the concentration of a number of neurochemicals and their role in healthy and unhealthy brains. For example, N-Acetylaspartate (NAA) is a marker, representing neuronal and axonal health and density, and reductions in the concentration of NAA can be a marker for disease (14, 16, 17). The amount of NAA as seen in 1H-MRS studies is thought to be a measure of neuronal integrity and may reflect soma integrity, the number of axon terminals (18), and/or mitochondrial function (19, 20). In a study on simian immunodeficiency virus in rhesus macaques, reductions in NAA were correlated with synaptophysin, indicating a relationship between NAA loss and poor synaptodendritic integrity (18). In addition, NAA forms the most robust spectral peak in 1H-MRS studies, as well as the most commonly studied nervous system–specific metabolite in ASD (21-23). Choline (Cho) levels represent cellular membrane proliferation and degradation (14, 17). Glutamate is related to oxidative energy production and excitatory neurotransmitter functions, while glutamine is involved with glutamate recycling and regulation of brain ammonia metabolism (17, 24). The combined Glx thus represents overall glutamate/glutamine levels and their functioning in the brain (17, 25, 26). Finally, creatine (Cr) plays a role in the central nervous system energy homeostasis, and

represents the most stable cerebral metabolite (14, 17). Thus, Cr is often used as an internal reference value, with levels of other metabolites reported in terms of their ratio to the level of Cr in the brain.

1H-MRS is a valuable technique for assessing neurobiological alterations in autism, which can potentially add deeper levels of biological insights into ASD that cannot be accomplished by traditional MRI. Previous studies have uncovered alterations in various neurochemicals in ASD, with reduced NAA in both gray and white matter serving as the most common finding (27). However, the majority of 1H-MRS studies in ASD has focused on children; and as 1H-MRS data are collected one voxel per acquisition, usually the data are limited to a few brain regions. In the current study, 1H-MRS is applied to study the dorsal anterior cingulate (dACC) and posterior cingulate (PCC) cortices. The cingulate cortex was chosen as the area of interest due to its widespread alterations in function, anatomy, and connectivity reported in autism. Previous fMRI studies in ASD have found significantly reduced ACC response for motor preparation (28), familiar faces (29), and for response inhibition (30); and significantly reduced PCC activation for spatial working memory (31), and for processing faces of familiar children (29), when compared to control individuals. Abnormalities in cingulate cortex volume (32-34) and alterations in the white matter underlying cingulate cortex (35-40) have also been reported in ASD. Functional connectivity MRI studies in ASD have also uncovered significant alterations in connectivity involving ACC and PCC during cognitive tasks (41-44) and during resting state (45-48).

Although a few previous research findings have examined the ACC using 1H-MRS, the results have been relatively inconsistent. Two studies found reduced Cho level

in left ACC (49) and reduced NAA/Cr in the ACC (50) in ASD children compared to TD children. Two additional studies examined adults with ASD, finding increased NAA/Cho in the ACC (51) and reduced Glx in right ACC (52) compared to typically developing (TD) peers. To date, the PCC has not been studied in ASD using 1H-MRS. As there are limited previous findings, with somewhat mixed results, and no previous examination of the PCC, the current study will apply 1H-MRS to investigate metabolites in the dACC and PCC of high-functioning adults with ASD. Based on functional, structural, and connectivity differences involving cingulate cortex, as well as previous 1H-MRS studies uncovering overall significantly reduced NAA in ACC (see (27) for a review), we expect to find alterations in metabolites in these regions, particularly within the ACC. In addition, to better understand the link between neurochemical markers in the brain in ASD and behavior, we will also correlate brain metabolites with neuropsychological measures. Utilizing 1H-MRS to examine the neurochemical levels in dACC and PCC in participants with ASD may provide valuable insights into the health of neurons in this disorder which in turn may shed light on the behavioral phenotype of autism.

Method & Materials

Participants

Twenty high-functioning adults with ASD (15 males/5 females; mean age: 26.8 years) and 20 typically developing (TD) peers (15 males/5 females; mean age: 24.9 years) participated in this study (see Table 1 for demographic information). The groups were equivalent on age and IQ. Full-scale IQ (FSIQ), verbal IQ (VIQ), and performance IQ (PIQ) were assessed using the Wechsler Abbreviated Scale of Intelligence (WASI) (53), handedness using the Edinburgh Handedness Inventory (54), and ASD symptoms

using the Ritvo Autism Asperger Diagnostic Scale-Revised (RAADS-R) (55). Age, FSIQ, VIQ, and PIQ were not significantly different between groups. The ASD group scored significantly higher on the RAADS-R compared to their TD peers (see Table 1). The study was approved by the Institutional Review Board of our university, and all participants provided informed consent for their participation in the study. Participants with ASD had received a previous diagnosis of an ASD based on Autism Diagnostic Interview-Revised (ADI-R) (56) symptoms and Autism Diagnostic Observation Schedule (ADOS) (57). TD participants were screened through a self-report history questionnaire to rule out neurological disorders, such as ASD, ADHD, or Tourette's Disorder, that could potentially confound the results. Several ASD participants reported taking medications, including stimulant medication (n=6), antidepressants (n=9), anxiety medication (n=1), and antipsychotic medication (n=1). Eight ASD participants reported no medications, and no TD participants reported taking medication. Finally, all participants were reported to be non-smokers.

1H-MRS Imaging

Imaging was performed on a 3T head-only scanner (Siemens Allegra, Erlangen, Germany) with a circularly polarized transmit/receive head coil. A series of sagittal, coronal, and axial T1-weighted anatomical scans were acquired for 1H-MRS voxel placement (gradient-recalled echo sequence; TR = 250ms, TE = 3.48ms, flip angle = 70 degrees, 512 x 512 matrix size, 5mm slice thickness, and 1.5mm gap). Slices were aligned to anatomical midline to control for head tilt. The 1H-MRS voxel for dACC (20 X 27 X 10 mm) was positioned around the center of the ACC, identified centrally in the gray matter above the anterior corpus callosum. The 1H-MRS voxel for PCC (20 X 27 X

20 mm) was positioned above the splenium of the corpus callosum with the long axis parallel to the parieto-occipital sulcus (See Figure 1 for sample voxel placement). These voxels were placed on the basis of the sagittal and coronal images, such that the amount of gray matter in the voxel as viewed on the T1-weighted images was maximized. Following manual shimming, to optimize field homogeneity across the voxel, water-suppressed spectra were collected with the point-resolved spectroscopy sequence (PRESS; TR/TE = 2000/80 ms, 1200 Hz spectral bandwidth, 1024 points, 128 averages, 4 min 24 s scanning time).

MRS data were processed in *jMRUI* (version 5.0) (58). The residual water peak was removed using the Hankel-Lanczos singular values decomposition filter (59). Spectra were quantified in the time domain by the AMARES algorithm (advanced method for accurate, robust, and efficient spectral fitting) (60). AMARES is a quantification method that has been used to compute the spectral fitting parameters (e.g., amplitudes, frequencies, and linewidths for the metabolite peaks). Ratios of NAA, Cho, Cr, and Glx, with respect to Cr were calculated using the amplitudes of the time domain signal resulting from the AMARES analysis. Cramer-Rao lower bounds (CRLB) were used as a measure of uncertainty of the fitting procedure. Inclusion in analyses required ratios to have CRLB less than 20%; all participants' ratios were within these limits and were included in the final analyses.

Voxel-based Morphometry

Anatomical images were acquired using high resolution T1-weighted scans using a 160 slice 3D magnetization-prepared rapid acquisition gradient-echo (MPRAGE) volume scan with a TR = 200ms, TE = 3.34 ms, flip angle = 12^0, FOV = 25.6 cm, 256 x

256 matrix size, and 1mm slice thickness. Anatomical data were processed using Statistical Parametric Mapping 8 (SPM8; Wellcome Trust Center for Neuroimaging) in MATLAB version 7.11.0 (Mathworks). Each participant's T1-weighted MPRAGE image was segmented into gray matter (GM), white matter (WM), and cerebrospinal fluid (CSF) using the segmentation routine in SPM8. Using native-space masks, we calculated the total GM, WM, and CSF volumes for the dACC and PCC regions of interest (ROI) using a script adapted from John's SPM Gems (http://www-personal.umich.edu/~nichols/JohnsGems.html) in MATLAB. The GM, WM, and CSF content were obtained in order to control for the tissue concentration of our acquired 1H-MRS voxels.

Statistical Analyses

Statistical analyses were performed in SPSS (version 11.5). Demographics were compared using independent samples *t*-tests. 1H-MRS ratios were compared using ANCOVA, covarying for age, GM content, and WM content. In exploratory analyses, Pearson's correlation coefficients were used to evaluate the relationship between metabolites and age and clinical measures (FSIQ, VIQ, PIQ, RAADS-R).

Results

The current study sought to examine the level of brain metabolites in anterior and posterior cingulate cortices in high-functioning adults with ASD. Our main findings include a significant reduction in NAA/Cr in the dACC for adults with ASD, compared to their TD peers, and a significant correlation between NAA/Cr and FSIQ in dACC in TD adults, but not in ASD adults. In addition, a significant partial correlation between NAA/Cr for dACC and RAADS-R scores (controlling for FSIQ) emerged for all

participants. No significant differences in Glx/Cr or Cho/Cr were found in dACC, and no significant alterations in neurochemicals were found in PCC between groups.

Metabolite Concentration

For the dACC, the mean NAA/Cr ratio for the ASD group was significantly reduced compared to the TD group, while there were no statistically significant group differences in Glx/Cr and Cho/Cr ratios (see Table 2). Mean amplitude for Cr, which was used as a reference, was not significantly different between the groups ($F = 3.03$, $p = 0.09$). For the PCC region, metabolite ratios did not significantly differ between the groups (see Table 2), and the mean amplitudes for Cr were not significantly different between groups ($F = 1.31$, $p = 0.25$).

NAA/Cr for the dACC was significantly positively correlated with FSIQ in TD adults ($r(18)= 0.55$, $p = 0.027$) but not in ASD adults ($r(18)=0.00$, $p = 0.99$) (See Figure 2). However, the difference in correlation coefficients between groups was not significant ($Z= -1.72$, $p = 0.08$). NAA/Cr for the dACC was also marginally significant in its correlation with age for TD adults ($r(18)= -0.42$, $p = 0.06$) and not significantly correlated with age for ASD adults ($r(18)=0.02$, $p = 0.92$). A significant negative correlation was found for all subjects between NAA/Cr for the dACC and symptom severity (RAADS-R) ($r(38)= -0.35$, $p = 0.02$) (See Figure 3). No significant correlations were found for either group for the dACC Cho/Cr or Glx/Cr levels and VIQ or PIQ. No significant correlations were found for either group with any of the metabolite ratios for PCC and PIQ or VIQ, and RAADS-R scores.

Discussion

Our finding of significantly reduced levels of NAA/Cr in dACC is in line with previous reports of reduced NAA concentration in adults with autism in the ACC (50), hippocampal-amygdala formation (61), and frontal, parietal, and occipital cortices (62). The reduction in NAA level suggests the possibility of continuing neuronal compromise in ACC (27). This is particularly important considering the cingulate cortex abnormalities in ASD reported widely in studies using functional MRI (48, 63, 64), MRI-based morphometry (32, 65), diffusion tensor imaging (35-40), PET (33, 65), single-photon emission computed tomography (66), and postmortem studies (67). Reduced NAA in ASD individuals has also been found in a number of additional brain areas in children and adolescents, including hippocampus-amygdala formation (68-70), thalamus (71, 72), cerebellum (69, 73, 74), frontal cortex (62, 73), temporal lobes (73, 75, 76), occipital cortex (73), and basal ganglia (76). However, all of these studies investigated metabolite concentrations in children and adolescents with ASD. The findings of the current study shed light on the neurochemical concentrations in relatively underexplored population of adults with ASD.

NAA is a neurochemical that is synthesized in the mitochondria of neurons, and it is present in most neuronal cell types, although it is highly concentrated in gray matter (2). The primary roles for NAA in the brain have been suggested to include facilitating energy metabolism in neuronal mitochondria, serving as a source of acetate for myelin synthesis in oligodendrocytes, and as a precursor for the biosynthesis of N-acetylaspartylglutamate (which modulates neurotransmitter release from the synapse (77, 78)) (2, 79). Within the 1H-MRS spectra, NAA serves as the largest peak, and it has been

shown to be fairly stable in healthy adults longitudinally (80). Thus, significant reductions in NAA are typically indicative of disease or neuronal damage. Indeed, reductions in NAA have been found in cases of brain cancer, multiple sclerosis, brain injury, and Alzheimer's Disease (81). NAA level decreases when there is tissue destruction and reversibly so when the neuronal tissue is suffering (82) thereby non-specifically reflecting the general state of the health of neurons. The significant reduction in NAA/Cr in dACC found in the current study could potentially be underscored by neuronal or axonal damage in that region in ASD. One previous study using postmortem and fresh-frozen tissue samples from ACC in individuals with ASD uncovered significantly greater astroglial reactions (and astrogliosis in some cases) and increases in proinflammatory and modulatory cytokines, compared to control tissue samples (9). Higher astroglial reactions and greater inflammatory processes, representing tissue damage and potential inhibition of neuronal repair, in cingulate cortex in ASD could support significant reductions in NAA measured using 1H-MRS. Reductions in NAA/Cr may also be indicative of a mitochondrial dysfunction, given the role of NAA in mitochondrial energy metabolism within neurons. Mitochondrial disease as well as biomarkers for mitochondrial dysfunction are prevalent at much higher rates in ASD children compared to the general population (see (83) for a review). In addition, altered expression of genes encoding the mitochondrial aspartate/glutamate carrier (AGC1) has been associated with ASD, marking a potential link between neuronal dysfunction and NAA levels in ASD (84-86). Our finding of reduced NAA/Cr in ASD adults may support the possibility of abnormal mitochondrial function in the brains of affected individuals.

NAA has also been found to predict the severity of illness in various neurodegenerative disorders (87-89) and to correlate with cognitive function in brain disorders (90, 91). Furthermore, reversals of NAA reduction have been observed with treatment in other brain disorders. For example, recovery of NAA/Cr levels (indicating a reversal of axonal damage) was uncovered in patients with multiple sclerosis after treatment of glatiramer acetate (an immunomodulator) (92) and fluoxetine (a selective serotonin reuptake inhibitor [SSRI]) (93). Significant increase in NAA/Cr was also found in obsessive compulsive disorder patients after twelve weeks of SSRI treatment (94). In addition, improvements in NAA levels due to drug treatments have also been linked to improvement in symptomatology for a few disorders, including increased NAA and improved symptoms in generalized anxiety disorder following riluzole (a glutamate release inhibitor) (95) and increased NAA with improved cognition in AIDS patients following highly active retroviral therapy (96). These findings have strong implications for the treatment of ASD, indicating the potential of pharmacological intervention to improve levels of NAA/Cr and possibly the behavior phenotype. Therefore, knowledge of NAA levels in autism can not only provide conceptual breakthroughs in basic neurobiology of autism, but also provide important insights into potential treatment options.

The current study did not find any significant differences in Glx/Cr between ASD and TD adults. Glutamate is the major excitatory neurotransmitter in the brain, and is strongly related to neurodevelopment (97). Reductions in Glx could have implications for cellular migration and signaling in ASD. In fact, a few studies have indicated glutamate receptor genes are associated with ASD (98-101). One study found altered glutamate

serum levels in adults with ASD (102), and two previous 1H-MRS studies found reduced Glx in children (73) and adults (52) with ASD. However, previous meta-analyses of 1H-MRS studies indicate reduced NAA to be the most consistent finding in ASD (27, 103). While a robust difference in NAA/Cr emerged between groups, our results do not indicate a reduction of Glx/Cr in the dACC in ASD adults. Despite its implications for brain function in ASD, based on our findings, significant alterations in glutamate may not be the mechanism specific to impaired anterior cingulate function.

It should also be noted that the current study did not find significant group differences in any of the measured metabolite levels in PCC. No previous study, to our knowledge, has examined this region using 1H-MRS in ASD. The lack of differences in metabolite level in PCC is surprising given previous findings of altered brain activity in this region in participants with ASD (29, 31). Nevertheless, one postmortem study of the PCC in ASD found no significant difference in densities of parvalbumin immunotractive interneurons and calbindin immunoreactive interneurons, although significantly abnormal cytoarchitecture was found in almost all cases (104). Another similar postmortem study revealed significant reductions in the number of GABA receptors, and higher binding affinity in the superficial layers of PCC for the ASD group (105). Although alterations in the function (29, 31) and structure (32, 34) of PCC in ASD have been found, the current study did not find significant group differences in the mean levels of neurochemicals in this region. It is possible that the findings related to cortical structure and function are stemming from other sources (e.g., poor functional and/or structural connectivity with other brain regions), and may not be specific to altered concentration of neurochemicals. It should also be noted that the anterior and posterior cortices are distinct in both their

function and cellular structure (106, 107), so abnormality in one region may not necessarily overlap with the other. Since no previous study has examined metabolite level in PCC in participants with ASD using 1H-MRS, it will be interesting to see the replication of this finding and its underlying mechanisms in future studies.

As neurochemical levels can determine neuronal health, it is possible that it may predict cognitive abilities, such as intelligence. We found a significant correlation between FSIQ and NAA/Cr for dACC in TD adults, but not ASD adults. The correlation between FSIQ and NAA/Cr in our control adults (r=0.55) is in fact very close to the correlation found in a previous study between NAA in occiptio-parietal areas and FSIQ (r=0.52) for healthy adults (108). As NAA is linked to neuronal health, it is natural that better neuronal health should indicate better overall brain function. For instance, white matter NAA has been shown to positively correlate with intelligence and with better cognitive performance (108-110). A positive correlation approaching significance was found for age and NAA/Cr for dACC in TD adults, but not in ASD adults. The lack of correlation of age and IQ with NAA levels in autism is consistent with the findings of previous studies showing an absence of such relationship in individuals with autism (111). Also, the marginally significant difference in age-related correlations may also be due to the limited age range of participants in the current study. Indeed, a meta-analysis of age-related changes from 1H-MRS findings in ASD uncovered decreased NAA in frontal, temporal, parietal, hippocampus-amygdala formation, and thalamus with age for children, but no significant reductions with age for adults with ASD (103). It is possible that a metabolic disruption in tissue in ASD develops early on, and is established before reaching adulthood. Thus, no significant reductions with age in ASD adults are noted. It

will be important for future studies to investigate the onset of metabolite abnormalities in children, and the developmental trajectory of neurochemicals across the lifespan in ASD. This could inform about the optimal window for potential treatment of NAA abnormalities in ASD. ASD symptom severity (measured by RAADS-R scores) was significantly negatively correlated with NAA/Cr for the dACC. In this case, lower levels of NAA/Cr were associated with greater ASD symptoms. This finding points to the potential link between levels of NAA in ACC and autistic behavior. This is in line with one previous study finding a correlation between NAA/Cr levels in ACC in children with ASD and their social quotient scores, with lower NAA/Cr levels for those participants with poorer social skills (50). A few other studies have found similar findings, linking levels of NAA in the brain with ASD behaviors (75, 112). Together, these studies suggest a potential connection between metabolic abnormalities in the brain in ASD and impaired social functioning in individuals.

Despite using a well-matched ASD and TD participant pool on different levels, our study also had a few limitations, such as medication use in some of the ASD participants. Medication could potentially alter metabolite levels in the brain, and possible differences in neurochemical concentrations could have been changed or masked by drug use. Future studies should examine potential drug effects in ASD. In addition, the current study was limited to high-functioning adults with average and above-average IQ scores. Perhaps more pronounced differences in metabolite levels could be uncovered (and their association with behavior better elucidated) with the inclusion of lower functioning adults. Finally, 1H-MRS data acquisition is restricted to only one isolated voxel at a time. Nevertheless, the findings of this study (lower levels of NAA/Cr in

dACC, but not in PCC, in adults with ASD provide evidence for significant metabolic dysfunction in dACC in ASD which may have an impact on neuronal quality, myelination, and connectivity. The relationship between NAA level and symptom severity suggests that alterations in neurochemicals may potentially impact symptom severity and social behavior in affected individuals. In all, this study provides evidence for abnormal levels of NAA in anterior cingulate cortex in ASD suggesting subtle cellular pathology intrinsic to dACC. This finding is important not only in better understanding the basic neuropathology in autism, but also in thinking about targeted clinical and pharmacological intervention.

Acknowledgments

The authors would like to thank the UAB College of Arts and Sciences Interdisciplinary Innovation Award to RK. The authors would also like to thank Thomas DeRamus, Hrishikesh Deshpande, and Dr. Nina Kraguljac for their assistance in the data collection and comments on earlier versions of this manuscript.

References

1. Isacson O (1993): On neuronal health. *Trends in Neurosciences*. 16:306-308.
2. Moffett JR, Ross B, Arun P, Madhavarao CN, Namboodiri A (2007): N-Acetylaspartate in the CNS: From neurodiagnostics to neurobiology. *Progress in neurobiology*. 81:89-131.
3. Anagnostou E, Taylor M (2011): Review of neuroimaging in autism spectrum disorders: what have we learned and where we go from here. *Molecular Autism*. 2:4.
4. Minshew NJ, Williams DL (2007): The new neurobiology of autism: cortex, connectivity, and neuronal organization. *Archives of neurology*. 64:945.
5. Schumann CM, Amaral DG (2006): Stereological analysis of amygdala neuron number in autism. *The journal of Neuroscience*. 26:7674-7679.
6. Courchesne E, Mouton PR, Calhoun ME, et al. (2011): Neuron number and size in prefrontal cortex of children with autism. *JAMA*. 306:2001-2010.
7. Buxhoeveden DP, Semendeferi K, Buckwalter J, Schenker N, Switzer R, Courchesne E (2006): Reduced minicolumns in the frontal cortex of patients with autism. *Neuropathology and Applied Neurobiology*. 32:483-491.
8. Casanova MF, Buxhoeveden DP, Switala AE, Roy E (2002): Minicolumnar pathology in autism. *Neurology*. 58:428-432.
9. Vargas DL, Nascimbene C, Krishnan C, Zimmerman AW, Pardo CA (2005): Neuroglial activation and neuroinflammation in the brain of patients with autism. *Annals of Neurology*. 57:67-81.
10. Sajdel-Sulkowska E, Xu M, McGinnis W, Koibuchi N (2011): Brain Region-Specific Changes in Oxidative Stress and Neurotrophin Levels in Autism Spectrum Disorders (ASD). *The Cerebellum*. 10:43-48.
11. López-Hurtado E, Prieto JJ (2008): A microscopic study of language-related cortex in autism. *American Journal of Biochemistry & Biotechnology*. 4.
12. Morgan JT, Chana G, Pardo CA, Achim C, Semendeferi K, Buckwalter J, et al. (2010): Microglial activation and increased microglial density observed in the dorsolateral prefrontal cortex in autism. *Biological psychiatry*. 68:368-376.
13. Stanley JA (2002): In vivo magnetic resonance spectroscopy and its application to neuropsychiatric disorders. *Canadian journal of psychiatry Revue canadienne de psychiatrie*. 47:315-326.
14. Fayed N, Olmos S, Morales H, Modrego PJ (2006): Physical basis of magnetic resonance spectroscopy and its application to central nervous system diseases. *American Journal of Applied Sciences*. 3:1836.
15. Ross B, Bluml S (2001): Magnetic resonance spectroscopy of the human brain. *The Anatomical Record*. 265:54-84.
16. Meyerhoff DJ, MacKay S, Bachman L, Poole N, Dillon W, Weiner M, et al. (1993): Reduced brain N-acetylaspartate suggests neuronal loss in cognitively impaired human immunodeficiency virus-seropositive individuals In vivo 1H magnetic resonance spectroscopic imaging. *Neurology*. 43:509-509.
17. Maddock RJ, Buonocore MH (2012): MR spectroscopic studies of the brain in psychiatric disorders. *Brain Imaging in Behavioral Neuroscience*: Springer, pp 199-251.
18. Lentz MR, Kim JP, Westmoreland SV, Greco JB, Fuller RA, Ratai EM, et al. (2005): Quantitative neuropathologic correlates of changes in ratio of N-acetylaspartate to creatine in macaque brain. *Radiology*. 235:461-468.
19. Bates TE, Strangward M, Keelan J, Davey GP, Munro PM, Clark JB (1996): Inhibition of N-acetylaspartate production: implications for 1H MRS studies in vivo. *Neuroreport*. 7:1397-1400.

20. Stork C, Renshaw P (2005): Mitochondrial dysfunction in bipolar disorder: evidence from magnetic resonance spectroscopy research. *Molecular psychiatry*. 10:900-919.
21. Tallan HH, Moore S, Stein WH (1956): N-Acetyl-L-aspartic acid in brain. *The Journal of biological chemistry*. 219:257-264.
22. Urenjak J, Williams SR, Gadian DG, Noble M (1993): Proton nuclear magnetic resonance spectroscopy unambiguously identifies different neural cell types. *The Journal of neuroscience*. 13:981-989.
23. Soares D, Law M (2009): Magnetic resonance spectroscopy of the brain: review of metabolites and clinical applications. *Clinical radiology*. 64:12-21.
24. Waagepetersen H, Sonnewald U, Schousboe A (2007): 1 Glutamine, Glutamate, and GABA: Metabolic Aspects. *Handbook of Neurochemistry and Molecular Neurobiology*: Springer, pp 1-21.
25. Rothman DL, Behar KL, Hyder F, Shulman RG (2003): In vivo NMR studies of the glutamate neurotransmitter flux and neuroenergetics: implications for brain function. *Annual review of physiology*. 65:401-427.
26. Yüksel C, Öngür D (2010): Magnetic resonance spectroscopy studies of glutamate-related abnormalities in mood disorders. *Biological psychiatry*. 68:785-794.
27. Ipser JC, Syal S, Bentley J, Adnams CM, Steyn B, Stein DJ (2012): 1H-MRS in autism spectrum disorders: a systematic meta-analysis. *Metabolic brain disease*. 27:275-287.
28. Rinehart NJ, Bradshaw JL, Brereton AV, Tonge BJ (2001): Movement preparation in high-functioning autism and Asperger disorder: a serial choice reaction time task involving motor reprogramming. *Journal of autism and developmental disorders*. 31:79-88.
29. Pierce K, Redcay E (2008): Fusiform function in children with an autism spectrum disorder is a matter of “who”. *Biological psychiatry*. 64:552-560.
30. Kana RK, Keller TA, Minshew NJ, Just MA (2007): Inhibitory control in high-functioning autism: decreased activation and underconnectivity in inhibition networks. *Biological psychiatry*. 62:198-206.
31. Luna B, Minshew N, Garver K, Lazar N, Thulborn K, Eddy W, et al. (2002): Neocortical system abnormalities in autism An fMRI study of spatial working memory. *Neurology*. 59:834-840.
32. Abell F, Krams M, Ashburner J, Passingham R, Friston K, Frackowiak R, et al. (1999): The neuroanatomy of autism: a voxel-based whole brain analysis of structural scans. *Neuroreport*. 10:1647-1651.
33. Haznedar MM, Buchsbaum MS, Metzger M, Solimando A, Spiegel-Cohen J, Hollander E (1997): Anterior cingulate gyrus volume and glucose metabolism in autistic disorder. *American Journal of Psychiatry*. 154:1047-1050.
34. Schumann CM, Bloss CS, Barnes CC, Wideman GM, Carper RA, Akshoomoff N, et al. (2010): Longitudinal magnetic resonance imaging study of cortical development through early childhood in autism. *The Journal of Neuroscience*. 30:4419-4427.
35. Barnea-Goraly N, Kwon H, Menon V, Eliez S, Lotspeich L, Reiss AL (2004): White matter structure in autism: preliminary evidence from diffusion tensor imaging. *Biological psychiatry*. 55:323-326.
36. Jou RJ, Jackowski AP, Papademetris X, Rajeevan N, Staib LH, Volkmar FR (2011): Diffusion tensor imaging in autism spectrum disorders: preliminary evidence of abnormal neural connectivity. *Australian and New Zealand Journal of Psychiatry*. 45:153-162.

37. Kumar A, Sundaram SK, Sivaswamy L, Behen ME, Makki MI, Ager J, et al. (2010): Alterations in frontal lobe tracts and corpus callosum in young children with autism spectrum disorder. *Cerebral cortex*. 20:2103-2113.
38. Noriuchi M, Kikuchi Y, Yoshiura T, Kira R, Shigeto H, Hara T, et al. (2010): Altered white matter fractional anisotropy and social impairment in children with autism spectrum disorder. *Brain research*. 1362:141-149.
39. Pardini M, Garaci F, Bonzano L, Roccatagliata L, Palmieri M, Pompili E, et al. (2009): White matter reduced streamline coherence in young men with autism and mental retardation. *European journal of neurology*. 16:1185-1190.
40. Thakkar KN, Polli FE, Joseph RM, Tuch DS, Hadjikhani N, Barton JJ, et al. (2008): Response monitoring, repetitive behaviour and anterior cingulate abnormalities in autism spectrum disorders (ASD). *Brain*. 131:2464-2478.
41. Kleinhans NM, Richards T, Sterling L, Stegbauer KC, Mahurin R, Johnson LC, et al. (2008): Abnormal functional connectivity in autism spectrum disorders during face processing. *Brain*. 131:1000-1012.
42. Agam Y, Joseph RM, Barton JJ, Manoach DS (2010): Reduced cognitive control of response inhibition by the anterior cingulate cortex in autism spectrum disorders. *Neuroimage*. 52:336-347.
43. Solomon M, Ozonoff SJ, Ursu S, Ravizza S, Cummings N, Ly S, et al. (2009): The neural substrates of cognitive control deficits in autism spectrum disorders. *Neuropsychologia*. 47:2515-2526.
44. Shih P, Keehn B, Oram JK, Leyden KM, Keown CL, Müller R-A (2011): Functional differentiation of posterior superior temporal sulcus in autism: a functional connectivity magnetic resonance imaging study. *Biological psychiatry*. 70:270-277.
45. Cherkassky VL, Kana RK, Keller TA, Just MA (2006): Functional connectivity in a baseline resting-state network in autism. *Neuroreport*. 17:1687-1690.
46. Monk CS, Peltier SJ, Wiggins JL, Weng S-J, Carrasco M, Risi S, et al. (2009): Abnormalities of intrinsic functional connectivity in autism spectrum disorders. *Neuroimage*. 47:764-772.
47. Weng S-J, Wiggins JL, Peltier SJ, Carrasco M, Risi S, Lord C, et al. (2010): Alterations of resting state functional connectivity in the default network in adolescents with autism spectrum disorders. *Brain Research*. 1313:202-214.
48. Assaf M, Jagannathan K, Calhoun VD, Miller L, Stevens MC, Sahl R, et al. (2010): Abnormal functional connectivity of default mode sub-networks in autism spectrum disorder patients. *Neuroimage*. 53:247-256.
49. Levitt JG, O'Neill J, Blanton RE, Smalley S, Fadale D, McCracken JT, et al. (2003): Proton magnetic resonance spectroscopic imaging of the brain in childhood autism. *Biological psychiatry*. 54:1355-1366.
50. Fujii E, Mori K, Miyazaki M, Hashimoto T, Harada M, Kagami S (2010): Function of the frontal lobe in autistic individuals: a proton magnetic resonance spectroscopic study. *J Med Invest*. 57:35-44.
51. Oner O, Devrimci-Ozguven H, Oktem F, Yagmurlu B, Baskak B, Munir K (2007): Proton MR spectroscopy: higher right anterior cingulate N-acetylaspartate/choline ratio in Asperger syndrome compared with healthy controls. *American Journal of Neuroradiology*. 28:1494-1498.
52. Bernardi S, Anagnostou E, Shen J, Kolevzon A, Buxbaum JD, Hollander E, et al. (2011): In vivo 1H-magnetic resonance spectroscopy study of the attentional networks in autism. *Brain research*. 1380:198-205.
53. Wechsler D (1999): *Wechsler abbreviated scale of intelligence*. Psychological Corporation.

54. Oldfield RC (1971): The assessment and analysis of handedness: the Edinburgh inventory. *Neuropsychologia*. 9:97-113.
55. Ritvo RA, Ritvo ER, Guthrie D, Ritvo MJ, Hufnagel DH, McMahon W, et al. (2011): The Ritvo Autism asperger diagnostic scale-revised (RAADS-R): a scale to assist the diagnosis of Autism spectrum disorder in adults: an international validation study. *Journal of autism and developmental disorders*. 41:1076-1089.
56. Rutter M, Le Couteur A, Lord C (2003): Autism diagnostic interview-revised. *Los Angeles, CA: Western Psychological Services*.
57. Lord C, Risi S, Lambrecht L, Cook Jr EH, Leventhal BL, DiLavore PC, et al. (2000): The Autism Diagnostic Observation Schedule—Generic: A standard measure of social and communication deficits associated with the spectrum of autism. *Journal of autism and developmental disorders*. 30:205-223.
58. Naressi A, Couturier C, Devos J, Janssen M, Mangeat C, De Beer R, et al. (2001): Java-based graphical user interface for the MRUI quantitation package. *Magnetic Resonance Materials in Physics, Biology and Medicine*. 12:141-152.
59. Pijnappel W, Van den Boogaart A, De Beer R, Van Ormondt D (1992): SVD-based quantification of magnetic resonance signals. *Journal of Magnetic Resonance (1969)*. 97:122-134.
60. Vanhamme L, van den Boogaart A, Van Huffel S (1997): Improved method for accurate and efficient quantification of MRS data with use of prior knowledge. *Journal of Magnetic Resonance*. 129:35-43.
61. Suzuki K, Nishimura K, Sugihara G, Nakamura K, Tsuchiya KJ, Matsumoto K, et al. (2010): Metabolite alterations in the hippocampus of high-functioning adult subjects with autism. *The International Journal of Neuropsychopharmacology*. 13:529-534.
62. Kleinhans NM, Schweinsburg BC, Cohen DN, Müller R-A, Courchesne E (2007): N-acetyl aspartate in autism spectrum disorders: Regional effects and relationship to fMRI activation. *Brain research*. 1162:85-97.
63. Chiu PH, Kayali MA, Kishida KT, Tomlin D, Klinger LG, Klinger MR, et al. (2008): Self responses along cingulate cortex reveal quantitative neural phenotype for high-functioning autism. *Neuron*. 57:463-473.
64. Lombardo MV, Chakrabarti B, Bullmore ET, Sadek SA, Pasco G, Wheelwright SJ, et al. (2010): Atypical neural self-representation in autism. *Brain*. 133:611-624.
65. Haznedar MM, Buchsbaum MS, Wei T-C, Hof PR, Cartwright C, Bienstock CA, et al. (2000): Limbic circuitry in patients with autism spectrum disorders studied with positron emission tomography and magnetic resonance imaging. *American Journal of Psychiatry*. 157:1994-2001.
66. Ohnishi T, Matsuda H, Hashimoto T, Kunihiro T, Nishikawa M, Uema T, et al. (2000): Abnormal regional cerebral blood flow in childhood autism. *Brain*. 123:1838-1844.
67. Bauman ML, Kemper TL (1994): Neuroanatomic observations of the brain in autism. *The neurobiology of autism*.119-145.
68. Otsuka H, Harada M, Mori K, Hisaoka S, Nishitani H (1999): Brain metabolites in the hippocampus-amygdala region and cerebellum in autism: an 1H-MR spectroscopy study. *Neuroradiology*. 41:517-519.
69. Mori K, Hashimoto T, Harada M, Yoneda Y, Shimakawa S, Fujii E, et al. (2001): Proton magnetic resonance spectroscopy of the autistic brain. *Brain and Development*. 33:329-335.
70. Gabis L, Huang W, Azizian A, DeVincent C, Tudorica A, Kesner-Baruch Y, et al. (2008): 1H-magnetic resonance spectroscopy markers of cognitive and language ability in clinical subtypes of autism spectrum disorders. *Journal of child neurology*. 23:766-774.

71. Hardan AY, Minshew NJ, Melhem NM, Srihari S, Jo B, Bansal R, et al. (2008): An MRI and proton spectroscopy study of the thalamus in children with autism. *Psychiatry Research: Neuroimaging*. 163:97-105.
72. Perich-Alsina J, Aduna dPM, Valls A, Muñoz-Yunta J (2002): Thalamic spectroscopy using magnetic resonance in autism. *Revista de neurologia*. 34:S68-71.
73. DeVito TJ, Drost DJ, Neufeld RW, Rajakumar N, Pavlosky W, Williamson P, et al. (2007): Evidence for cortical dysfunction in autism: a proton magnetic resonance spectroscopic imaging study. *Biological Psychiatry*. 61:465-473.
74. Chugani DC, Sundram BS, Behen M, Lee M-L, Moore GJ (1999): Evidence of altered energy metabolism in autistic children. *Progress in Neuro-Psychopharmacology and Biological Psychiatry*. 23:635-641.
75. Endo T, Shioiri T, Kitamura H, Kimura T, Endo S, Masuzawa N, et al. (2007): Altered chemical metabolites in the amygdala-hippocampus region contribute to autistic symptoms of autism spectrum disorders. *Biological Psychiatry*. 62:1030-1037.
76. Friedman S, Shaw D, Artru A, Richards T, Gardner J, Dawson G, et al. (2003): Regional brain chemical alterations in young children with autism spectrum disorder. *Neurology*. 60:100-107.
77. Xi Z-X, Baker DA, Shen H, Carson DS, Kalivas PW (2002): Group II metabotropic glutamate receptors modulate extracellular glutamate in the nucleus accumbens. *Journal of Pharmacology and Experimental Therapeutics*. 300:162-171.
78. Zhao J, Ramadan E, Cappiello M, Wroblewska B, Bzdega T, Neale JH (2001): NAAG inhibits KCl-induced [3H]-GABA release via mGluR3, cAMP, PKA and L-type calcium conductance. *European Journal of Neuroscience*. 13:340-346.
79. Madhavarao CN, Namboodiri AM (2006): NAA synthesis and functional roles. *N-Acetylaspartate*: Springer, pp 49-66.
80. Rigotti DJ, Kirov II, Djavadi B, Perry N, Babb JS, Gonen O (2011): Longitudinal whole-brain N-acetylaspartate concentration in healthy adults. *American Journal of Neuroradiology*. 32:1011-1015.
81. Danielsen E, Ross B (1999): Magnetic resonance spectroscopy diagnosis of neurological diseases., 1999. New York: Marcel Dekker, Inc.
82. De Stefano N, Matthews PM, Fu L, Narayanan S, Stanley J, Francis GS, et al. (1998): Axonal damage correlates with disability in patients with relapsing-remitting multiple sclerosis. Results of a longitudinal magnetic resonance spectroscopy study. *Brain*. 121:1469-1477.
83. Rossignol D, Frye R (2012): Mitochondrial dysfunction in autism spectrum disorders: a systematic review and meta-analysis. *Molecular psychiatry*. 17:290-314.
84. Ramoz N, Reichert JG, Smith CJ, Silverman JM, Bespalova IN, Davis KL, et al. (2004): Linkage and association of the mitochondrial aspartate/glutamate carrier SLC25A12 gene with autism. *American Journal of Psychiatry*. 161:662-669.
85. Segurado R, Conroy J, Meally E, Fitzgerald M, Gill M, Gallagher L (2005): Confirmation of association between autism and the mitochondrial aspartate/glutamate carrier SLC25A12 gene on chromosome 2q31. *American Journal of Psychiatry*. 162:2182-2184.
86. Palmieri L, Papaleo V, Porcelli V, Scarcia P, Gaita L, Sacco R, et al. (2010): Altered calcium homeostasis in autism-spectrum disorders: evidence from biochemical and genetic studies of the mitochondrial aspartate/glutamate carrier AGC1. *Molecular psychiatry*. 15:38-52.
87. Brooks W, Sabet A, Sibbitt Jr W, Barker P, Van Zijl P, Duyn J, et al. (1997): Neurochemistry of brain lesions determined by spectroscopic imaging in systemic lupus erythematosus. *The Journal of rheumatology*. 24:2323-2329.

88. Brooks WM, Stidley CA, Petropoulos H, Jung RE, Weers DC, Friedman SD, et al. (2000): Metabolic and cognitive response to human traumatic brain injury: a quantitative proton magnetic resonance study. *Journal of neurotrauma*. 17:629-640.
89. Friedman SD, Brooks WM, Jung RE, Hart BL, Yeo RA (1998): Proton MR spectroscopic findings correspond to neuropsychological function in traumatic brain injury. *American Journal of Neuroradiology*. 19:1879-1885.
90. Ross AJ, Sachdev PS (2004): Magnetic resonance spectroscopy in cognitive research. *Brain Research Reviews*. 44:83-102.
91. Ross AJ, Sachdev PS, Wen W, Valenzuela MJ, Brodaty H (2005): Cognitive correlates of 1H MRS measures in the healthy elderly brain. *Brain research bulletin*. 66:9-16.
92. Khan O, Shen Y, Caon C, Bao Fe, Ching W, Reznar M, et al. (2005): Axonal metabolic recovery and potential neuroprotective effect of glatiramer acetate in relapsing-remitting multiple sclerosis. *Multiple Sclerosis*. 11:646-651.
93. Mostert JP, Sijens PE, Oudkerk M, De Keyser J (2006): Fluoxetine increases cerebral white matter NAA/Cr ratio in patients with multiple sclerosis. *Neuroscience letters*. 402:22-24.
94. Jang J, Kwon J, Jang D, Moon W-J, Lee J-M, Ha T, et al. (2006): A proton MRSI study of brain N-acetylaspartate level after 12 weeks of citalopram treatment in drug-naive patients with obsessive-compulsive disorder. *American Journal of Psychiatry*. 163:1202-1207.
95. Mathew SJ, Price RB, Mao X, Smith EL, Coplan JD, Charney DS, et al. (2008): Hippocampal N-Acetylaspartate Concentration and Response to Riluzole in Generalized Anxiety Disorder. *Biological psychiatry*. 63:891-898.
96. Stankoff B, Tourbah A, Suarez S, Turell E, Stievenart J, Payan C, et al. (2001): Clinical and spectroscopic improvement in HIV-associated cognitive impairment. *Neurology*. 56:112-115.
97. Coyle J, Leski M, Morrison J (2002): The diverse roles of L-glutamic acid in brain signal transduction. *Davis, K; Charney, D; Coyle, J*.71-90.
98. Jamain S, Betancur C, Quach H, Philippe A, Fellous M, Giros B, et al. (2002): Linkage and association of the glutamate receptor 6 gene with autism. *Molecular psychiatry*. 7:302.
99. Shuang M, Liu J, Jia MX, Yang JZ, Wu SP, Gong XH, et al. (2004): Family-based association study between autism and glutamate receptor 6 gene in Chinese Han trios. *American Journal of Medical Genetics Part B: Neuropsychiatric Genetics*. 131:48-50.
100. Serajee F, Zhong H, Nabi R, Huq AM (2003): The metabotropic glutamate receptor 8 gene at 7q31: partial duplication and possible association with autism. *Journal of medical genetics*. 40:e42-e42.
101. Purcell A, Jeon O, Zimmerman A, Blue M, Pevsner J (2001): Postmortem brain abnormalities of the glutamate neurotransmitter system in autism. *Neurology*. 57:1618-1628.
102. Shinohe A, Hashimoto K, Nakamura K, Tsujii M, Iwata Y, Tsuchiya KJ, et al. (2006): Increased serum levels of glutamate in adult patients with autism. *Progress in Neuro-Psychopharmacology and Biological Psychiatry*. 30:1472-1477.
103. Aoki Y, Kasai K, Yamasue H (2012): Age-related change in brain metabolite abnormalities in autism: a meta-analysis of proton magnetic resonance spectroscopy studies. *Transl Psychiatry*. 2:e69.
104. Oblak AL, Rosene DL, Kemper TL, Bauman ML, Blatt GJ (2011): Altered posterior cingulate cortical cytoarchitecture, but normal density of neurons and interneurons in the posterior cingulate cortex and fusiform gyrus in autism. *Autism Research*. 4:200-211.

105. Oblak AL, Gibbs TT, Blatt GJ (2011): Reduced GABA A receptors and benzodiazepine binding sites in the posterior cingulate cortex and fusiform gyrus in autism. *Brain research*. 1380:218-228.
106. Vogt BA, Finch DM, Olson CR (1992): Functional heterogeneity in cingulate cortex: the anterior executive and posterior evaluative regions. *Cerebral cortex*. 2:435-443.
107. Leech R, Sharp DJ (2014): The role of the posterior cingulate cortex in cognition and disease. *Brain*. 137:12-32.
108. Jung RE, Brooks WM, Yeo RA, Chiulli SJ, Weers DC, Sibbitt WL (1999): Biochemical markers of intelligence: a proton MR spectroscopy study of normal human brain. *Proceedings of the Royal Society of London Series B: Biological Sciences*. 266:1375-1379.
109. Ferguson KJ, MacLullich AM, Marshall I, Deary IJ, Starr JM, Seckl JR, et al. (2002): Magnetic resonance spectroscopy and cognitive function in healthy elderly men. *Brain*. 125:2743-2749.
110. Valenzuela M, Sachdev P, Wen W, Shnier R, Brodaty H, Gillies D (2000): Dual Voxel Proton Magnetic Resonance Spectroscopy in the Healthy Elderly: Subcortical-Frontal Axonal N-Acetylaspartate Levels Are Correlated with Fluid Cognitive Abilities Independent of Structural Brain Changes. *Neuroimage*. 12:747-756.
111. Aoki Y, Abe O, Yahata N, Kuwabara H, Natsubori T, Iwashiro N, et al. (2012): Absence of age-related prefrontal NAA change in adults with autism spectrum disorders. *Translational psychiatry*. 2:e178.
112. Kleinhans N, Richards T, Weaver K, Liang O, Dawson G, Aylward E (2009): Brief Report: Biochemical Correlates of Clinical Impairment in High Functioning Autism and Asperger's Disorder. *Journal of Autism and Developmental Disorders*. 39:1079-1086.

Table 1. Participant demographics.

	Autism			Control			Group difference	
	N = 20			*N* = 20				
	Mean	Range	s.d.	Mean	Range	s.d.	*t*-value	*p*-value
Age	26.8	19-40	1.35	24.9	19-38	1.13	1.04	0.30
Verbal IQ	113.7	95-139	3.15	113.8	88-141	2.91	0.01	0.98
Performance IQ	113.9	94-138	3.18	115.1	99-133	2.84	0.27	0.78
Full-scale IQ	115.4	99-140	2.88	117.5	103-140	2.51	0.53	0.59
RAADS-R total	128.7	72-181	6.66	39.15	13-77	3.84	11.4	<0.0001

Table 2. 1H-MRS ANCOVA results between ASD and TD groups for dACC and PCC regions.

		ASD (n = 20)	TD (n=20)	Group Differences	
ROI	Metabolite	Mean (SD)	Mean (SD)	*F*-statistic	p-value
dACC	NAA/Cr	1.39(0.08)	1.47(0.09)	*F*(1,35)=4.69	0.038
	CRLB,%	4.54(0.003)	5.16(0.003)		
	Glx/CR	0.73(0.09)	0.77(0.10)	*F*(1,35)=0.85	0.363
	CRLB,%	8.73(0.007)	9.42(0.006)		
	Cho/Cr	0.80(0.09)	0.78(0.09)	*F*(1,35)=0.01	0.901
	CRLB,%	3.32(0.002)	3.62(0.002)		
	Linewidth, Hz	4.82(0.85)	4.63(0.65)	*F*(1,38)=0.58	0.450
PCC	NAA/Cr	1.49(0.06)	1.51(0.08)	*F*(1,35)=1.13	0.295
	CRLB,%	3.16(0.001)	3.55(0.002)		
	Glx/Cr	0.73(0.07)	0.75(0.08)	*F*(1,35)=0.79	0.379
	CRLB,%	5.91(0.002)	6.72(0.004)		
	Cho/Cr	0.59(0.06)	0.58(0.06)	*F*(1,35)=0.54	0.468
	CRLB,%	2.00(0.0008)	2.20(0.001)		
	Linewidth, Hz	5.08(0.59)	5.22(1.51)	*F*(1,38)=0.16	0.691

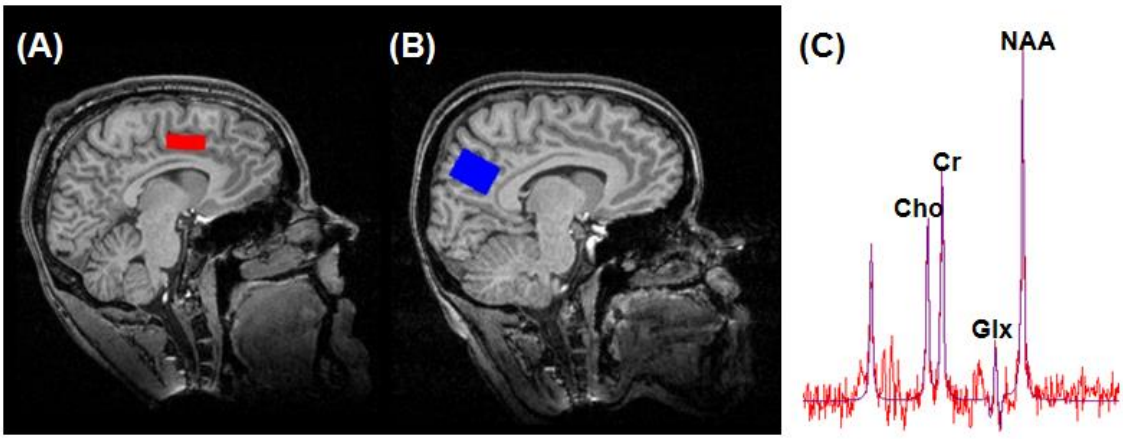

Figure 1. Example 1H-MRS voxel position for (a) dACC and (b) PCC from one participant; (c) Sample spectrum (red) from the dACC with jMRUI AMARES fitting (blue).

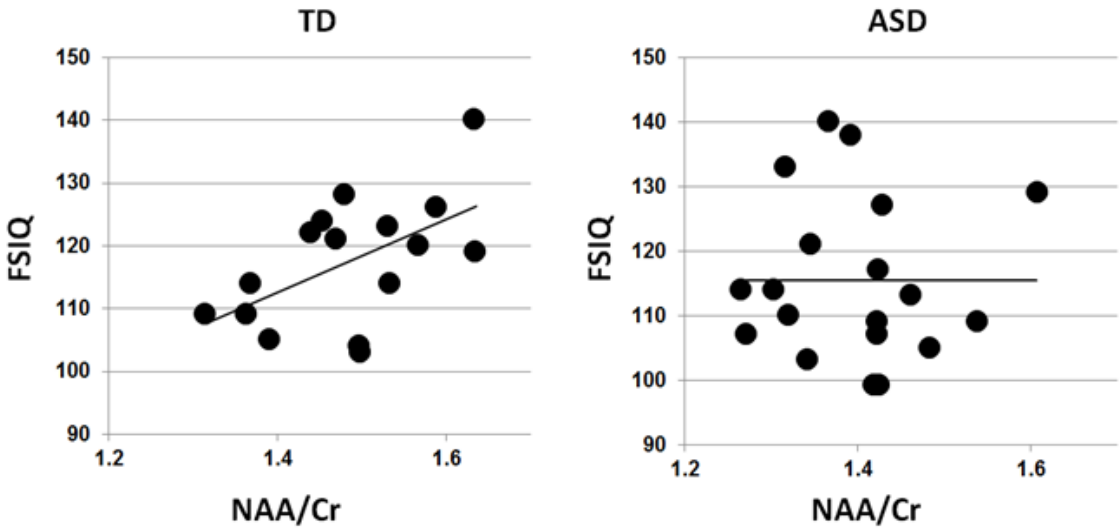

Figure 2. Correlation between full scale IQ (FSIQ) and NAA/Cr in the dACC voxel for TD (r=0.55) and ASD (r=0.00) groups.

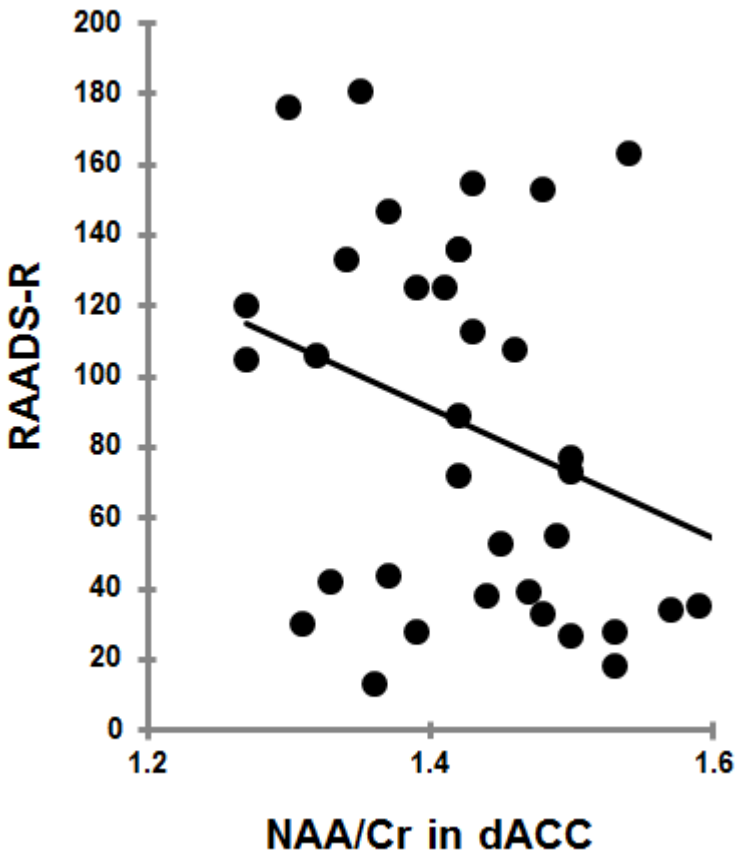

Figure 3. Correlation between ASD symptom severity (RAADS-R) and NAA/Cr in the dACC voxel for all (r = -0.35) participants.

MULTIMODAL NEUROIMAGING BASED CLASSIFICATION OF AUTISM SPECTRUM DISORDER USING ANATOMICAL, NEUROCHEMICAL, AND WHITE MATTER CORRELATES

by

LAUREN E. LIBERO, THOMAS P. DERAMUS, ADRIENNE C. LAHTI, GOPIKRISHNA DESHPANDE, AND RAJESH K. KANA

In preparation for *NeuroImage: Clinical*

Format adapted for dissertation

Abstract

Neuroimaging studies of autism spectrum disorder (ASD) have uncovered evidence for widespread functional and anatomical brain abnormalities suggesting it to be a system-wide neural systems disorder. Such evidence of abnormalities has mainly come from fMRI, structural MRI, diffusion tensor imaging (DTI), and proton magnetic resonance spectroscopy (1H-MRS) studies. Nevertheless, most previous studies have focused on examining one index of neuropathology through a single neuroimaging modality, and seldom using multiple modalities to examine the same cohort of individuals. The current study aims to bring together multiple brain imaging modalities (MRI, DTI, and 1H-MRS) to investigate the neural architecture of the same set of individuals with ASD. Nineteen high-functioning adults with ASD and 18 typically developing (TD) peers were included in this study. Adults with ASD were found to have increased cortical thickness across the left cingulate, left pars opercularis, left inferior temporal, and right precuneus, and reduced cortical thickness in right cuneus and right precentral gyrus, compared to the TD group. DTI analyses showed that ASD adults had reduced fractional anisotropy and increased radial diffusivity for two clusters on the forceps minor of the corpus callosum. 1H-MRS results showed a significant reduction in N-acetylaspartate in ASD participants across the brain. A decision tree classification analysis resulted in classification accuracy of 91.9% with a model including radial diffusivity and fractional anisotropy from the forceps minor of the corpus callosum and cortical thickness for pars opercularis. A decision tree regression analysis predicting symptom severity resulted in a root mean square error for prediction of 18.72, finding measures of diffusion and cortical thickness predicting symptom severity. Examining the same cohort of adults with ASD and their TD peers, this study found significant alterations in measurements of cortical thickness, white matter connectivity, and

neurochemical concentration. These neural measures were investigated as potential predictors for diagnostic status of participants in a classification analysis, finding cortical thickness and DTI measures serving as the best predictors of diagnosis and symptom severity. These findings underscore the potential for multimodal imaging to better inform on the neural characteristics most relevant to the disorder.

Introduction

Autism spectrum disorder (ASD) has been characterized as a disorder of neurodevelopmental origin, with abnormalities such as altered cortical anatomy (Amaral, Schumann, & Nordahl, 2008; Nickl-Jockschat et al., 2012), abnormal white matter integrity (Travers et al., 2012), altered brain function and connectivity (Anagnostou & Taylor, 2011; Kana, Libero, & Moore, 2011; Libero & Kana, 2013; Maximo, Cadena, & Kana, 2014; Schipul, Keller, & Just, 2011), increase in neuron number (Courchesne et al., 2011), numerous and smaller cortical minicolumns (Casanova et al., 2002; 2006), and alterations in synaptic connections and the organization of neurons within cortex (Avino & Hutsler, 2010; Hutsler, Love, & Zhang, 2007; Hutsler & Zhang, 2010; Stoner et al., 2014). Such abnormalities point to a complex and multilayered picture of the neurobiology of autism. While this may be a true reflection of the multidimensional manifestation of the behavioral symptoms of autism, uncovering the neural underpinnings of this disorder certainly poses immense challenge to neuroscientists.

With regard to cortical anatomy, there has been reports of consistent and early overgrowth in brain volume (Courchesne, Campbell, & Solso, 2011; Hazlett et al., 2005; Hazlett et al., 2011; Stanfield et al., 2008), followed by abnormal decline and degeneration during adolescence and adulthood (Courchesne et al., 2011). However, regional volumetric differences found in ASD have been variable with no consensus on any single region to be the main culprit. The relatively more consistent findings are increased gray matter volume in frontal, temporal, parietal, and limbic areas, decreased white matter volume in frontal, temporal, and limbic areas

(Chen, Jiao, & Herskovits, 2011; Stanfield et al., 2008), and volumetric abnormalities in amygdala, hippocampus, corpus callosum, and cerebellum (Brambilla et al., 2003; Stanfield et al., 2008). Surface based examinations of brain structure in ASD, on the other hand, have uncovered alterations in cortical thickness in regions across the entire brain (Chung et al., 2005; Christine Ecker et al., 2013; Hadjikhani, Joseph, Snyder, & Tager-Flusberg, 2006; Hardan, Muddasani, Vemulapalli, Keshavan, & Minshew, 2006; Hyde, Samson, Evans, & Mottron, 2010; Mak-Fan, Taylor, Roberts, & Lerch, 2012; Raznahan et al., 2010; Scheel et al., 2011; Wallace, Dankner, Kenworthy, Giedd, & Martin, 2010). As cortical thickness and volume are related to dendritic arborization (Huttenlocher, 1990), myelination (Sowell et al., 2004), and the migration of neurons and organization of minicolumns (Rakic, 1988), abnormalities in surface features of cortex in ASD may imply significant alterations at a cellular and developmental level.

While volumetric examinations provide valuable information about the neuroanatomical organization, it does not address the microstructural aspects of tissues like white matter. With advanced neuroimaging techniques like Diffusion tensor imaging (DTI), studying the structural integrity of white matter in disorders like autism has become more sophisticated. DTI is a technique that allows the measurement of the diffusion of water molecules along white matter tracts in the brain, indicating potential pathological differences in the shape, structure, and organization of white matter fibers. Whole brain studies of diffusion in ASD have found reduced fractional anisotropy (FA; an index of the directionality of diffusion) and increased mean diffusivity (MD; average diffusion in all directions) in overall white matter in ASD participants (Groen, Buitelaar, Van Der Gaag, & Zwiers, 2011; Shukla, Keehn, Lincoln, & Müller, 2010), suggesting significant disturbance in white matter integrity across the brain. At a finer level, DTI studies in ASD examining specific regions or white matter tracts have most consistently found

reduced FA, indicating alterations in white matter tract integrity, in a number of tracts including corpus callosum, cingulum bundle, and tracts projecting to the temporal lobes, such as the uncinate fasciculus, inferior longitudinal fasciculus, and superior longitudinal fasciculus ((A. L. Alexander et al., 2007; Barnea-Goraly et al., 2004; Bloemen et al., 2010; Keller, Kana, & Just, 2007; Lee et al., 2007); see (Travers et al., 2012) for a review). These findings indicate significant microstructural abnormalities and alterations in the organization of white matter fibers in ASD, which may translate into impairments in brain activation and functional connectivity.

While cortical anatomy and white matter fiber orientation provide two different aspects of brain organization, the health of individual neurons is yet another factor which determines the structural and functional makeup of the brain. Proton magnetic resonance spectroscopy (1H-MRS) measures tissue metabolite concentration, and can be used as an indirect measure of neuronal health and function in living tissue (Fayed, Olmos, Morales, & Modrego, 2006; Stanley, 2002). 1H-MRS is applied to examine the concentration of specific neurochemicals in the brain, and their potential role in disease and treatment. This technique can measure various neurochemicals, including N-acetylaspartate (NAA; a marker for neuronal and axonal health and density), choline (Cho; marking cellular membrane proliferation), glutamate/glutamine (Glx; measuring glutamate/glutamine levels), and creatine (Cr; marking energy homeostasis). Previous 1H-MRS studies in ASD have found reductions of NAA in both gray and white matter in children and adults with ASD most consistently (Ipser et al., 2012). These findings suggest significant alterations in neurochemicals in certain regions of the ASD brain, specifically pointing to poorer neuronal health or possible cellular damage or inflammation.

Thus, neuroimaging evidence coming from morphometry, DTI, and 1H-MRS studies in ASD have provided information about alterations in brain structure, white matter integrity, and neuronal health; yet, these findings span diffuse and spatially distinct brain regions, with poor constancy and overlap of results across studies. While heterogeneity among individuals with autism may be an important factor driving the inconsistency in findings, what's striking is that studies rarely, if ever, have investigated all indices of brain organization (anatomy, white matter integrity, and neurochemical level) from the same set of participants. Therefore, it is difficult to derive a convincing inference that is comprehensive and reliable in representing the neuropathology in autism. The current study is an attempt to address this gap by using multimodal neuroimaging data from the same participants across three modalities of neuroimaging, MRI, DTI, and 1H-MRS. This approach is novel and provides a promising venue for understanding the neuropathology of autism.

Another objective of this study was to identify patterns across findings from different modalities and to apply that knowledge to classify participants into autism and TD control groups. Utilizing pattern classification of neuroimaging data, several studies have aimed to identify a predictive model for ASD diagnosis. For example, functional brain activation and connectivity were used for pattern classification to separate ASD from TD peers (Anderson et al., 2011; Coutanche, Thompson-Schill, & Schultz, 2011; Deshpande, Libero, Sreenivasan, Deshpande, & Kana, 2013; Kaiser & Pelphrey, 2012; Murdaugh et al., 2012; Spencer et al., 2011). A few studies have also applied classification analyses to volumetric and surface based structural measures (Akshoomoff et al., 2004; Christine Ecker, Marquand, et al., 2010; Christine Ecker, Rocha-Rego, et al., 2010; Yun Jiao et al., 2010; Uddin et al., 2011) and DTI data (Ingalhalikar, Parker, Bloy, Roberts, & Verma, 2011; Lange et al., 2010) to predict ASD group

membership. One study has also used a combination of cortical volume and thickness measures, along with single-nucleotide polymorphisms (Y Jiao et al., 2011) to predict group membership. Thus, accurate and reliable classification of participants with autism is a promising step towards the diagnostic utility of such measures. For a neurodevelopmental disorder that relies on behavioral diagnosis, an applied neural classifier could be useful, at least in deciding difficult cases. Attempts at neural classifiers thus far have mainly relied on measures of brain function, based on experimental tasks, which may be inappropriate for many individuals with ASD, particularly those who would be considered low-functioning or young children. ASD has been identified as a neural systems disorder with complex neurobiology, and any biomarker will need to be multivariate, possibly including several aspects of biology and genetics (C Ecker, Spooren, & Murphy, 2013). Ultimately, a multimodal technique could become more sensitive to symptomatology, which can lead to not only better diagnosis of autism, but also aid in designing more tailored interventions. The current study is novel in that it marks the first one to examine three neuroimaging modalities (SBM, DTI, and 1H-MRS) in the same subjects with ASD, and to apply such measures to a diagnostic classification of autism.

Method & Materials

Participants

Nineteen high-functioning adults with ASD (15 males/4 females; mean age: 27.1 years) and 18 typically developing (TD) peers (14 males/4 females; mean age: 24.6 years) participated in this study (see Table 1 for demographic information). The groups were equivalent on age and IQ. This sample is the same as the sample included in Manuscript 3, but with one ASD participant and two TD participants excluded as they did not have DTI data. Full-scale IQ (FSIQ), verbal IQ (VIQ), and performance IQ (PIQ) were assessed using the Wechsler

Abbreviated Scale of Intelligence (WASI) (Wechsler, 1999), handedness using the Edinburgh Handedness Inventory (Oldfield, 1971), and ASD symptoms using the Ritvo Autism Asperger Diagnostic Scale-Revised (RAADS-R) (Ritvo et al., 2011). Age, FSIQ, VIQ, and PIQ were not significantly different between groups. The ASD group scored significantly higher on the RAADS-R compared to their TD peers (see Table 1). Participants with ASD had received a previous diagnosis of an ASD based on Autism Diagnostic Interview-Revised (ADI-R) (Rutter, Le Couteur, & Lord, 2003) symptoms and Autism Diagnostic Observation Schedule (ADOS) (Lord et al., 2000). TD participants were screened through a self-report history questionnaire to rule out neurological disorders, such as ASD, ADHD, or Tourette's Disorder, that could potentially confound the results. Several ASD participants reported taking medications, including stimulant medication (n=6), antidepressants (n=8), anxiety medication (n=1), and antipsychotic medication (n=1). Eight ASD participants reported no medications, and no TD participants reported taking medication. Finally, all participants were reported to be non-smokers. The study was approved by the Institutional Review Board of our university, and all participants provided informed consent for their participation in the study.

MRI Data Acquisition & Surface Based Morphometry

MRI images were acquired using a 3T Siemens Allegra head-only scanner (Siemens Medical Inc., Erlangen, Germany) housed at the Civitan International Research Center, UAB. Anatomical images have been acquired using high resolution T1-weighted scans using a 160 slice 3D MPRAGE volume scan with a TR = 200ms, TE = 3.34 ms, flip angle = 12, FOV = 25.6, 256 x 256 matrix size, and 1mm slice thickness. 3D volumes were visually examined by three researchers independently to confirm data quality (examining images for significant distortion

due to head motion or scanner artifact). No participants needed to be excluded due to poor data quality.

Structural images were analyzed using *FreeSufer* image analysis suite, which is documented and freely available (http://surfer.nmr.mgh.harvard.edu/) (Fischl, 2012; Fischl & Dale, 2000). The technical details of these procedures can be found in previous publications (Dale, Fischl, & Sereno, 1999; Dale & Sereno, 1993; Fischl & Dale, 2000; Fischl, Liu, & Dale, 2001; Fischl, Salat, et al., 2004; Fischl, Sereno, & Dale, 1999; Fischl, Sereno, Tootell, & Dale, 1999; Han et al., 2006; Jovicich et al., 2006; Ségonne et al., 2004). Images undergo skull stripping using a watershed/surface deformation procedure to remove non-brain tissue (Ségonne et al., 2004), transformation to Talairach space, segmentation of subcortical white and gray matter structures (Fischl et al., 2002; Fischl, van der Kouwe, et al., 2004), intensity normalization (Sled, Zijdenbos, & Evans, 1998) in order to correct for MR intensity non-uniformity mainly arising from variations in the sensitivity of the reception coil and from gradient-driven eddy currents (Sled et al., 1998) , tessellation of the gray matter/white matter boundaries, automated topology correction (Fischl et al., 2001; Ségonne, Pacheco, & Fischl, 2007), and surface deformation following intensity gradients to optimally place the gray/white and gray/CSF borders that most accurately define the transition to the other tissue class (Dale et al., 1999; Dale & Sereno, 1993; Fischl & Dale, 2000). Segmented images were visually inspected for acceptable segmentation. These images were then inflated and registered to a spherical atlas which separated the cortex into 66 regions of interest (Desikan et al., 2006; Fischl, Salat, et al., 2004; Fischl, Sereno, & Dale, 1999). Segmented data were then parceled into units based on gyral and sulcal structure, resulting in values for cortical thickness, surface area, and volume (Desikan et al., 2006; Fischl, Salat, et al., 2004). Cortical thickness measurements as

implemented in FreeSurfer have been validated against manual measurements (Kuperberg et al., 2003; Salat et al., 2004) and histological analysis (Rosas et al., 2002). Previous studies have found FreeSurfer morphometric procedures to have sufficient test-retest reliability across scanner manufacturers, field strengths, and other imaging parameters (Han et al., 2006; Jovicich et al., 2006; Wonderlick et al., 2009). Groups were compared on the resulting cortical thickness values using ANCOVAs conducted using SPSS 22.0 software. Age was used as a covariate for all between-group analyses, as well as average hemispheric cortical thickness

1H-MRS Imaging

Imaging was performed on a 3T head-only scanner (Siemens Allegra, Erlangen, Germany) with a circularly polarized transmit/receive head coil. A series of sagittal, coronal, and axial T1-weighted anatomical scans were acquired for 1H-MRS voxel placement (gradient-recalled echo sequence; TR = 250ms, TE = 3.48ms, flip angle = 70 degrees, 512 x 512 matrix size, 5mm slice thickness, and 1.5mm gap). Slices were aligned to anatomical midline to control for head tilt. The 1H-MRS voxel for dorsal anterior cingulate cortex (dACC) (20 X 27 X 10 mm) was positioned around the center of the ACC, identified centrally in the gray matter above the anterior corpus callosum. The 1H-MRS voxel for posterior cingulate cortex (PCC) (20 X 27 X 20 mm) was positioned above the splenium of the corpus callosum with the long axis parallel to the parieto-occipital sulcus. These voxels were placed on the basis of the sagittal and coronal images, such that the amount of gray matter in the voxel as viewed on the T1-weighted images is maximized. Following manual shimming, to optimize field homogeneity across the voxel, water-suppressed spectra were collected with the point-resolved spectroscopy sequence (PRESS; TR/TE = 2000/80 ms, 1200 Hz spectral bandwidth, 1024 points, 128 averages, 4 min 24 s scanning time).

MRS data were processed in *jMRUI* (version 5.0) (Naressi et al., 2001). The residual water peak was removed using the Hankel-Lanczos singular values decomposition filter (Pijnappel, Van den Boogaart, De Beer, & Van Ormondt, 1992). Spectra were quantified in the time domain by the AMARES algorithm (advanced method for accurate, robust, and efficient spectral fitting) (Vanhamme, van den Boogaart, & Van Huffel, 1997). AMARES is a quantification method that has been used to compute the spectral fitting parameters (e.g., amplitudes, frequencies, and linewidths for the metabolite peaks). Ratios of NAA, Cho, Cr, and Glx, with respect to Cr were calculated using the amplitudes of the time domain signal resulting from the AMARES analysis. Cramer-Rao lower bounds (CRLB) were used as a measure of uncertainty of the fitting procedure. Inclusion in analyses required ratios to have CRLB less than 20%; all participants' ratios were within these limits and were included in the final analyses.

High resolution anatomical data were processed using Statistical Parametric Mapping 8 (SPM8; Wellcome Trust Center for Neuroimaging) in MATLAB version 7.11.0 (Mathworks). Each participant's T1-weighted MPRAGE image was segmented into gray matter (GM), white matter (WM), and cerebrospinal fluid (CSF) using the segmentation routine in SPM8. Using native-space masks, we calculated the total GM, WM, and CSF volumes for the dACC and PCC regions of interest (ROI) using a script adapted from John's SPM Gems (http://www-personal.umich.edu/~nichols/JohnsGems.html) in MATLAB. The GM, WM, and CSF content were obtained in order to control for the tissue concentration of our acquired 1H-MRS voxels. Statistical analyses were performed in SPSS 22.0. 1H-MRS ratios were compared using ANCOVA, covarying for age, and GM content.

Diffusion Tensor Imaging

Diffusion weighted images were collected using a single-shot, spin-echo, EPI sequence. A diffusion weighted, single-shot, spin–echo, echo-planar imaging sequence was used (TR = 7000 ms, TE = 90 ms, bandwidth = 2790 Hz/voxel, FOV = 220 mm, and matrix size = 128 x 128 x 27, resulting in an in-plane resolution of 1.7 X 1.7 X 3 mm^3). Twenty-seven 3-mm thick slices were imaged (no slice gap) with no diffusion-weighting (b = 0s/mm2) and with diffusion-weighting (b = 1000s/mm^2) gradients applied in 46 orthogonal directions. Ninety-two images of each slice by gradient direction combination were acquired and averaged to produce the final diffusion imaging dataset for each participant.

Diffusion images were preprocessed using the *mrDiffusion* package (Stanford VISTA Lab). Through this pipeline, participant head motion and eddy current distortions were removed by a 14-parameter constrained non-linear co-registration based on the expected pattern of distortions for each phase-encoded direction of the data (Rohde, Barnett, Basser, Marenco, & Pierpaoli, 2004). Diffusion weighted images were aligned to the unweighted (b=0) images, and then rigid-body aligned to each subject's anatomical T1 reference image. Data were resampled to 2 X 2 X 2 mm^3 voxels with a 7^{th} order b-spline interpolation, taking into account head motion-correction, eddy-current distortion correction, and anatomical alignment transforms (Friston & Ashburner, 2004). The rotation matrices from the alignment steps were combined and applied to correctly orient the resampled data to their respective vectors. Finally, the tensor model was fit using a robust least-squares algorithm, and the resulting eigenvalues were used to compute fractional anisotropy (FA), mean diffusivity (MD), radial diffusivity (RD), and axial diffusivity (AD) (Basser & Pierpaoli, 1996).

The preprocessed data were analyzed using *Automated Fiber Quantification* (AFQ) (Yeatman, Dougherty, Myall, Wandell, & Feldman, 2012). The data for each participant were subjected to whole-brain tractography (using deterministic tractography). The data were then segmented into tracts for left thalamic radiation, right thalamic radiation, left corticospinal, right corticospinal, left cingulum cingulate, right cingulum cingulate, left cingulum hippocampus, right cingulum hippocampus, callosum forceps major, callosum forceps minor, left inferior fronto-occipital fasciculus, right inferior fronto-occipital fasciculus, left inferior longitudinal fasciculus, right inferior longitudinal fasciculus, left superior longitudinal fasciculus, right superior longitudinal fasciculus, left uncinate, right uncinate, left arcuate, and right arcuate. Next, stray fibers were removed, and tract properties (FA, RD, MD, and AD) were computed for 100 points along each tract for each participant. Norms for each tract were determined using control group data. For some participants, tract properties for specific tracts could not be computed (due to artifact, head motion, or qualities [e.g., size or crossing fibers] of the tissue). Tracts with greater than 10% of participants missing data (due to incomplete tractography) were removed from further analyses. These tracts included the left and right cingulum bundles. To compare the ASD and TD groups on FA, RD, MD, and AD, t-tests were conducted point-wise along each fiber tract for 100 points. A permutation based multiple comparison correction was applied to determine statistical significance (Nichols & Holmes, 2002), $p < 0.05$.

Decision Tree Pattern Classification and Regression

Decision tree is a class of Hierarchical Optimal Discriminant Predictive Models which map several input observations into the value of a target variable. When the target variable is discrete, the decision tree is referred to as a classification tree and when the target variable is continuous, it is referred to as a regression tree. The decision tree is derived by recursively

partitioning the values of observed variables using top-down induction greedy search (Quinlan, 1986). Specifically we used the CART (Classification And Regression Trees) algorithm (Barros, Basgalupp, Carvalho, & Freitas, 2011; Loh, 2011) to perform this greedy search. The algorithm was initiated with one of the many given variables (FA/RD, CT or NAA) as the head node. At each node (including the head node), we determined the variable to be tested and the many possible splits of the variable's values. Each possible split yields a partition into two child nodes and we chose the partitions which resulted in a tree that minimized the weighted sum of the class impurities of each branch of the split. The recursion was stopped when further splitting did not improve the prediction. Class impurities were determined using the Gini impurity index (Coppersmith, Hong, & Hosking, 1999). Decision tree based classification was used for predicting the diagnostic label (TD or ASD) of a given subject while and regression was used for predicting symptom severity (RAADS-R). Leave-one-subject-out cross validation was performed for both regression and classification. Many previous studies have demonstrated the efficacy of decision trees for applications in MR-based diagnostics (Douglas, Harris, Yuille, & Cohen, 2011; Nair et al., 2013; Schiffmann & van der Knaap, 2009).

Results

Cortical Thickness

Cortical thickness was significantly increased in ASD participants, relative to TD controls, in left caudal anterior cingulate cortex ($F[2,35]=5.46$, $p=0.025$), left posterior cingulate cortex ($F[2,35]=5.84$, $p=0.021$), left isthmus cingulate cortex ($F[2,35]=7.21$, $p=0.011$), left pars opercularis aspect of the inferior frontal gyrus ($F[2,35]=4.87$, $p=0.034$), left inferior temporal gyrus ($F[2,35]=5.16$, $p=0.029$), and right precuneus ($F[2,35]=5.07$, $p=0.03$) (See Table 2). Regions with significant reduction in cortical thickness in ASD participants, compared to TD

peers, included right cuneus (F[2,35]=4.20, p=0.048), and right precentral gyrus (F[2,35]=5.54, p=0.024) (See Table 2). Many of these regions are considered to be part of the social brain.

Neural Metabolite Concentration

For the dACC, the mean NAA/Cr ratio for the ASD group was significantly reduced compared to the TD group, while there were no statistically significant group differences in Glx/Cr and Cho/Cr ratios (see Table 3). Mean amplitude for Cr, which was used as a reference, was not significantly different between the groups ($F = 2.60$, $p = 0.11$). For the PCC region, metabolite ratios did not significantly differ between the groups (see Table 3), and the mean amplitude for Cr were not significantly different between groups ($F = 1.39$, $p = 0.24$). Results remain consistent as the original study (described in Manuscript 3), which was to be expected as the current study sample contains almost all of the same participants as the original sample reported in the previous study.

White Matter Integrity

The main finding here is a significant difference in white matter integrity of the forceps minor of the corpus callosum, with ASD participants showing significantly reduced FA compared to their TD peers on two clusters ($p<0.05$, corrected) (See Figure 1). Differences in FA occurred on two clusters of the forceps minor, one left and one right, towards the middle of each half, with no differences in FA in the middle most points of the tract (see Figure 1 for a graph representing mean FA for both ASD and TD groups for the statistically significant cluster on the forceps minor). The same two clusters on the forceps minor also showed significant increases in RD for the ASD group compared to the TD group ($p<0.05$, corrected). No significant differences in FA, RD, MD, or AD emerged between groups for the remaining 19 tracts after correcting for multiple comparisons.

Pattern Classification: Decision Tree

Decision trees were generated based on combinations of the data to determine the best model for classification of participants by diagnostic group. Three sets of data points (DTI measurements, surface based cortical thickness measures, and neurochemical concentration) were combined with two predictions (ASD or TD diagnosis). The data points included were the resulting values of the statistical analyses of separate neuroimaging modalities. The best decision tree model returned classification accuracy of 91.9% +/- 0.42, including RD for the right forceps minor, FA for the left forceps minor, and CT for the pars opercularis aspect of the inferior frontal gyrus as the best predictors (See Figure 2). According to the decision tree, when the RD cluster is high, having higher FA in the left forceps minor results in a TD classification. Likewise, when the RD cluster is low, having lower CT in left pars opercularis of the IFG results in a TD classification.

In order to establish the relationship between the neuroimaging measures and autism symptom severity (measured by the RAADS-R), a regression analysis was conducted, resulting in a root mean square error for predicting RAADS-R score of 18.72. Based on the decision tree for this model, a number of relationships with symptom severity emerged (See Figures 3 and 4). First, low FA in the left hemisphere cluster predicted higher symptom severity for all subjects. Next, higher symptom severity was predicted when the left FA measure was high, but measures of CT for left isthmus cingulate, left posterior cingulate, and right cuneus were low, and lower symptom severity was predicted when right cuneus CT was higher. Finally, when FA for left forceps minor was high, higher cortical thickness for left isthmus cingulate and left posterior cingulate and RD for the forceps minor resulted in moderate symptom severity, while low RD for the right forceps minor resulted in low symptom severity.

Discussion

The current study examined a cohort of adults with ASD and their TD peers using multiple neuroimaging techniques, and found significant alterations in measurements of cortical thickness, white matter connectivity, and neurochemical concentration in participants with ASD. Measures of significant difference between groups were investigated as potential predictors for diagnostic status of participants in a pattern classification analysis, pointing to the potential of multimodal imaging to better inform on the neural characteristics most relevant to the disorder.

Surface based brain measures resulted in significant differences between the ASD and TD groups. Reduced precentral and cuneus CT and increased CT in cingulate, IFG, and temporal cortex is in line with previous studies of surface based features in ASD (Ecker et al., 2013; Hyde et al., 2010; Mak-Fan et al., 2012; Wallace et al., 2010). These may reflect underlying cellular alterations in organization and density of neurons, and dendritic arborization/synaptic pruning. In postmortem studies of ASD, more numerous, smaller, and less compact minicolumns, compared to TD individuals, have been reported within middle temporal, superior and middle frontal, and temporoparietal cortices (Casanova, Buxhoeveden, & Brown, 2002; Casanova, Buxhoeveden, Switala, & Roy, 2002; Casanova et al., 2006), holding implications for the alterations seen in CT.

Reduced FA found in the forceps minor of the corpus callosum in autism is in line with general alterations in FA reported in autism. The forceps minor crosses the genu of the corpus callosum and radiates to the lateral and medial sides of prefrontal cortex. Previous studies have also found reduced FA (Jou et al., 2011; Keller et al., 2007) and increased RD (Alexander et al., 2007; Ameis et al., 2011) across the forceps minor and genu of the corpus callosum. Alterations

in this tract could potentially affect the communication between the two hemispheres in the prefrontal cortex, and in how each side connects to the rest of the brain.

Our finding of significantly reduced levels of NAA/Cr in dACC is in line with previous reports of lower NAA concentration in adults with autism in the ACC (Fujii et al., 2010), hippocampal-amygdala formation (Suzuki et al., 2010), and frontal, parietal, and occipital cortices (Kleinhans, Schweinsburg, Cohen, Müller, & Courchesne, 2007). This finding is also consistent with our finding in Manuscript 3, as the sample included in the current study consists of the same adult participants. NAA is a neurochemical representing neuronal and axonal health and density, and reductions in its concentration can be an indication of disease (Fayed et al., 2006; Maddock & Buonocore, 2012; Meyerhoff et al., 1993). The amount of NAA as measured by 1H-MRS studies is thought to be a measure of neuronal integrity and its reductions in ASD may reflect alterations in soma integrity, the number of axon terminals (Lentz et al., 2005), and/or mitochondrial function (Bates et al., 1996; Stork & Renshaw, 2005).

It should be noted that while our study found significant alterations in many neural measures, it did not find differences in some of the regions and tracts examined. It is possible that these areas are unaffected in ASD; or perhaps these measures differ with age or symptomatology, resulting in findings to differ from cohort to cohort (and study to study). The marked heterogeneity in ASD population affects the consistency across neuroimaging findings in ASD. A recent postmortem study found abnormalities in laminar cytoarchitecture and disorganization of neurons in ASD, but noted that the cellular disorganization varied from case to case, indicating the possibility of different functional systems being affected impacting different symptom presentation in different individuals (Stoner et al., 2014). Future studies should seek to examine the brain in very large samples of participants and include individuals

with varied presentation to clarify whether some regions are intact, or just unaffected in certain subsamples of individuals with ASD.

Alterations found across all three neuroimaging modalities in our study point to ASD as a multilayered neural disorder, with widespread problems in cortical structure, white matter integrity, and neuronal health. Our classification analyses sought to examine how these measures may be useful in identifying participants with ASD, and the relationships between the predictors. As a result, predictors from DTI and SBM returned the highest classification accuracy. In addition, higher FA in the left forceps minor reduced the chance of an ASD diagnosis when RD in the right forceps minor was high; and lower CT in pars opercularis of the IFG reduced one's chance of an ASD diagnosis when coupled with lower RD in the right forceps minor. In summary, more accurate classification of ASD was made possible by contributions from both DTI and SBM modalities. Other variables from these modalities, along with the predictor from 1H-MRS, did not contribute the most accurate classification model. While these differences may contribute to abnormalities specific to individuals or subgroups, some variables may not be sufficient to separate participants for diagnostic group membership. However, overall, a multimodal approach returned the highest classification percentage, indicative of the benefit of including brain measures from many systems.

The current study also investigated the relationship between the predictor variables and symptom severity. As a result, relationships emerged between FA for forceps minor and symptom severity, as well as combinations of DTI and SBM measures predicting high, moderate, and low symptom severity for all participants. Interestingly the DTI and SBM data interacted to produce varying severity of ASD. This suggests different neural systems are related to different symptomatology, with perhaps not one modality explaining everything. Also, different

combinations of variables potentially explain different behavioral outcomes. We found measures of CT, FA, and RD came together to impact symptom severity. Thus, varying combinations of neural abnormalities could account for the heterogeneity in behavior in ASD. Further research in these lines may aid establishing this relationship with symptoms, and in potentially identifying subgroups of individuals who share similar behavioral and neural profiles. Identifying subsets of individuals with differences in DTI, SBM, and 1H-MRS measures could lead to interventions that target the specific areas needed and have the most impact. This could be most fruitful for a disorder where treatment cannot be one size fits all.

The current study makes a vital contribution to the literature on the neuropathology of ASD, with its integrated approach and its application to testing the diagnostic utility of these measures. This method could potentially be applied to younger or lower functioning individuals in the future, increasing the utility of this approach. Finally, through regression analysis, we found measures from different modalities coming together to predict ASD symptom severity, demonstrating the importance of exploring the interrelatedness of impairments across the brain in ASD. Future studies should apply multimodal imaging to investigate classification and apply such a method to a validation cohort (participants who were not included in the analysis determining the predictors to include) to test the validity of this method. In addition, future studies should investigate the application of multimodal neuroimaging classification in younger children and lower functioning individuals, those who may most benefit from such a technique. Overall, this study marks a contribution to the literature on neural markers of ASD, and is the first to employ three neuroimaging modalities together and apply the results to classification models of the disorder. This is a step towards applied classification, and a better understanding of how differences in the brain may be interconnected and related to behavioral symptoms.

References

Akshoomoff, N., Lord, C., Lincoln, A. J., Courchesne, R. Y., Carper, R. A., Townsend, J., & Courchesne, E. (2004). Outcome classification of preschool children with autism spectrum disorders using MRI brain measures. *Journal of the American Academy of Child & Adolescent Psychiatry, 43*(3), 349-357.

Alexander, A. L., Lee, J. E., Lazar, M., Boudos, R., DuBray, M. B., Oakes, T. R., . . . McMahon, W. M. (2007). Diffusion tensor imaging of the corpus callosum in Autism. *Neuroimage, 34*(1), 61-73.

Alexander, A. L., Lee, J. E., Lazar, M., Boudos, R., DuBray, M. B., Oakes, T. R., . . . McMahon, W. M. (2007). Diffusion tensor imaging of the corpus callosum in autism. *Neuroimage, 34*(1), 61-73.

Amaral, D. G., Schumann, C. M., & Nordahl, C. W. (2008). Neuroanatomy of autism. *Trends in neurosciences, 31*(3), 137-145.

Ameis, S. H., Fan, J., Rockel, C., Voineskos, A. N., Lobaugh, N. J., Soorya, L., . . . Anagnostou, E. (2011). Impaired structural connectivity of socio-emotional circuits in autism spectrum disorders: a diffusion tensor imaging study. *PLoS One, 6*(11), e28044.

Anagnostou, E., & Taylor, M. J. (2011). Review of neuroimaging in autism spectrum disorders: what have we learned and where we go from here. *Mol Autism, 2*(4).

Anderson, J. S., Nielsen, J. A., Froehlich, A. L., DuBray, M. B., Druzgal, T. J., Cariello, A. N., . . . Fletcher, P. T. (2011). Functional connectivity magnetic resonance imaging classification of autism. *Brain, 134*(12), 3742-3754.

Avino, T. A., & Hutsler, J. J. (2010). Abnormal cell patterning at the cortical gray–white matter boundary in autism spectrum disorders. *Brain research, 1360*, 138-146.

Barnea-Goraly, N., Kwon, H., Menon, V., Eliez, S., Lotspeich, L., & Reiss, A. L. (2004). White matter structure in autism: preliminary evidence from diffusion tensor imaging. *Biological psychiatry, 55*(3), 323-326.

Barros, R., Basgalupp, M., Carvalho, A., & Freitas, A. (2011). A Survey of Evolutionary Algorithms for Decision-Tree Induction. *IEEE Transactions on Systems, Man and Cybernetics, Part C: Applications and Reviews, 42*(3), 291-312.

Basser, P. J., & Pierpaoli, C. (1996). Microstructural and Physiological Features of Tissues Elucidated by Quantitative-Diffusion-Tensor MRI. *Journal of Magnetic Resonance, Series B, 111*(3), 209-219. doi: http://dx.doi.org/10.1006/jmrb.1996.0086

Bates, T. E., Strangward, M., Keelan, J., Davey, G. P., Munro, P. M., & Clark, J. B. (1996). Inhibition of N-acetylaspartate production: implications for 1H MRS studies in vivo. *Neuroreport, 7*(8), 1397-1400.

Bloemen, O. J., Deeley, Q., Sundram, F., Daly, E. M., Barker, G. J., Jones, D. K., . . . Murphy, K. C. (2010). White matter integrity in Asperger syndrome: a preliminary diffusion tensor magnetic resonance imaging study in adults. *Autism Research, 3*(5), 203-213.

Brambilla, P., Hardan, A., di Nemi, S. U., Perez, J., Soares, J. C., & Barale, F. (2003). Brain anatomy and development in autism: review of structural MRI studies. *Brain research bulletin, 61*(6), 557-569.

Casanova, M. F., Buxhoeveden, D. P., & Brown, C. (2002). Clinical and macroscopic correlates of minicolumnar pathology in autism. *Journal of Child Neurology, 17*(9), 692-695.

Casanova, M. F., Buxhoeveden, D. P., Switala, A. E., & Roy, E. (2002). Minicolumnar pathology in autism. *Neurology, 58*(3), 428-432. doi: 10.1212/wnl.58.3.428

Casanova, M. F., van Kooten, I. A., Switala, A. E., van Engeland, H., Heinsen, H., Steinbusch, H. W., . . . Schmitz, C. (2006). Minicolumnar abnormalities in autism. *Acta neuropathologica, 112*(3), 287-303.

Chen, R., Jiao, Y., & Herskovits, E. H. (2011). Structural MRI in autism spectrum disorder. *Pediatric research, 69*, 63R-68R.

Chung, M. K., Robbins, S. M., Dalton, K. M., Davidson, R. J., Alexander, A. L., & Evans, A. C. (2005). Cortical thickness analysis in autism with heat kernel smoothing. *NeuroImage, 25*(4), 1256-1265.

Coppersmith, D., Hong, S., & Hosking, J. (1999). Partitioning Nominal Attributes in Decision Trees. *Data Mining and Knowledge Discovery, 3*, 197–217.

Courchesne, E., Campbell, K., & Solso, S. (2011). Brain growth across the life span in autism: age-specific changes in anatomical pathology. *Brain research, 1380*, 138-145.

Coutanche, M. N., Thompson-Schill, S. L., & Schultz, R. T. (2011). Multi-voxel pattern analysis of fMRI data predicts clinical symptom severity. *Neuroimage, 57*(1), 113-123.

Dale, A. M., Fischl, B., & Sereno, M. I. (1999). Cortical surface-based analysis: I. Segmentation and surface reconstruction. *Neuroimage, 9*(2), 179-194.

Dale, A. M., & Sereno, M. I. (1993). Improved localizadon of cortical activity by combining eeg and meg with mri cortical surface reconstruction: A linear approach. *Journal of cognitive neuroscience, 5*(2), 162-176.

Deshpande, G., Libero, L. E., Sreenivasan, K. R., Deshpande, H. D., & Kana, R. K. (2013). Identification of neural connectivity signatures of autism using machine learning. *Frontiers in human neuroscience, 7*.

Desikan, R. S., Ségonne, F., Fischl, B., Quinn, B. T., Dickerson, B. C., Blacker, D., . . . Hyman, B. T. (2006). An automated labeling system for subdividing the human cerebral cortex on MRI scans into gyral based regions of interest. *Neuroimage, 31*(3), 968-980.

Douglas, P., Harris, S., Yuille, A., & Cohen, M. (2011). Performance comparison of machine learning algorithms and number of independent components used in fMRI decoding of belief vs. disbelief. *NeuroImage, 56*(2), 544-553.

Ecker, C., Ginestet, C., Feng, Y., Johnston, P., Lombardo, M. V., Lai, M.-C., . . . Murphy, C. M. (2013). Brain surface anatomy in adults with autism: the relationship between surface area, cortical thickness, and autistic symptoms. *JAMA psychiatry, 70*(1), 59-70.

Ecker, C., Marquand, A., Mourão-Miranda, J., Johnston, P., Daly, E. M., Brammer, M. J., . . . Williams, S. C. (2010). Describing the brain in autism in five dimensions—magnetic resonance imaging-assisted diagnosis of autism spectrum disorder using a multiparameter classification approach. *The Journal of Neuroscience, 30*(32), 10612-10623.

Ecker, C., Rocha-Rego, V., Johnston, P., Mourao-Miranda, J., Marquand, A., Daly, E. M., . . . Murphy, D. G. (2010). Investigating the predictive value of whole-brain structural MR scans in autism: a pattern classification approach. *Neuroimage, 49*(1), 44-56.

Ecker, C., Spooren, W., & Murphy, D. (2013). Translational approaches to the biology of Autism: false dawn or a new era&quest. *Molecular psychiatry, 18*(4), 435-442.

Fayed, N., Olmos, S., Morales, H., & Modrego, P. J. (2006). Physical basis of magnetic resonance spectroscopy and its application to central nervous system diseases. *American Journal of Applied Sciences, 3*(5), 1836.

Fischl, B. (2012). FreeSurfer. *Neuroimage, 62*(2), 774-781.

Fischl, B., & Dale, A. M. (2000). Measuring the thickness of the human cerebral cortex from magnetic resonance images. *Proceedings of the National Academy of Sciences, 97*(20), 11050-11055.

Fischl, B., Liu, A., & Dale, A. M. (2001). Automated manifold surgery: constructing geometrically accurate and topologically correct models of the human cerebral cortex. *Medical Imaging, IEEE Transactions on, 20*(1), 70-80.

Fischl, B., Salat, D. H., Busa, E., Albert, M., Dieterich, M., Haselgrove, C., . . . Klaveness, S. (2002). Whole brain segmentation: automated labeling of neuroanatomical structures in the human brain. *Neuron, 33*(3), 341-355.

Fischl, B., Salat, D. H., van der Kouwe, A. J., Makris, N., Ségonne, F., Quinn, B. T., & Dale, A. M. (2004). Sequence-independent segmentation of magnetic resonance images. *Neuroimage, 23*, S69-S84.

Fischl, B., Sereno, M. I., & Dale, A. M. (1999). Cortical surface-based analysis: II: Inflation, flattening, and a surface-based coordinate system. *Neuroimage, 9*(2), 195-207.

Fischl, B., Sereno, M. I., Tootell, R. B., & Dale, A. M. (1999). High-resolution intersubject averaging and a coordinate system for the cortical surface. *Human brain mapping, 8*(4), 272-284.

Fischl, B., van der Kouwe, A., Destrieux, C., Halgren, E., Ségonne, F., Salat, D. H., . . . Kennedy, D. (2004). Automatically parcellating the human cerebral cortex. *Cerebral cortex, 14*(1), 11-22.

Friston, K. J., & Ashburner, J. (2004). Generative and recognition models for neuroanatomy. *Neuroimage, 23*(1), 21-24. doi: 10.1016/j.neuroimage.2004.04.021

Fujii, E., Mori, K., Miyazaki, M., Hashimoto, T., Harada, M., & Kagami, S. (2010). Function of the frontal lobe in autistic individuals: a proton magnetic resonance spectroscopic study. *J Med Invest, 57*(1-2), 35-44.

Groen, W. B., Buitelaar, J. K., Van Der Gaag, R. J., & Zwiers, M. P. (2011). Pervasive microstructural abnormalities in autism: a DTI study. *Journal of psychiatry & neuroscience: JPN, 36*(1), 32.

Hadjikhani, N., Joseph, R. M., Snyder, J., & Tager-Flusberg, H. (2006). Anatomical differences in the mirror neuron system and social cognition network in autism. *Cerebral cortex, 16*(9), 1276-1282.

Han, X., Jovicich, J., Salat, D., van der Kouwe, A., Quinn, B., Czanner, S., . . . Killiany, R. (2006). Reliability of MRI-derived measurements of human cerebral cortical thickness: the effects of field strength, scanner upgrade and manufacturer. *Neuroimage, 32*(1), 180-194.

Hardan, A., Muddasani, S., Vemulapalli, M., Keshavan, M., & Minshew, N. (2006). An MRI study of increased cortical thickness in autism. *American Journal of Psychiatry, 163*(7), 1290-1292.

Hazlett, H. C., Poe, M., Gerig, G., Smith, R. G., Provenzale, J., Ross, A., . . . Piven, J. (2005). Magnetic resonance imaging and head circumference study of brain size in autism: birth through age 2 years. *Archives of general psychiatry, 62*(12), 1366-1376.

Hazlett, H. C., Poe, M. D., Gerig, G., Styner, M., Chappell, C., Smith, R. G., . . . Piven, J. (2011). Early brain overgrowth in autism associated with an increase in cortical surface area before age 2 years. *Archives of general psychiatry, 68*(5), 467-476.

Hutsler, J. J., Love, T., & Zhang, H. (2007). Histological and magnetic resonance imaging assessment of cortical layering and thickness in autism spectrum disorders. *Biological psychiatry, 61*(4), 449-457.

Hutsler, J. J., & Zhang, H. (2010). Increased dendritic spine densities on cortical projection neurons in autism spectrum disorders. *Brain research, 1309*, 83-94.

Huttenlocher, P. R. (1990). Morphometric study of human cerebral cortex development. *Neuropsychologia, 28*(6), 517-527.

Hyde, K. L., Samson, F., Evans, A. C., & Mottron, L. (2010). Neuroanatomical differences in brain areas implicated in perceptual and other core features of autism revealed by cortical

thickness analysis and voxel-based morphometry. *Human brain mapping, 31*(4), 556-566.

Ingalhalikar, M., Parker, D., Bloy, L., Roberts, T. P., & Verma, R. (2011). Diffusion based abnormality markers of pathology: toward learned diagnostic prediction of ASD. *Neuroimage, 57*(3), 918-927.

Ipser, J. C., Syal, S., Bentley, J., Adnams, C. M., Steyn, B., & Stein, D. J. (2012). 1H-MRS in autism spectrum disorders: a systematic meta-analysis. *Metabolic brain disease, 27*(3), 275-287.

Jiao, Y., Chen, R., Ke, X., Cheng, L., Chu, K., Lu, Z., & Herskovits, E. (2011). Predictive models for subtypes of autism spectrum disorder based on single-nucleotide polymorphisms and magnetic resonance imaging. *Advances in medical sciences, 56*(2), 334-342.

Jiao, Y., Chen, R., Ke, X., Chu, K., Lu, Z., & Herskovits, E. H. (2010). Predictive models of autism spectrum disorder based on brain regional cortical thickness. *Neuroimage, 50*(2), 589-599.

Jou, R., Mateljevic, N., Kaiser, M., Sugrue, D., Volkmar, F., & Pelphrey, K. (2011). Structural neural phenotype of autism: preliminary evidence from a diffusion tensor imaging study using tract-based spatial statistics. *American Journal of Neuroradiology, 32*(9), 1607-1613.

Jovicich, J., Czanner, S., Greve, D., Haley, E., van der Kouwe, A., Gollub, R., . . . MacFall, J. (2006). Reliability in multi-site structural MRI studies: effects of gradient non-linearity correction on phantom and human data. *Neuroimage, 30*(2), 436-443.

Kaiser, M. D., & Pelphrey, K. A. (2012). Disrupted action perception in autism: behavioral evidence, neuroendophenotypes, and diagnostic utility. *Developmental cognitive neuroscience, 2*(1), 25-35.

Kana, R. K., Libero, L. E., & Moore, M. S. (2011). Disrupted cortical connectivity theory as an explanatory model for autism spectrum disorders. *Physics of life reviews, 8*(4), 410-437.

Keller, T. A., Kana, R. K., & Just, M. A. (2007). A developmental study of the structural integrity of white matter in autism. *Neuroreport, 18*, 23-27.

Kleinhans, N. M., Schweinsburg, B. C., Cohen, D. N., Müller, R.-A., & Courchesne, E. (2007). N-acetyl aspartate in autism spectrum disorders: Regional effects and relationship to fMRI activation. *Brain research, 1162*, 85-97.

Kuperberg, G. R., Broome, M. R., McGuire, P. K., David, A. S., Eddy, M., Ozawa, F., . . . van der Kouwe, A. J. (2003). Regionally localized thinning of the cerebral cortex in schizophrenia. *Archives of general psychiatry, 60*(9), 878-888.

Lange, N., DuBray, M. B., Lee, J. E., Froimowitz, M. P., Froehlich, A., Adluru, N., . . . Bigler, E. D. (2010). Atypical diffusion tensor hemispheric asymmetry in autism. *Autism research, 3*(6), 350-358.

Lee, J. E., Bigler, E. D., Alexander, A. L., Lazar, M., DuBray, M. B., Chung, M. K., . . . McMahon, W. M. (2007). Diffusion tensor imaging of white matter in the superior temporal gyrus and temporal stem in autism. *Neuroscience letters, 424*(2), 127-132.

Lentz, M. R., Kim, J. P., Westmoreland, S. V., Greco, J. B., Fuller, R. A., Ratai, E. M., . . . Gonzalez, R. G. (2005). Quantitative neuropathologic correlates of changes in ratio of N-acetylaspartate to creatine in macaque brain. *Radiology, 235*(2), 461-468. doi: 10.1148/radiol.2352040003

Libero, L. E., & Kana, R. K. (2013). Advancing our understanding of the brain in autism: contribution of functional MRI and diffusion tensor imaging. *Imaging in Medicine, 5*(5), 453-465.

Loh, W.-Y. (2011). Classification and regression trees. *Data Mining and Knowledge Discovery, 1*, 14–23.

Lord, C., Risi, S., Lambrecht, L., Cook Jr, E. H., Leventhal, B. L., DiLavore, P. C., . . . Rutter, M. (2000). The Autism Diagnostic Observation Schedule—Generic: A standard measure of social and communication deficits associated with the spectrum of autism. *Journal of autism and developmental disorders, 30*(3), 205-223.

Maddock, R. J., & Buonocore, M. H. (2012). MR spectroscopic studies of the brain in psychiatric disorders *Brain Imaging in Behavioral Neuroscience* (pp. 199-251): Springer.

Mak-Fan, K. M., Taylor, M. J., Roberts, W., & Lerch, J. P. (2012). Measures of cortical grey matter structure and development in children with autism spectrum disorder. *Journal of autism and developmental disorders, 42*(3), 419-427.

Maximo, J. O., Cadena, E. J., & Kana, R. K. (2014). The Implications of Brain Connectivity in the Neuropsychology of Autism. *Neuropsychology review, 24*(1), 16-31.

Meyerhoff, D. J., MacKay, S., Bachman, L., Poole, N., Dillon, W., Weiner, M., & Fein, G. (1993). Reduced brain N-acetylaspartate suggests neuronal loss in cognitively impaired human immunodeficiency virus-seropositive individuals In vivo 1H magnetic resonance spectroscopic imaging. *Neurology, 43*(3 Part 1), 509-509.

Murdaugh, D. L., Shinkareva, S. V., Deshpande, H. R., Wang, J., Pennick, M. R., & Kana, R. K. (2012). Differential deactivation during mentalizing and classification of autism based on default mode network connectivity. *PloS one, 7*(11), e50064.

Nair, S., Tan, L., Mohd Ramli, N., Lim, S., Rahmat , K., & Mohd Nor, H. (2013). A decision tree for differentiating multiple system atrophy from Parkinson's disease using 3-T MR imaging. *European Radiology, 23*(6), 1459-1466.

Naressi, A., Couturier, C., Devos, J., Janssen, M., Mangeat, C., De Beer, R., & Graveron-Demilly, D. (2001). Java-based graphical user interface for the MRUI quantitation package. *Magnetic Resonance Materials in Physics, Biology and Medicine, 12*(2-3), 141-152.

Nichols, T. E., & Holmes, A. P. (2002). Nonparametric permutation tests for functional neuroimaging: a primer with examples. *Human brain mapping, 15*(1), 1-25.

Nickl-Jockschat, T., Habel, U., Maria Michel, T., Manning, J., Laird, A. R., Fox, P. T., . . . Eickhoff, S. B. (2012). Brain structure anomalies in autism spectrum disorder—a meta-analysis of VBM studies using anatomic likelihood estimation. *Human brain mapping, 33*(6), 1470-1489.

Oldfield, R. C. (1971). The assessment and analysis of handedness: the Edinburgh inventory. *Neuropsychologia, 9*(1), 97-113.

Pijnappel, W., Van den Boogaart, A., De Beer, R., & Van Ormondt, D. (1992). SVD-based quantification of magnetic resonance signals. *Journal of Magnetic Resonance (1969), 97*(1), 122-134.

Quinlan, J. (1986). Induction of Decision Trees. *Machine Learning, 1*, 81-106.

Rakic, P. (1988). Specification of cerebral cortical areas. *Science, 241*(4862), 170-176.

Raznahan, A., Toro, R., Daly, E., Robertson, D., Murphy, C., Deeley, Q., . . . Murphy, D. G. (2010). Cortical anatomy in autism spectrum disorder: an in vivo MRI study on the effect of age. *Cerebral cortex, 20*(6), 1332-1340.

Ritvo, R. A., Ritvo, E. R., Guthrie, D., Ritvo, M. J., Hufnagel, D. H., McMahon, W., . . . Attwood, T. (2011). The Ritvo Autism asperger diagnostic scale-revised (RAADS-R): a scale to assist the diagnosis of Autism spectrum disorder in adults: an international validation study. *Journal of autism and developmental disorders, 41*(8), 1076-1089.

Rohde, G. K., Barnett, A. S., Basser, P. J., Marenco, S., & Pierpaoli, C. (2004). Comprehensive approach for correction of motion and distortion in diffusion-weighted MRI. *Magn Reson Med, 51*(1), 103-114. doi: 10.1002/mrm.10677

Rosas, H., Liu, A., Hersch, S., Glessner, M., Ferrante, R., Salat, D., . . . Fischl, B. (2002). Regional and progressive thinning of the cortical ribbon in Huntington's disease. *Neurology, 58*(5), 695-701.

Rutter, M., Le Couteur, A., & Lord, C. (2003). Autism diagnostic interview-revised. *Los Angeles, CA: Western Psychological Services*.

Salat, D. H., Buckner, R. L., Snyder, A. Z., Greve, D. N., Desikan, R. S., Busa, E., . . . Fischl, B. (2004). Thinning of the cerebral cortex in aging. *Cerebral cortex, 14*(7), 721-730.

Scheel, C., Rotarska-Jagiela, A., Schilbach, L., Lehnhardt, F. G., Krug, B., Vogeley, K., & Tepest, R. (2011). Imaging derived cortical thickness reduction in high-functioning autism: key regions and temporal slope. *Neuroimage, 58*(2), 391-400.

Schiffmann, R., & van der Knaap, M. (2009). Invited article: an MRI-based approach to the diagnosis of white matter disorders. *Neurology, 72*(8), 750-759.

Schipul, S. E., Keller, T. A., & Just, M. A. (2011). Inter-regional brain communication and its disturbance in autism. *Front Syst Neurosci, 5*(10), 7.

Ségonne, F., Dale, A., Busa, E., Glessner, M., Salat, D., Hahn, H., & Fischl, B. (2004). A hybrid approach to the skull stripping problem in MRI. *Neuroimage, 22*(3), 1060-1075.

Ségonne, F., Pacheco, J., & Fischl, B. (2007). Geometrically accurate topology-correction of cortical surfaces using nonseparating loops. *Medical Imaging, IEEE Transactions on, 26*(4), 518-529.

Shukla, D. K., Keehn, B., Lincoln, A. J., & Müller, R.-A. (2010). White matter compromise of callosal and subcortical fiber tracts in children with autism spectrum disorder: a diffusion tensor imaging study. *Journal of the American Academy of Child & Adolescent Psychiatry, 49*(12), 1269-1278. e1262.

Sled, J. G., Zijdenbos, A. P., & Evans, A. C. (1998). A nonparametric method for automatic correction of intensity nonuniformity in MRI data. *Medical Imaging, IEEE Transactions on, 17*(1), 87-97.

Sowell, E. R., Thompson, P. M., Leonard, C. M., Welcome, S. E., Kan, E., & Toga, A. W. (2004). Longitudinal mapping of cortical thickness and brain growth in normal children. *The Journal of Neuroscience, 24*(38), 8223-8231.

Spencer, M., Holt, R., Chura, L., Suckling, J., Calder, A., Bullmore, E., & Baron-Cohen, S. (2011). A novel functional brain imaging endophenotype of autism: the neural response to facial expression of emotion. *Translational psychiatry, 1*(7), e19.

Stanfield, A. C., McIntosh, A. M., Spencer, M. D., Philip, R., Gaur, S., & Lawrie, S. M. (2008). Towards a neuroanatomy of autism: a systematic review and meta-analysis of structural magnetic resonance imaging studies. *European Psychiatry, 23*(4), 289-299.

Stanley, J. A. (2002). In vivo magnetic resonance spectroscopy and its application to neuropsychiatric disorders. *Canadian journal of psychiatry. Revue canadienne de psychiatrie, 47*(4), 315-326.

Stoner, R., Chow, M. L., Boyle, M. P., Sunkin, S. M., Mouton, P. R., Roy, S., . . . Courchesne, E. (2014). Patches of Disorganization in the Neocortex of Children with Autism. *New England Journal of Medicine, 370*(13), 1209-1219.

Stork, C., & Renshaw, P. (2005). Mitochondrial dysfunction in bipolar disorder: evidence from magnetic resonance spectroscopy research. *Molecular psychiatry, 10*(10), 900-919.

Suzuki, K., Nishimura, K., Sugihara, G., Nakamura, K., Tsuchiya, K. J., Matsumoto, K., . . . Sugiyama, T. (2010). Metabolite alterations in the hippocampus of high-functioning adult subjects with autism. *The International Journal of Neuropsychopharmacology, 13*(04), 529-534.

Travers, B. G., Adluru, N., Ennis, C., Tromp do, P. M., Destiche, D., Doran, S., . . . Alexander, A. L. (2012). Diffusion tensor imaging in autism spectrum disorder: a review. *Autism Res, 5*(5), 289-313. doi: 10.1002/aur.1243

Uddin, L. Q., Menon, V., Young, C. B., Ryali, S., Chen, T., Khouzam, A., . . . Hardan, A. Y. (2011). Multivariate searchlight classification of structural magnetic resonance imaging in children and adolescents with autism. *Biological psychiatry, 70*(9), 833-841.

Vanhamme, L., van den Boogaart, A., & Van Huffel, S. (1997). Improved method for accurate and efficient quantification of MRS data with use of prior knowledge. *Journal of Magnetic Resonance, 129*(1), 35-43.

Wallace, G. L., Dankner, N., Kenworthy, L., Giedd, J. N., & Martin, A. (2010). Age-related temporal and parietal cortical thinning in autism spectrum disorders. *Brain, 133*(12), 3745-3754.

Wechsler, D. (1999). *Wechsler abbreviated scale of intelligence*: Psychological Corporation.

Wonderlick, J., Ziegler, D. A., Hosseini-Varnamkhasti, P., Locascio, J., Bakkour, A., Van Der Kouwe, A., . . . Dickerson, B. C. (2009). Reliability of MRI-derived cortical and subcortical morphometric measures: effects of pulse sequence, voxel geometry, and parallel imaging. *Neuroimage, 44*(4), 1324-1333.

Yeatman, J. D., Dougherty, R. F., Myall, N. J., Wandell, B. A., & Feldman, H. M. (2012). Tract profiles of white matter properties: automating fiber-tract quantification. *PLoS one, 7*(11), e49790.

Table 1. Participant demographic information.

	Autism			Control			Group difference	
	N = 19			*N* = 18				
	Mean	Range	s.d.	Mean	Range	s.d.	*t*-value	*P*-value
Age	27.1	19-40	1.38	24.6	19-38	1.22	1.39	0.17
Verbal IQ	113.7	95-139	3.15	113.0	88-141	3.04	0.15	0.88
Performance IQ	113.9	89-138	3.18	115.2	99-133	3.08	0.27	0.78
Full-scale IQ	115.4	99-140	2.88	117.1	103-140	2.73	0.41	0.68
RAADS total	128.9	72-181	7.04	39.8	13-77	3.99	10.8	<0.0001

Table 2. Group differences in cortical thickness, comparing TD and ASD adults.

Region	F-statistic	P-value	Direction
(1) L Caudal Anterior Cingulate	5.46	0.025	ASD>TD
(2) L Posterior Cingulate	5.84	0.021	ASD>TD
(3) L Isthmus Cingulate	7.27	0.011	ASD>TD
(4) L Pars Opercularis	4.87	0.034	ASD>TD
(5) L Inferior Temporal	5.16	0.029	ASD>TD
(6) R Cuneus	4.2	0.048	TD>ASD
(7) R Precentral	5.54	0.024	TD>ASD
(8) R Precuneus	5.07	0.03	ASD>TD

Table 3. Group differences in neurochemical concentrations for of the dACC and PCC, comparing ASD and TD adults.

		ASD (n = 19)	TD (n=18)	Group Differences	
ROI	Metabolite	Mean (SD)	Mean (SD)	*F*-statistic	p-value
dACC	NAA/Cr	1.39(0.08)	1.47(0.08)	$F(1,33)=4.94$	0.033
	CRLB,%	4.57(0.003)	5.03(0.003)		
	Glx/CR	0.74(0.09)	0.78(0.09)	$F(1,33)=0.914$	0.346
	CRLB,%	8.82(0.007)	9.16(0.006)		
	Cho/Cr	0.80(0.09)	0.79(0.07)	$F(1,33)=0.004$	0.952
	CRLB,%	3.35(0.002)	3.57(0.002)		
	Linewidth, Hz	4.84(0.87)	4.55(0.68)	$F(1,36)=1.26$	0.269
PCC	NAA/Cr	1.49(0.06)	1.51(0.08)	$F(1,33)=0.814$	0.373
	CRLB,%	3.17(0.001)	3.56(0.002)		
	Glx/Cr	0.74(0.07)	0.75(0.08)	$F(1,33)=0.294$	0.591
	CRLB,%	5.96(0.002)	6.72(0.005)		
	Cho/Cr	0.59(0.06)	0.57(0.07)	$F(1,33)=0.960$	0.334
	CRLB,%	2.01(0.0008)	2.21(0.001)		
	Linewidth, Hz	5.10(0.60)	5.18(1.57)	$F(1,36)=0.04$	0.846

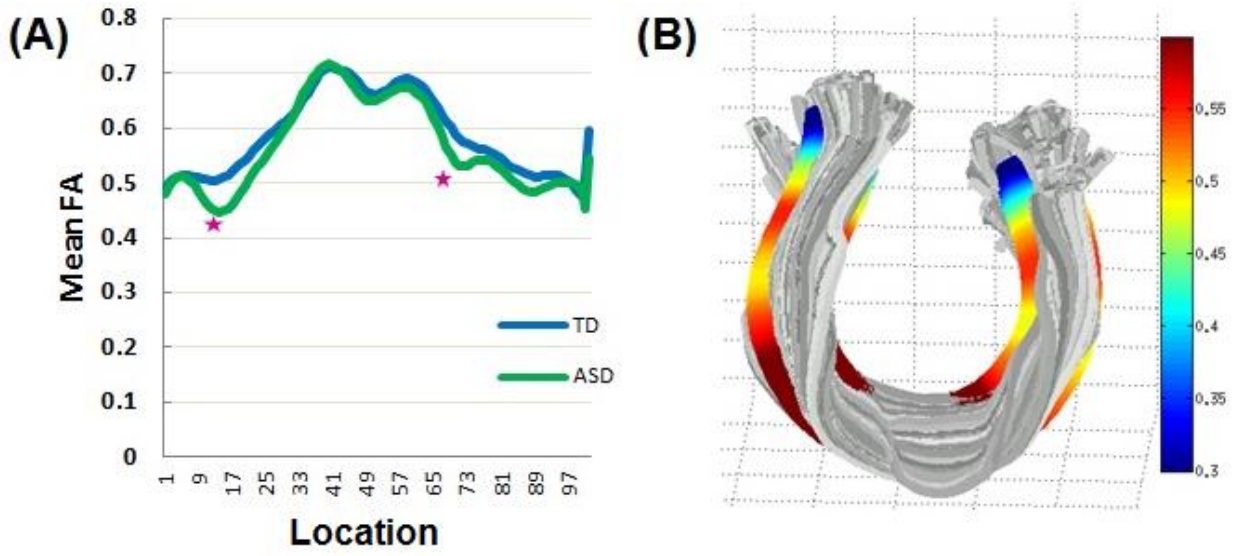

Figure 1. (A) Group means for fractional anisotropy (FA) for the nodes along the forceps minor of the corpus callosum for the TD (depicted in blue) and ASD (depicted in green) groups. The clusters with significant reduction in FA in ASD participants ($p<0.05$, corrected) are indicated with a star; (B) A rendering of FA measurements for the forceps minor of the corpus callosum for one subject as a visualization of the tract properties.

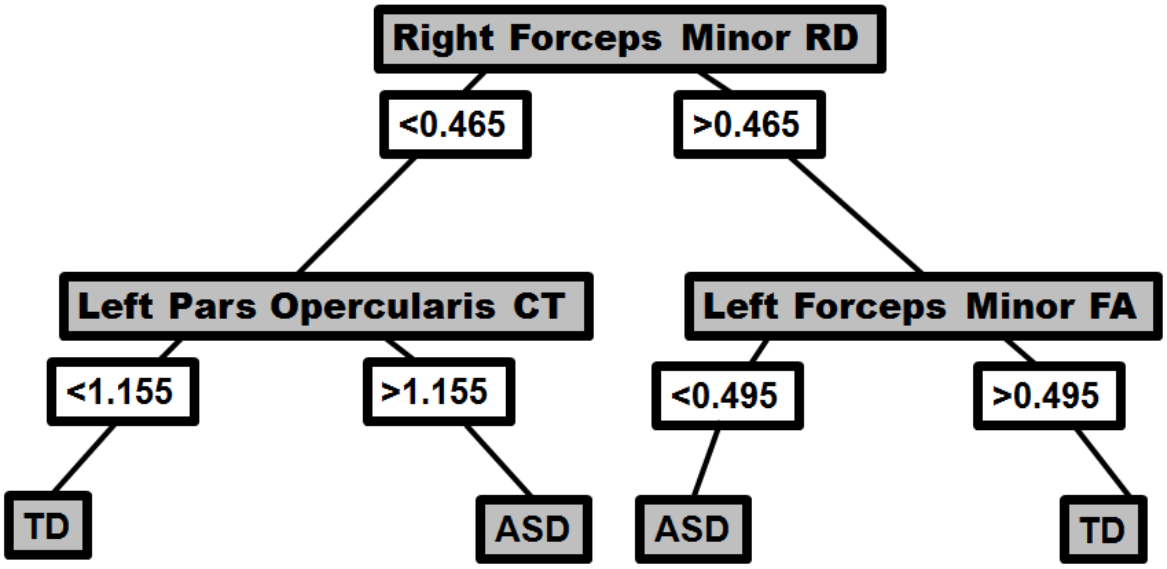

Figure 2: Decision tree for classification of autism (ASD) and typically developing (TD) groups, including the following predictors: right forceps minor radial diffusivity (RD), left Inferior Frontal Gyrus pars opercularis cortical thickness (CT), and left forceps minor fractional anisotropy (FA). Classification accuracy reached 91.9% +/- 0.42.

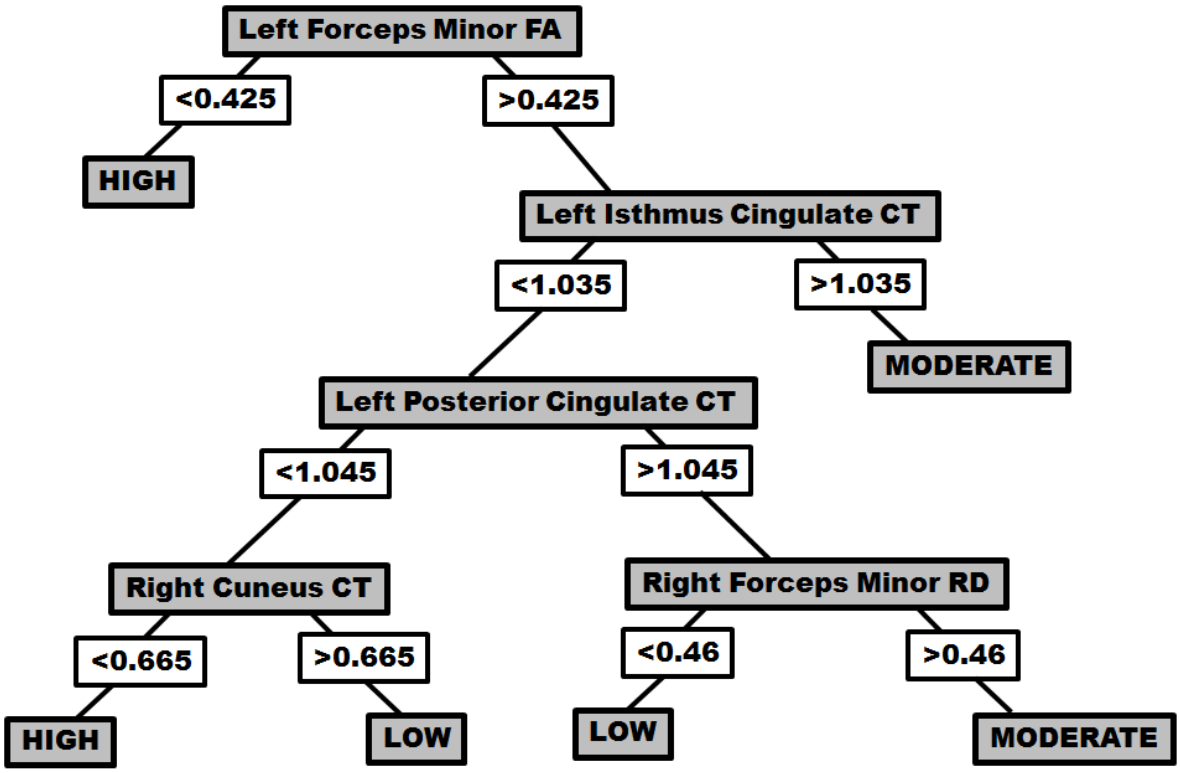

Figure 3: Decision tree for a regression model including symptom severity scores (measured by RAADS-R) and significant factors including left forceps minor fractional anisotropy (FA), cortical thickness (CT) for left isthmus cingulate, left posterior cingulate, and right cuneus, and radial diffusivity (RD) for right forceps minor.

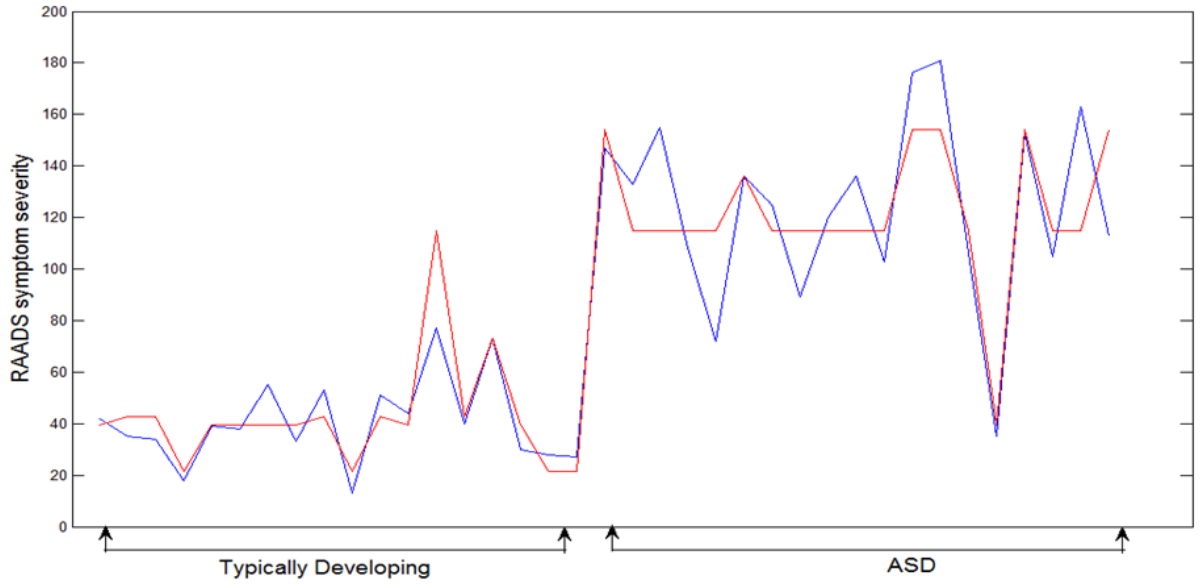

Figure 4: Original (blue) and predicted (red) symptom severity (measured by RAADS-R) using a regression model including typically developing (TD) and autism (ASD) participants.

SUMMARY

By studying ASD from the perspective of three MRI techniques, this project aimed to gain a more comprehensive understanding of the structural integrity and organization of the brain in autism. The current study examined brain structure, diffusion, and metabolite levels in relation to age and behavioral functioning of children and adults with ASD. Although previous studies have found alterations in diffuse and spatially distant brain regions in ASD, these findings have been relatively inconsistent. An understanding of the neural systems affected by ASD is critical in: 1) characterizing its etiology; 2) in using neural markers for diagnostic purpose; and 3) in designing neurobiologically informed and targeted intervention for individuals with autism. This project used multimodal MRI to investigate brain structure, white matter integrity, neurochemical concentrations, and classification in children and adults with ASD.

We found significant alterations in cortical volume, cortical thickness, surface area, and gyrification in children and adults with ASD. The ASD participants had significantly reduced cortical thickness in right rostral anterior cingulate cortex, right superior parietal lobule, and reduced gyrification in right precentral gyrus. Whereas, measures were significantly greater for the ASD group for volume of the right posterior cingulate cortex and TPJ, cortical thickness for right pars orbitalis, left TPJ, and left superior frontal, and surface area for right posterior cingulate cortex and left TPJ. Age-related relationships emerged for both groups for many of the regions that showed significant group differences for surface based measures, with several correlations differing between ASD and TD. Overall, these findings represent widespread alterations in surface brain measures in children and adults with ASD, potentially underscoring the behavioral abnormalities that are characteristic of autism.

The results of our DTI study indicate a significant reduction in fractional anisotropy (FA) for the left superior longitudinal fasciculus (LSLF) in ASD children and adults, compared to their TD peers. A significant increase in radial diffusivity for ASD participants was also found in the same cluster along the LSLF. In addition, a significant positive correlation emerged for all subjects between FA for the LSLF and age, with FA increasing with age. Finally, a significant negative correlation was found between FA in the LSLF and autism symptom severity in adults with ASD, indicating greater abnormalities in white matter as the severity of autism increased. These findings point to alterations in long distance white matter connectivity in children and adults with ASD, potentially underscoring the relationship between white matter microstructure and the ASD phenotype. These results also suggest that the white matter abnormalities in autism may be subtle and related to symptom severity and the developmental trajectory.

This project also investigated levels of neurochemicals in the cingulate cortex in adults with ASD using 1H-MRS. The main findings include a significant reduction in NAA/Cr in the anterior cingulate for adults with ASD, compared to their TD peers. No significant differences in Glx/Cr or Cho/Cr were found in dorsal anterior cingulate cortex. Nor were there any significant alterations in NAA/Cr, Cho/Cr, and Glx/Cr in the posterior cingulate cortex. Results of this study provide evidence for metabolic dysfunction in the anterior cingulate cortex in adults with ASD, suggesting poor neuronal health in that area. Poor neuronal health in dACC can have significant impact on the structural and functional integrity of this region in individuals with ASD.

The information gained from the current project could potentially be used for diagnostic purposes, or classification of individuals into subgroups for more targeted treatment. Currently ASD is diagnosed by clinical observations during a short period of time in a clinical evaluation. This is coupled with the fact that the presentation of ASD varies greatly from child to child,

making diagnosis that much more challenging. Because of these limitations, the median earliest age of ASD diagnosis is 4.4 years (Autism and Developmental Disabilities Monitoring Network, 2014**)**, while most children receive a diagnosis much later. As it is very difficult to identify children earlier by observing behaviors, a neural marker can make a significant difference in early diagnosis and hence early intervention for affected children. A neural marker (founded in multimodal measurements of neural features) for the disorder could be applied to babies or toddlers who are too young for current ASD behavioral tests. This has strong implications for early intervention and increasing the success of ASD treatment as earlier intervention has proven to be effective with higher achievement (Sheinkopf & Siegel, 1998; Harris & Handleman, 2000). The current study found cortical thickness and diffusion measures (FA and RD) were significant in classifying participants with ASD apart from the TD participants. In addition, cortical thickness features and diffusion variables were also interactive in their relationship with ASD symptom severity. This line of research could potentially become very useful for clinical diagnosis as it applied to younger and younger participants with ASD.

This project extends previous findings of alterations in brain structure, organization, and health in ASD. In addition, we demonstrate the utility of combining these measures to better understand ASD and the features most relevant to diagnosis. Together, the results provide a better understanding of the neural features of ASD, and contribute to the literature on the neural systems affected by ASD. Information about surface based features, white matter integrity, and brain metabolite concentrations gives us insight into the overall makeup of the ASD brain. The information gained about brain structure, white matter integrity, and metabolite levels in ASD may also be useful in future studies for identifying specific pathways or tracts to target for intervention in ASD. Improving brain organization, connectivity, or metabolite levels could

improve cognition and ASD behavior, as has been seen in previous studies in other clinical populations like dyslexia (Temple et al., 2003; Keller & Just, 2009; Krafnick, Flowers, Napoliello, & Eden, 2011), bipolar disorder (Davanzo et al., 2001), and Alzheimer's disease (Jessen et al., 2006).

Overall, the current project found significant alterations in brain structure, white matter connectivity, and neuronal health in participants with ASD. These measures were also useful in developing a classification model for identifying participants with ASD. The multimodal brain imaging evidence from this study provides a more comprehensive characterization, which spans several levels and layers, of the neural organization and health of autism.

GENERAL REFERENCES

Alexander, A. L., Lee, J. E., Lazar, M., Boudos, R., DuBray, M .B., Oakes, T. R., Miller, J. N., Lu, J., Jeong, E. K., McMahon, W. M., Bigler, E. D., & Lainhart, J. E. (2007). Diffusion tensor imaging of the corpus callosum in autism. *Neuroimage, 34*, 61–73.

Amaral, D. G., Schumann, C. M., & Nordahl, C. W. (2008). Neuroanatomy of autism. *Trends Neurosci., 31,* 137-145. doi: 10.1016/j.tins.2007/12.005

Akshoomoff, N., Lord, C., Lincoln, A., Courchesne, R., Carper, R., Townsend, J., & Courchesne, E. (2004). Outcome classification of preschool children with autism spectrum disorder using MRI brain measures. *J. Amer. Acad. Child Adolesc. Psyc., 43,* 349-357.

Anderson, J., Nielsen, J., Froehlich, A., DuBray, M., Druzgal, T., Cariello, A., Cooperrider, J., Zielinski, B., Ravichandran, C., Fletcher, P., Alexander, A., Bigler, E., Lange, N., & Lainhart, J. (2011). Functional connectivity magnetic resonance imaging classification of autism. *Brain, 12,* 3742-3754. doi: 10.1093/brain/awr263

Ashburner, J., & Frison, K. J. (2000). Voxel-based morphometry—the methods. *Neuroimage, 11,* 805-821. doi: 10.1006/nimg.2000.0582

Auzias, G., Viellard, M., Takerkart, S., Villeneuve, N., Poinso, F., Da Fonseca, D., Deruelle, C. (2014). Atypical sulcal anatomy in young children with autism spectrum disorder. *Neuroimage Clinical.*

Barnea-Goraly, N., Kwon, H., Menon, V., Eliez, S., Lotspeich, L., & Reiss, A. L. (2004). White matter structure in autism: preliminary evidence from diffusion tensor imaging. *Biol. Psychiatry, 55*, 323-326.

Basser, P. J. (1995). Inferring microstructural features and the physiological state of tissues from diffusion-weighted images. *NMR Biomed., 8*, 333–344.

Beaulieu, C. (2002). The basis of anisotropic water diffusion in the nervous system - a technical review. *NMR Biomed., 15*, 435–455.

Bernardi, S., Anagnostou, E., Shen, J., Kolevzon, A., Buxbaum, J., Hollander, E., Hof, P. R., & Fan, J. (2011). In vivo 1H-magnetic resonance spectroscopy study of the attentional networks in autism. *Brain Res., 1380,* 198-205. doi: 10.1016/j.brainres.2010.12.057

Bloemen, O. J., Deeley, Q., Sundram, F., Daly, E. M., Barker, G. J., Jones, D. K., van Amelsvoort, T. A., Schmitz, N., Robertson, D., Murphy, K. C., & Murphy, D. G. (2010). White matter integrity in Asperger syndrome: a preliminary diffusion tensor magnetic resonance imaging study in adults. *Autism res., 3*, 203-213. doi: 10.1002/aur.146

Bookstein, F. (2001). Voxel-based morphometry should not be used with imperfectly registered

images. *Neuroimage, 14,* 1454-1462.

Brambilla, P., Hardan, A., di Nemi, U. S., Perez, J., Soares, J. C., & Barale, F. (2003). Brain anatomy and development in autism: review of structural MRI studies. *Brain Res. Bull., 61,* 557-569.

Calderoni, S., Retico, A., Biagi, L., Tancredi, R., Muratori, F., & Tosetti, M. (2012). Female children with autism spectrum disorder: An insight from mass-univariate and pattern classification analyses. *NeuroImage, 59,* 1013-1022.

Chen, R., Jiao, Y., & Herskovits, E. H. (2011). Structural MRI in autism spectrum disorder. *Pediatr. Res., 69,* 63R-68R. doi: 10.1203/PDR.0b013e318212c2b3

Chugani, D. C., Sundram, B. S., Behen, M., Lee, M. L., & Moore, G. J. (1999). Evidence of altered energy metabolism in autistic children. *Prog. Neuropsychopharmacol. Biol. Psychiatry, 23,* 635–641.

Courchesne, E., Carper, R. A., & Akshoomoff, N. A. (2003). Evidence of brain overgrowth in the first year of life in autism. *JAMA,* 290, 337-344.

Courchesne, E., Karns, C. M., Davis, H. R., Ziccardi, R., Carper, R. A., Tigue, Z. D., Chisum, H. J., Moses, P., Pierce, K., Lord, C., Lincoln, A. J., Pizzo, S., Schreibman, L., Haas, R. H., Akshoomoff, N. A., & Courchesne, R. Y. (2001). Unusual brain growth patterns in early life in patients with autistic disorder: an MRI study. *Neurology,* 57, 245-254.

Coutanche, M., Thompson-Schill, S., & Schultz, R. (2011). Multi-voxel pattern analysis of fMRI data predicts clinical symptom severity. *NeuroImage, 1,* 113-123. doi: 10.1016/j.neuroimage.2011.04.016

Davanzo, P., Thomas, M. A., Yue, K., Oshiro, T., Belin, T., Strober, M., & McCracken, J. (2001). Decreased anterior cingulate myo-inositol/creatine spectroscopy resonance with lithium treatment in children with bipolar disorder. *Neuropsychopharmacology, 24,* 359-369.

Davatzikos, C. (2004). Why voxel-based morphometric analysis should be used with great caution when characterizing group differences. *Neuroimage, 23,* 17-20.

Deshpande, G., Libero, L., Sreenivasan, K., Deshpande, H., & Kana, R. (2013). Identification of neural connectivity signatures of autism using machine learning. *Front. Hum. Neurosci., 7,* 670. doi: 10.3389/fnhum.2013.00670

Devito, T., Drost, D. J., Neufeld, R. W., Rajakumar, N., Pavlosky, W., Williamson, P., & Nicholson, R. (2007). Evidence for cortical dysfunction in autism: a proton magnetic resonance spectroscopic imaging study. *Biol. Psychiatry, 6,* 465–473.

Ecker, C., Ginestet, C., Feng, Y., Johnston, P., Lombardo, M., Lai, M., Suckling, J.,

Palaniyappan, L., Daly, E., Murphy, C. M., Williams, S. C., Bullmore, E. T., Baron-Cohen, S., Brammer, M., Murphy, D. G., & MRC AIMS Consortium (2013). Brain surface anatomy in adults with autism: the relationship between surface area, cortical thickness, and autistic symptoms. *JAMA Psychiatry, 70,* 59-70. doi: 10.1001/jamapsychiatry.2013.265

Ecker, C., Marquand, A., Mourao-Miranda, J., Johnston, P., Daly, E., Brammer, M., Maltezos, S., Murphy, C., Robertson, D., Williams, S., & Murphy, D. (2010a). Describing the brain in autism in five dimensions—magnetic resonance imaging-assisted diagnosis of autism spectrum disorder using a multiparameter classification approach. *J. Neurosci, 30,* 10612-10623. doi: 10.1523/JNEUROSCI.5413-09.2010

Ecker, C., Rocha-Rego, V., Johnston, P., Mourao-Miranda, J., Marquand, A., Daly, E., Brammer, M., Murphy, C., Murphy, D., & MRC AIMS Consortium 1 (2010b). Investigating the predictive value of whole-brain structural MR scans in autism: A pattern classification approach. *NeuroImage, 49,* 44-56. doi: 10.1016/j.neuroimage.2009.08.024

Ecker, C., Spooren, W., & Murphy, D. (2013). Translational approaches to the biology of autism: false dawn or a new era? *Molecular Psychiatry, 18,* 435-442. doi: 10.1038/mp.2012.102

Ecker, C., Suckling, J., Deoni, S. C., Lombardo, M. V., Bullmore, E. T., Baron-Cohen, S., Catani, M., Jezzard, P., Barnes, A., Bailey, A. J., Williams, S. C., Murphy, D. G., & MRC AIMS Consortium (2012). Brain anatomy and its relationship to behavior in adults with autism spectrum disorder: a multicenter magnetic resonance imaging study. *Arch. Gen. Psychiatry, 69,* 195-209. doi: 10.1001/archgenpsychiatry.2011.1251

Endo, T., Shioiri, T., Kitamura, G., Kimua, T., Endo, S., Masuzawa, N., & Someya, T. (2007). Altered chemical metabolites in the amygdala-hippocampus region contribute to autistic symptoms of autism spectrum disorders. *Biol. Psychiatry, 62,* 1030-1037.

Fayed, N., & Modrego, P. (2005). Comparative study of cerebral white matter in autism and attention-deficit/hyperactivity disorder by means of magnetic resonance spectroscopy. *Acad. Radiol., 12,* 566–569.

Fayed, N., Olmos, S., Morales, H., & Modrego, P. J. (2006). Physical basis of magnetic resonance spectroscopy and its application to central nervous system diseases. *Am. J. Applied Sci, 3,* 1836-1845. doi: 10.3844/ajassp.2006.1836.1845

Friedman, S., Shaw, D., Artru, A., Richards, T., Gardner, J., Dawson, G., Posse, S., & Dager, S. (2003). Regional brain chemical alterations in young children with autism spectrum disorder. *Neurology, 60,* 100-107.

Fujii, E., Mori, K., Miyazaki, M., Hashimoto, T., Harada, M., & Kagami, S. (2010). Function of the frontal lobe in autistic individuals: a proton magnetic resonance spectroscopic study.

J. Med. Invest., 57, 35–44.

Gabis, L., Huang, W., Azizian, A., DeVincent, C., Tudorica, A., Kesner-Baruch, Y., Roche, P., & Pomeroy, J. (2008). 1H-Magnetic resonance spectroscopy markers of cognitive and language ability in clinical subtypes of autism spectrum disorders. *J. Child Neurol., 23*, 788-774. doi: 10.1177/0883073808315423

Ghosh, S., Kakunoori, S., Augustinack, J., Nieto-Castanon, A., Kovelman, I., Gaab, N., Christodoulou, J., Triantafyllou, C., Gabrieli, J., & Fischl, B. (2011). Evaluating the validity of volume-based and surface-based brain image registration for developmental cognitive neuroscience studies in children 4-to-11 years of age. *Neuroimage, 53,* 85-93.

Hadjikhani, N., Joseph, R. M., Snyder, J., & Tager-Flusberg, H. (2006). Anatomical differences in the mirror neuron system and social cognition network in autism. *Cereb. Cortex, 16,* 1276–1282.

Hallahan, B., Daly, E., McAlonan, G., Loth, E., Toal, F., O'Brien, F., Roberston, D., Hales, S., Murphy, C., Murphy, K. C., & Murphy, D. G. M. (2009). Brain morphometry volume in autistic spectrum disorder: a magnetic resonance imaging study of adults. *Psychol. Med., 39,* 337-346. doi: 10.1017/S0033291708003383

Hardan, A. Y., Jou, R. J., Keshavan, M. S., Varma, R., & Minshew, N. J. (2004). Increased frontal cortical folding in autism: a preliminary MRI study. *Psychiatry Res., 131,* 263–268.

Hardan, A., Libove, R., Keshavan, M., Melhem, N., & Minshew, N. (2009). A preliminary longitudinal magnetic resonance imaging study of brain volume and cortical thickness in autism. *Biological Psychiatry, 66,* 320-326. doi: 10.1016/j.biopsych.2009.04.024

Hardan, A. Y., Minshew, N. J., Melhem, N. M., Srihari, S., Jo, B., Bansal, R., Keshavan, M. S., & Stanley, J. A. (2008). An MRI and proton spectroscopy study of the thalamus in children with autism. *Psychiatry Res.,163,* 97-105. doi: 10.1016/j.pscychresns.2007.12.002

Hardan, A. Y., Muddasani, S., Vemulapalli, M., Keshavan, M. S., & Minshew, N. J. (2006). An MRI study of increased cortical thickness in autism. *Am. J. Psychiatry, 163,* 1290–1292.

Harris, S., & Handleman, J. (2000). Age and IQ at Intake as Predictors of Placement for Young Children with Autism: A Four- to Six-Year Follow-Up. *J. Autism Dev.Disord., 30,* 137-142.

Hazlett, G., Poe, M., Gerig, G., Smith, R. G., Provenzale, J., Ross, A., Gilmore, J., & Piven, J. (2005), Magnetic resonance imaging and head circumference study of brain size in autism. *Arch. Gen. Psychiatry, 62, 1366-1376.*

Hazlett, H., Poe, M., Gerig, G., Styner, M., Chappell, C., Smith, R. G., Vachet, C., & Piven, J. (2011). Early brain overgrowth in autism associated with an increase in cortical surface area before age 2 years. *Arch. Gen. Psychiatry, 68,* 467-476. doi: 10.1001/archgenpsychiatry.2011.39

Herbert, M. R., Ziegler, D. A., Makris, N., Filipek, P. A., Kemper, T. L., Normandin, J. J., Sanders, H. A., Kennedy, D. N., & Caviness, V. S. (2004). Localization of white matter volume increase in autism and developmental language disorder. *Ann. Neurol.,* 55, 530-540.

Hyde, K. L., Samson, F., Evans, A. C., & Mottron, L. (2010). Neuroanatomical differences in brain areas implicated in perceptual and other core features of autism revealed by cortical thickness analysis and voxel-based morphometry. *Hum. Brain Mapp., 31,* 556–566. doi: 10.1002/hbm.20887

Ingalhalikar, M., Parker, D., Bloy, L., Robers, T., & Verma, R. (2011). Diffusion based abnormality markers of pathology: Toward learned diagnostic prediction of ASD. *NeuroImage, 57,* 918-927.

Ipser, J., Bentley, J., Adnams, C., Steyn, B., & Stein, D. (2012). 1H-MRS in autism spectrum disorders: a systematic meta-analysis. *Metabolic brain disease, 27,* 275-287.

Jessen, F., Traeber, F., Freymann, K., Maier, W., Schild, H., & Block, W. (2006). Treatment monitoring and response prediction with proton MR spectroscopy in AD. *Neurology, 67,* 528-530.

Jiao, Y., Chen, R., Ke, X., Chu, K., Lu, Z., & Herskovits, E. H. (2010). Predictive models of autism spectrum disorder based on brain regional cortical thickness. *Neuroimage, 50,* 589–599. doi: 10.1016/j.neuroimage.2009.12.047

Jiao, Y., Chen, R., Ke, X., Chu, K., Lu, Z., & Herskovits, E. H. (2011). Predictive models for subtypes of autism spectrum disorder based on single-nucleotide polymorphisms and magnetic resonance imaging. *Advances in Medical Sciences, 56,* 334-342. doi: 10.2478/v10039-011-0042-y

Jou, R., Minshew, N., Keshavan, M., & Hardan, H. (2010). Cortical gyrification in autism and Asperger disorders: a preliminary magnetic resonance imaging study. *J. Child Neurol., 25,* 1482-1487. doi: 10.1177/0883073810368311

Kaiser, M. & Pelphrey, K. (2012). Disrupted action perception in autism: Behavioral evidence, neuroendophenotypes, and diagnostic utility. *Devel. Cog. Neurosci., 2,* 25-35. doi: 10.1016/j.dcn.2011.05.005

Kana, R. K., Libero, L. E., Hu, C. P., Deshpande, H. D., & Colburn, J.S. (2012). Functional brain networks and white matter underlying theory-of-mind in autism. *SCAN, 7.*

Kana, R. K., Libero, L. E., & Moore, M. S. (2011). Disrupted cortical connectivity theory as an explanatory model for autism spectrum disorders. *Phys. Life Rev., 8,* 410-437. doi: 10.1016/j.plrev.2011.10.001

Kates, W., Ikuta, I., & Burnette, C. (2009). Gyrification patterns in monozygotic twin pairs varying in discordance for autism. *Autism Res., 2,* 267-278. doi: 10.1002/aur.98

Keller, T. A., & Just, M. A. (2009). Altering cortical connectivity: remediation-induced changes in the white matter of poor readers. *Neuron, 64,* 624-631. doi: 10.1016/j.neuron.2009.10.018

Keller, T. A., Kana, R. K., & Just, M. A. (2007). A developmental study of the structural integrity of white matter in autism. *Neuroreport, 18,* 23-27.

Kleinhans, N. M., Richards, T., Weaver, K. E., Liang, O., Dawson, G., & Aylaward, E. (2009). Biochemical correlates of clinical impairment in high functioning autism Asperger's disorder. *J. Autism Dev. Disord., 39,* 1079–1086. doi: 10.1007/s10803-009-0707-6

Kleinhans, N., Schweinsburg, B., Cohen, D., Müller, R., & Courchesne, E. (2007). N-acetyl aspartate in autism spectrum disorders: regional effects and relationship to fMRI activation. *Brain Res., 1162,* 85–97.

Krafnick, A. J., Flowers, D. L., Napoliello, E. M., & Eden, G. F. (2011). Gray matter volume changes following reading intervention in dyslexic children. *Neuroimage, 57,* 733-741. doi: 10.1016/j.neuroimage.2010.10.062

Lange, N., Dubray, M. B., Lee, J. E., Froimowitz, M. P., Froehlich, A., Adluru, N., Wright, B., Ravichandran, C., Fletcher, P. T., Bigler, E. D., Alexander, A. L., & Lainhard, J. E. (2010). Atypical diffusion tensor hemispheric asymmetry in autism. *Autism Res., 3,* 350-358. doi: 10.1002/aur.162

Lee, J. E., Chung, M. K., Lazar, M., DuBray, M. B., Kim, J., Bigler, E. D., Lainhart, J. E., & Alexander, A. L. (2009). A study of diffusion tensor imaging by tissue-specific, smoothing-compensated voxel-based analysis. *Neuroimage, 44,* 870-883. doi: 10.1016/j.neuroimage.2008.09.041

Levitt, J., Blanton, R., Smalley, S., Thompson, P., Guthrie, D., McCracken, J., & Toga, A. (2003). Cortical sulcal maps in autism. *Cerebral Cortex, 13,* 728-735.

Levitt, J., O'Neill, J., Blanton, R., Smalley, S., Fedale, D., McCracken, J.T., Guthrie, D., Toga, J.R. (2003). Proton magnetic resonance spectroscopic imaging of the brain in childhood autism. *Biol. Psychiatry, 54:* 1355–1366.

Maddock, R. J., & Buonocore, M. H. (2012). MR spectroscopic studies of the brain in psychiatric disorders. *Curr. Top. Behav. Neurosci., 11,* 199-251.

Mak-Fan, K. M., Morris, D., Vidal, J., Anagnostou, E., Roberts, W., & Taylor, M. J. (2012). White matter and development in children with an autism spectrum disorder. *Autism.* doi: 10.1177/1362361312442596

Meyerhoff, D. J., MacKay, S., Bachman, L., Poole, N., Dillon, W. P., Weiner, M. W., & Fein, G. (1993). Reduced brain N-acetylaspartate suggests neuronal loss in cognitively impaired Human immunodeficiency virus-seropositive individuals: in vivo 1H magnetic resonance spectroscopic imaging. *Neurology, 43,* 509–515.

Mori, K., Hashimoto, T., Harada, M., Toneda, Y., Shimakawa, S., Fujii, E., Yamaue, T., Miyazaki, M., Saijo, T., & Kuroda, Y. (2001). Proton magnetic resonance spectroscopy of the autistic brain. *Brain & Development, 33*, 329-335.

Murdaugh, D., Shinkareva, S., Deshpande, H., Wang, J., Pennick, M., & Kana, R. (2012). Differential deactivation during mentalizing and classification of autism based on default mode network connectivity. *PLOS One.* doi: 10.1371/journal.pone.0050064

Murphy, D., Critchley, H., Schmitz, N., McAlonan, G., Van Amelsvoort, T., Robertson, D., Daly, E., Rowe, A., Russell, A., Simmons, A., Murphy, K., & Howlin, P. (2002). Asperger syndrome: a proton magnetic resonance spectroscopy study of brain. *Arch. Gen. Psychiatry*, *59,* 885-891.

Nickl-Jockschat, T., Habel, U., Michel, T. M., Manning, J., Laird, A. R., Fox, P. T., Schneider, F., & Eickhoff, S. B. (2012). Brain structure anomalies in autism spectrum disorder-a meta-analysis of VBM studies using anatomic likelihood estimation. *Hum. Brain Mapp., 33*, 1470-1489.

Nordahl, C., Dierker, D., Mostafavi, I., Schumann, C., Rivera, S., Amaral, D., & Van Essen, D. (2007). Cortical folding abnormalities in autism revealed by surface-based morphometry. *J. Neurosci,, 27,* 11725-11735.

Oner, O., Devrimci-Ozguven, H., Oktem, F., Yagmurlu, B., Baskak, B., & Munir, K. M. (2007). Proton MR spectroscopy: higher right anterior cingulate N-acetylaspartate/choline ratio in Asperger syndrome compared with healthy controls. *AJNR Am. J. Neuroradiol., 28,* 1494–1498.

Otsuka, H., Harada, M., Mori, K., Hisaoka, S., & Nishitani, H. (1999). Brain metabolites in the hippocampus- amygdala region and cerebellum in autism: an 1H-MR spectroscopy study. *Neuroradiology, 41*, 517-519.

Page, L., Daly, E., Schmitz, N., Simmons, A., Toal, F., Deeley, Q., Amberly, F., McAlonan, G. M., Murphy, K. C., & Murphy, G. M. (2006). In vivo 1H-Magnetic resonance spectroscopy study of amygdala-hippocampal and parietal regions in autism. *Am. J. Psychiatry, 163*, 2189-2192.

Perich-Alsina, J., Aduna de Paz, M., Valls, A., & Munoz-Yunta, J. A. (2002). Thalamic

spectroscopy using magnetic resonance in autism. *Rev. Neurol., 34 Suppl 1*, S68-71.

Pierpaoli, C., & Basser, P. J. (1996). Toward a quantitative assessment of diffusion anisotropy. *Magn. Reson. Med., 36,* 893–906.

Prevalence of Autism Spectrum Disorders Among Children Aged 8 Years—Autism and Developmental Disabilities Monitoring Network, 11 Sites, United States, 2010 (2014). *Surveillance Summaries*. *Morbidity and Mortality Weekly Report* 63(SS02), 1-21.

Raznahan, A. M., Toro, R., Daly, E., Robertson, D., Murphy, C., Deeley, Q., Bolton, P. F., Paus, T., & Murphy, D. (2010). Cortical anatomy in autism spectrum disorder: an in vivo MRI study on the effect of age. *Cereb. Cortex*, *20*, 1332-1340. doi: 10.1093/cercor/bhp198

Ross, B., & Bluml, S. (2001). Magnetic resonance spectroscopy of the human brain. *Anat. Rec., 2*, 54–84. doi: 10.1002/ar.1058

Rothman, D. L., Behar, K. L., Hyder, F., & Shulman, R. G. (2003). In vivo NMR studies of the Glutamate neurotransmitter flux and neuroenergetics: implications for brain function. *Annu. Rev. Physiol.,65*, 401–427.

Sheinkopf, S. J., & Siegel, B. (1998). Home-based behavioral treatment of young children with autism. *J. Autism Dev. Disord., 28*, 15-23.

Scheel, C., Rotarska-Jagiela, A., Schilbach, L., Legnhardt, F. G., Krug, B., Vogeley, K., & Tepest, R. (2011). Imaging derived cortical thickness reduction in high-functioning autism: Key regions and temporal slope. *Neuroimage, 58*, 391-400. doi: 10.1016/j.neuroimage.2011.06.040

Shokouhi, M., Williams, J., Waiter, G., & Condon, B. (2012). Changes in sulcal size associated with autism spectrum disorder revealed by sulcal morphometry. *Autism Res., 5*, 245-252. doi: 10.1002/aur.1232

Spencer, M., Holt, R., Chura, L., Suckling, J., Calder, A., Bullmore, E., & Baron-Cohen, S. (2011). A novel functional brain imaging endophenotype of autism: the neural response of facial expression of emotion. *Transl. Psych., 1,* e19. doi: 10.1038/tp.2011.18

Stanfield, A., McIntosh, A. M., Spencer, M. D., Philip, R., Gaur, S., & Lawrie, S. M. (2008). Towards a neuroanatomy of autism: a systematic review and meta-analysis of structural magnetic resonance imaging studies. *European Psychiatry, 23*, 289-299.

Stanley, J. A. (2002). In vivo magnetic resonance spectroscopy and its application to neuropsychiatric disorders. *Can. J. Psychiatry*, *47*, 315-326.

Suzuki, K., Nishimura, K., Sugihara, G., Nakamura, K., Tsuchiya, K. J., Matsumoto, K., Takebayashi, K., Isoda, H., Sakahara, H., Sugiyama, T., Tsujii, M., Takei, N., & Mori, N. (2010). Metabolites alteration in the hippocampus of high-functioning adult subjects with

autism. *Int. J. Neuropsychopharm., 13,* 529–534. doi: 10.1017/S1461145709990952

Temple, E., Deutsch, G. K., Poldrack, R. A., Miller, S. L., Tallal, P., Merzenich, M. M., & Gabrieli, J. D. (2003). Neural deficits in children with dyslexia ameliorated by behavioral remediation: Evidence from functional MRI. *Proc. Natl. Acad. Sci. U. S. A., 100,* 2860-2865.

Travers, B. G., Adluru, N., Ennis, C., Tromp do, P. M., Destiche, D., Doran, S., Bigler, E. D., Lange, N., Lainhart, J. E., & Alexander, A. L. (2012). Diffustion tensor imaging in autism spectrum disorder: a review. *Autism Res., 5,* 289-313. doi: 10.1002/aur.1243

Uddin, L., Menon, V., Young, C., Ryali, S., Chen, T., Khouzam, A., Minshew, N., & Hardan, A. (2011). Multivariate searchlight classification of structural magnetic resonance imaging in children and adolescents with autism. *Biol. Psychiatry, 70,* 833-841. doi: 10.1016/j.biopsych.2011.07.014

Vasconcelos, M. M., Brito, A. R., Domingues, R. C., Cruz, L. C., Werner, J., & Gonçalves, J. P. (2007). Proton magnetic resonance spectroscopy in school-aged autistic children. *J. Neuroimaging, 18,* 288–295. doi: 10.1111/j.1552-6569.2007.00200.x

Waagepetersen, H. S., Sonnewald, U., & Schousboe, A. (2007) Glutamine, Glutamate, and GABA: metabolic aspects. In A. Lajtha, S. Oja, A. Schousboe, & P. Saransaari (Eds.), *Handbook of neurochemistry and molecular neurobiology: Amino acids and peptides in the nervous system* (pp. 1-21). New York: Springer.

Waiter, G. D., Williams, J. H., Murray, A. D., Gilchrist, A., Perrett, D. I., & Whiten, A. (2005). Structural white matter deficits in high-functioning individuals with autistic spectrum disorder: a voxel-based investigation. *Neuroimage, 24,* 455-461.

Wallace, G., Dankner, N., Kenworth, L., Giedd, J., & Martin, A. (2010). Age-related temporal and parietal cortical thinning in autism spectrum disorders. *Brain, 133,* 3745-3754. doi: 10.1093/brain/awq279

Wallace, G., Robustelli, B., Dankner, N., Kenworthy, L., Giedd, J., & Martin, A. (2013). Increased gyrification, but comparable surface area in adolescents with autism spectrum disorders. *Brain, 136,* 1956-1967. doi: 10.1093/brain/awt106

Williams, D. L., & Minshew, N. J. (2007). Understanding autism and related disorders: what has imaging taught us?. *Neuroimaging. Clin. N. Am., 17,* 495-509.

Yuksel, C., & Ongur, D. (2010), Magnetic resonance spectroscopy studies of glutamate-related abnormalities in mood disorders. *Biol. Psychiatry, 68,* 785–794. doi: 10.1016/j.biopsych.2010.06.016

Zilles, K., Armstrong, E., Schleicher, A., & Kretschmann, H. (1988). The human pattern of gyrification in the cerebral cortex. *Anatomy and Embryology, 179,* 173-179.

APPENDIX

IRB APPROVAL FORM

THE UNIVERSITY OF ALABAMA AT BIRMINGHAM

Institutional Review Board for Human Use

DATE: July 31, 2013

MEMORANDUM

TO: Lauren E Libero
Principal Investigator

FROM: Cari Oliver, CIP
Assistant Director
Office of the Institutional Review Board (OIRB)

RE: Request for Determination—Human Subjects Research
IRB Protocol #N130725009 – Anatomical and Neurochemical Investigation of the Brain in Autism

A member of the Office of the IRB has reviewed your Application for Not Human Subjects Research Designation for above referenced proposal.

The reviewer has determined that this proposal is **not** subject to FDA regulations and is **not** Human Subjects Research. Note that any changes to the project should be resubmitted to the Office of the IRB for determination.

470 Administration Building
701 20th Street South
205.934.3789
Fax 205.934.1301
irb@uab.edu

The University of
Alabama at Birmingham
Mailing Address:
AB 470
1720 2ND AVE S
BIRMINGHAM AL 35294-0104